Food and Agriculture Organization of the United Nations

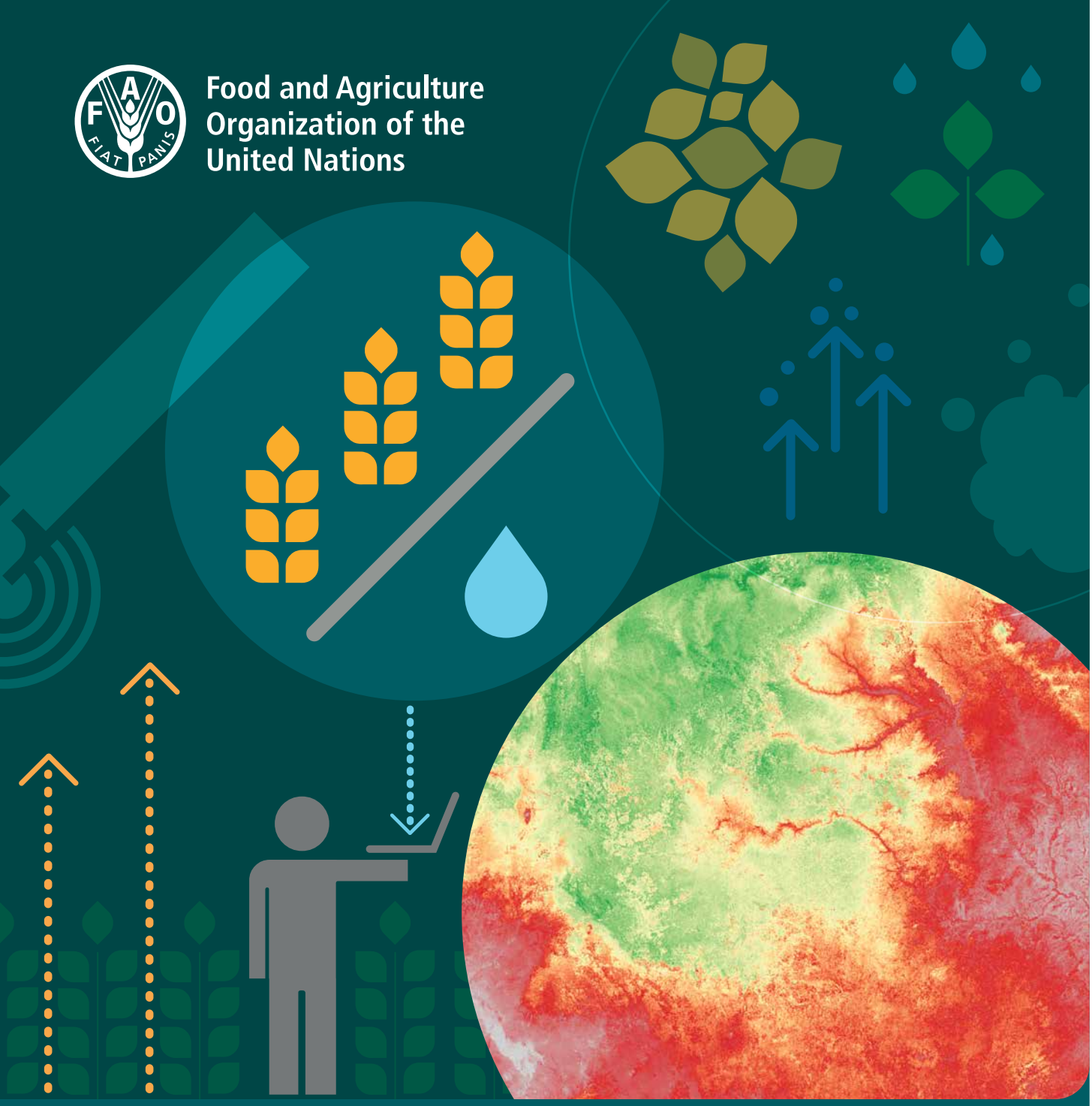

WaPOR quality assessment

Technical report on the data quality of the WaPOR FAO database version 1.0

UNESCO | IHE DELFT

WaPOR quality assessment

Technical report on the data quality of the WaPOR FAO database version 1.0

Food and Agriculture Organization of the United Nations
Rome, 2019

Required citation: FAO and IHE Delft. 2019. WaPOR quality assessment. Technical report on the data quality of the WaPOR FAO database version 1.0. Rome. 134 pp.

ISBN 978-92-5-131535-4

Contents

Figures

Tables

Acknowledgements

This report was prepared by Marloes Mul and Wim Bastiaanssen, with contributions from: Jonna van Opstal, Xueliang Cai, Ann van Griensven, Imeshi Weerasinghe, Bich Tran, Tim Hessels, Bert Coerver, Claire Michailovsky, Elga Salvadore, Ate Poortinga, Poolad Karimi, and Li Jia.

The FAO Land and Water Division commissioned this study and provided layout and editorial work in the framework of the the project ´Using Remote Sensing in support of solutions to reduce agricultural water productivity gaps`, funded by the Government of The Netherlands. The work was carried out by a team in IHE-Delft as an independent quality assessment of the WaPOR database and, as such, the views expressed in the report are those of the authors.

The report contains various type of analysis and quality checks. Most of the data has been assembled during the last two years. During the writing of the report, new global datasets became available. Some of them are included – or could be included in a future version of this report. It is the intention of the authors to include more ground measurements collected by IHE Delft students for the current and next academic year and intensify the exchanges with the various international partners in Africa and Near East. The continuation of quality control can benefit from the strengths and weaknesses found in the current report. Validation of the rich database of WaPOR with unprecedented possibilities is an evolving effort.

The essence of this validation report is to collect independent datasets and make comparative analysis. While most spatial data layers can be accessed through the public domain (although not all), the real value comes from the data sharing of third parties. We are therefore indebted to many international partners. We thank the team at Global Runoff Data Centre (GRDC), 56 068 Koblenz, Germany for providing the discharge data. We acknowledge the sharing of sap flow field measurements conducted by Karim Bergaoui and Makhram Belhaj Fraj from Tunisia. Michael Gilmont from the University of Oxford kindly made his field measurements from Jordan and Israel available. Jiro Ariyama from the FAO office in Cairo kindly assisted in the flux analysis of the eddy covariance towers in the Nile Delta of Egypt. Caren Jarmain, Colin Everson, Alistair Clulow and Graham Jewitt from the University of Kwazulu Natal provided flux tower data from South Africa, including the Cathedral Peak data from the South African Environmental Observation Network (SEAON), and the Lebanese Agricultural Research Institute (LARI) made the weather data available for the Bekaa Valley, and the Wonji Shoa Research Centre and factory made the yield data available in the Wonji irrigation scheme. Finally, the Ministry of Water Resources and Irrigation of Egypt provided data for the Fayoum irrigation scheme.

Some spatial maps were provided for making extra analysis feasible. For example, AETI data products were made available by various people and we are grateful for their support, this includes Li Jia for making the ETMonitor data available, Albert van Dijk for the CMRSET and Xuelong for the SEBS data, Seyed Hamed Alemohammad for the WECANN data and Martha Anderson for the ALEXI data. The National Council for Scientific Research of Lebanon is acknowledged for sharing the land use map of the Litani Basin. The Water for Growth Rwanda (W4GR) project kindly made their land use map available. The team of Miriam Coenders–Gerrits at TUDelft shared with us the newest T and I maps following their Budyko methodology. The SERVIR Mekong team kindly made code available for global WP analysis on the Earth Engine.

Abbreviations and Acronyms

AETI	Actual Evapotranspiration and Interception
AGBP	Above Ground Biomass Production
ALEXI	Atmosphere Land Exchange Inverse (model)
ARC	African Rainfall Climatology
CHIRPS	Climate Hazards Group InfraRed Precipitation with Stations
CMORPH	Climate Prediction Center's morphing technique
CMRSET	CSIRO MODIS ReScaled potential ET
CNRS	National Council for Scientific Research (Lebanon)
CRU	Climatic Research Unit
DEM	Digital Elevation Model
DM	Dry Matter
E	Evaporation (from soil)
ETLook	EvapoTranspiration Look (model)
EWEMBI	EartH_2Observe observations, WFDEI and ERA-Interim data Merged and Bias-corrected for ISIMIP
FAO	Food and Agricultural Organization of the United Nations
FLUXNET	Flux Network for in situ measurements of turbulent fluxes (H20, CO2, heat)
FRAME	FAO Remote sensing Assessment for Monitoring and Evaluation (Consortium)
GBWP	Gross Biomass Water Productivity
GIAM	Global Irrigated Area Map
GMIA	Global Map of Irrigated Areas
GLDAS	Global Land Data Assimilation System
GLEAM	Global Land surface Evaporation: the Amsterdam Methodology
GOES-5	Geostationary Operational Environmental Satellite system
GRDC	Global Runoff Data Centre
GT	Ground truth
HC	Harvest Choice
I	Interception
ITC	International Institute for Geo-Information Science and Earth Observation
ITCZ	Inter Tropical Convergence Zone
IWMI	International Water Management Institute
LAI	Leaf Area Index

LandFluxEval	Land Flux Evaluation data base
LCC	Land Cover Classification
LRA	Litani River Authority
MENA	Middle East and Northern Africa
MERRA	Modern-Era Retrospective Analysis for Research and Applications
MODIS	MODerate resolution Imaging Spectroradiometer
MSG	Meteosat Second Generation
MTE	Model Tree Ensemble
NBWP	Net Biomass Water Productivity
NDVI	Normalized Difference Vegetation Index
NPP	Net Primary Production
PCP	Precipitation
PERSIANN-CDR	Precipitation Estimation from Remotely Sensed Information using Artificial Neural Networks
RCMRD	Regional Centre for Mapping of Resources for Development
RET	Reference Evapotranspiration
RFE	African Rainfall Estimation
RWFA	Rwanda Water and Forestry Authority
SEBS	Surface Energy Balance System
SERVIR-Mekong	geospatial data-for-development program for the Lower Mekong SSEBop Operational Simplified Surface Energy Balance
SWAT+	Soil and Water Assessment Tool
T	Transpiration
TAMSAT	Tropical Applications of Meteorology using SATellite
TBP	Total Biomass Production
TC	TerraClimate
TE	Transpiration Efficiency
TRMM	Tropical Rainfall Measuring Mission
USGS	United States Geological Survey
VITO	Flemish Institute for Technological Research
WA+	Water Accounting plus
WACMOS-ET	WAter Cycle Observation Multi-mission Strategy - EvapoTranspiration
WaPOR	FAO portal to monitor Water Productivity through Open access of Remotely sensed derived data
WB	Water Balance
WECANN	Water, Energy, and Carbon with Artificial Neural Networks
WP	Water Productivity

Executive summary

This report describes the quality assessment of the FAO's data portal to monitor Water Productivity through Open access of Remotely sensed derived data (WaPOR 1.0). The WaPOR 1.0 data portal has been prepared as a major output of the project: ´Using Remote Sensing in support of solutions to reduce agricultural water productivity gaps', funded by the Government of The Netherlands. The WaPOR database is a comprehensive database that provides information on biomass production (for food production) and evapotranspiration (for water consumption) for Africa and the Near East in near real time covering the period 1 January 2009 to date. This report is the result of an independent quality assessment of the different datasets available in WaPOR prepared by IHE-Delft. The quality assessment checks the consistency of the different layers and compares the individual layers to various other independent data sources, including: spatial data; auxiliary data and in-situ data. The report describes the results of the quality assessment per data layer for each specific theme as available on the portal:

Precipitation (PCP)

The PCP dataset posted on the WaPOR data portal is a copy of CHIRPS, with a few modifications for data gaps in agricultural areas. This dataset has been validated by different independent and international science teams. The CHIRPS database is among the top PCP databases available online and performs specifically well on decadal timescales.

Reference Evapotranspiration (RET)

The WaPOR RET data is able to correctly express RET climatic evapotranspiration across the continent. On the continental level, variations in RET between years are low (varying less than 25 mm per year, 0.6%). A similar trend is also observed for one weather station. The WaPOR RET data is able to identify the impacts of 2009 El Nino event, with higher than average RET in Southern and West Africa and lower RET values in East Africa, consistent with El Nino anomalies. However, some more validation with ground-based weather station data remains necessary.

Actual Evapotranspiration and Interception (AETI)

Compared to similar remote sensing databases of actual evapotranspiration, WaPOR AETI is reliable for a longer period (e.g. a year) and larger areas (e.g. a sub-basin). The annual AETI for Litani basin in Lebanon is excellent. The quality reduces with a higher aridity such as in Egypt and South Africa. The 250m and 100m pixels are less suitable for detecting AETI of vegetables and fruit crops; 30 m pixels add a lot of value. However there are several challenges with the breakdowns of annual AETI into monthly and decadal values, and also spatially for local agricultural fields. The latter is manifested in the validation with individual flux tower data (eddy covariance and surface renewal). WaPOR AETI for the crop season is systematically underestimated (20-60%). Hence, a spatial and temporal refinement of AETI is required. It is fair to note that field measurements on AETI often have their own uncertainties.

Transpiration, Evaporation, Interception (T, E, I)

All three products individually showed reasonable ranges in values and spatial variability. Compared to ETMonitor, WaPOR T estimates are high and WaPOR E estimates are low. The high WaPOR ratio of T/AETI is consistent with the Budyko approach, exceeding at the continental scale 0.7 ratio. While this does not always match with the general

opinion, 0.7 ratio and higher for tropical forest and permanent crops are very acceptable. For the selected irrigation systems in Ethiopia, Egypt, Lebanon and Ghana similar high T/AETI are found (>0.73), consistent for vegetated areas.

Above Ground Biomass Production (AGBP)

Agro-ecological production is commonly expressed as Net Primary Production (NPP) in remote sensing terminology, or crop yield in agronomic terms. A direct comparison against AGBP from other sources is difficult. The comparison against NPP from MODIS and global ecological production models does not identify serious problems at the continental scale: the absolute values and aerial patterns of NPP are very acceptable. This is confirmed from the crop yield analysis for sugarcane (Ethiopia), grapes (Lebanon), rice and bananas (Ghana) and wheat (Egypt). Fresh crop yield could be very well approximated, provided that local calibration of Harvest Index and the moisture content of the harvestable product is considered and the cropping season is defined on the basis of local information. This implies that local agronomical knowledge is necessary to convert AGBP into crop yield. Some warning on the role of the default 0.65 shoot-root ratio and default C3 crop maximum light use efficiency of 2.49 gr/MJ of total dry matter for all C3 and C4 crops should be mentioned in the information section of the WaPOR website.

Land cover classification

Land cover classification, as all data layers, has been created with different spatial resolutions. The single most relevant class for water productivity is the distinction between rainfed and irrigated crops. While the WaPOR irrigated area extent is at times comparable to the GMIA from FAO AQUASTAT, verification with other sources and field measurements indicated that a serious underestimation occurs. The procedure applied for mapping irrigated areas may need to be improved.

Phenology

The crop phenology is essential for assessing the accumulated values of biomass production (AGBP and TBP) and water consumption (AETI). This study finds that the accuracy of the phenology is poor and does not match with local cropping calendars. This is a serious limitation for approximating the accumulated values between dates of emergence and date of harvest. This part of WaPOR can currently not be used without local information or validation, and an appropriate warning should be provided through the WaPOR portal.

Water productivity

The water productivity layer in WaPOR is a compilation of other WaPOR layers (phenology, land use, AGBP, AETI and T), errors in those layers are therefore compounded in the water productivity layer. The errors in the phenology and land cover classification layers were overcome by applying the start and end date of the season and using a polygon of the field obtained from observations. The analyses show very good comparisons with a slight deviation due to the inclusion of fallow land within the polygons. For example the WP analyses for sugarcane (Ethiopia) is therefore underestimated with non farm land (fallow land, buildings, roads and open water) showing low WP. On the other hand, WP for wheat and maize (Egypt) can be overestimated as included fallow areas show high WP. Finally, WP analyses in a humid zone (Southern Ghana) shows little distinction between the agricultural lands and the surrounding natural vegetation. It is clear that detailed cropping maps are required to exclude this kind of noise from the WP analyses.

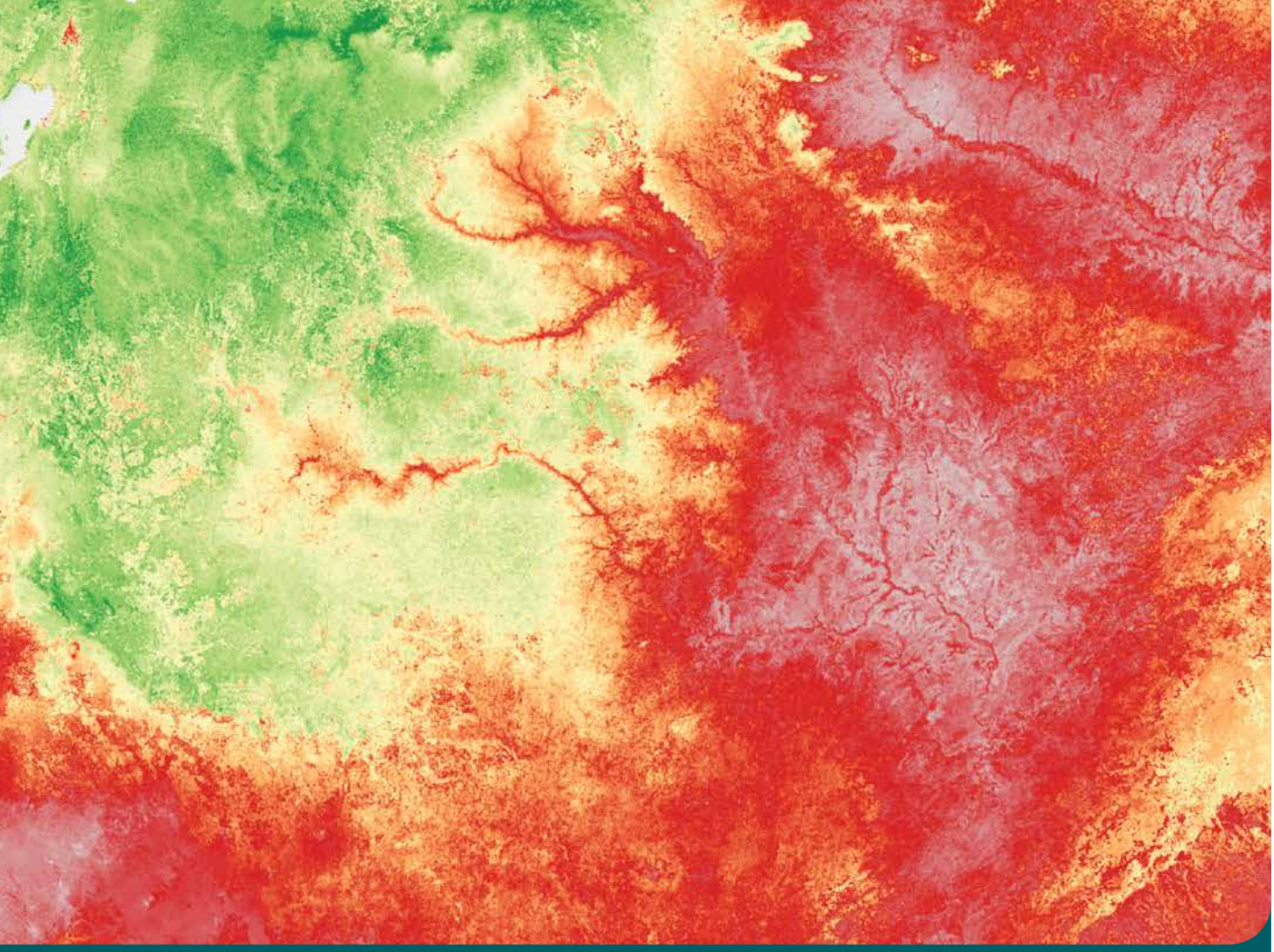

Detail of WaPOR Map "Gross Biomass Water Productivity 2018 - Kenya, Somalia and Ethiopia"

1. Introduction

A. Overview

This report is an output of the project "Using Remote Sensing in support of solutions to reduce agricultural water productivity gaps", funded by the Government of The Netherlands. The project is lead by FAO with the following project partners: FRAME consortium, IHE Delft and IWMI. The objective of the project is monitoring water productivity, identifying water productivity gaps, proposing solutions to reduce these gaps and contributing to a sustainable increase of agricultural production. The main output is to develop an open access data portal on remotely sensed derived water productivity in Africa and the MENA region, hosted by FAO. The FRAME consortium, consisting of eLEAF, VITO, ITC, and the WaterWatch Foundation, is responsible for creating and providing the remote sensing data for the project. In April 2017, FAO's portal to monitor Water Productivity through Open access of Remotely sensed derived data (WaPOR) was launched as a Beta version. Two parallel independent quality assessments of the Beta version were implemented by IHE Delft and ITC. Recommendations from these assessments were used to prioritize improvements for WaPOR version 1.0. In August 2018, this improved version was made available through the link: https://wapor.apps.fao.org (version 1.0), in December 2018 some additional improvements on the user interface of the portal were made available through version 1.1. An overview of the available WaPOR data is provided in Table 1.

Table 1

Thematic areas and WaPOR data components available for different spatial resolutions*

Thematic area	Layers	Level 1 (250 m)	Level 2 (100 m)	Level 3 (30 m)
Climate	Precipitation (PCP)	Daily/decadal/ annual (5km)		
	Reference Evapotranspiration (RET)	Daily/decadal/ annual (20km)		
Water	Actual Evapotranspiration and Interception (AETI)	Decadal/annual	Decadal/ seasonal/ annual	Decadal/ seasonal/ annual
	Transpiration (T)			
	Evaporation (E)			
	Interception (I)			
Land	Above ground biomass production (AGBP)	Annual	Decadal/ seasonal	Decadal/ seasonal
	Land cover classification (LCC)	Annual	Annual	Decadal
	Phenology		Seasonal	Seasonal
	Net Primary Production (NPP)	Decadal	Decadal	Decadal
Water Productivity (WP)	Gross WP	Annual	Seasonal	Seasonal
	Net WP	Annual	Seasonal	Seasonal

* currently available products in the WaPOR portal

The WaPOR database is the first comprehensive dataset that combines biomass production (for food production) and AETI information (for water consumption) at continental scale near real time covering the period 1 January 2009 to date. It should be emphasized that the Gross WP and Net WP are based on Above Ground Biomass Production and not on the fresh crop yield as is often done for international WP studies. The reason for avoiding crop dependent information is the lack of accuracy to determine crop layers from earth observation data. The validation of AGBP and WP can however only be done through conversion into crop yield data, because AGBP is rarely measured under actual field conditions.

B. Quality Assessment

Output 2 of the project includes a quality assessment of the WaPOR database. Results of this independent assessment by IHE Delft are presented in this report. It is meant for an independent verification of WaPOR version 1.0 data and it forms a basis for including improvements in WaPOR version 2.0. This quality assessment checks the consistency of the different layers and compares the individual layers to various products:

Table 2
Overview of comparisons made for each layer

Thematic area	Layers	Spatial data	Auxiliary data	In situ observations
Climate	PCP	CRU		
	RET	GLDAS, TerraClimate		Weather station data (Bekaa and Port Said)
Water	AETI	Various remote sensing data products, SWAT modelling output	Water balance for large river basins in Africa, Litani River Basin, Nile sub-basins, Fayoum irrigation scheme, field scale soil water (Jordan, Israel)	Flux towers (South Africa, Ghana, Senegal, Egypt)
	T	Remote sensing data products (ETMonitor, GLDAS), Budyko approach		Sap flow Tunisia
	E			
	I			
Land	AGBP	Remote sensing products (MODIS)	Comparisons with known yields (Wonji, Fayoum, Kpong, Bekaa Valley irrigation scheme)	
	LCC	Other databases (GMIA, GIAM)	National statistics Rwanda	GIAM Ground truth data points for Benin, Ethiopia
	Phenology		FAO crop calendars[a] , case study information (Wonji, Fayoum, Kpong, Bekaa)	
WP	Gross WP	WP MODIS & Servir Mekong	Case study data (Wonji, Fayoum, Bekaa)	
	Net WP			

[a] http://www.fao.org/agriculture/seed/cropcalendar/welcome.do

- Spatial data products
- Auxiliary data comparison
- In-situ data comparison

Table 2 presents an overview of the comparisons made between the WaPOR database and other data sources.

Consistency check

For each layer the general spatial trend is analysed, as well as the range of values in the layer. This is implemented at continental level (WaPOR Level 1, 250 m resolution). The authors used their expert judgement to evaluate if the values are in reasonable ranges.

Spatial data

Next to the WAPOR data, there are many other spatial data products available that monitor various WaPOR parameters. These spatial data products are either derived from remote sensing, similarly to WaPOR, or derived through other means (e.g. modelling). The products were compared on their general trends and statistical properties and differences with the WaPOR data were calculated and analysed. These analyses were done at continental level using the WaPOR Level 1 data (250 m resolution).

Auxiliary data

Several WaPOR layer products can be compared indirectly with auxiliary and independently gathered datasets. One such example is the water balance calculations, which derives actual ET using observed data for a specific area. The advantage of this method is that it integrates parameters over a specific area using observed and often validated datasets. Depending on the scale of the analyses, the WaPOR data with the highest available resolution was used.

In situ observations

Where possible, the WaPOR data layers are compared with in situ observations. As the WaPOR data has very high resolution (250 m to 30 m on selected pilot areas), it is possible to validate the product using point observations. This comparison has the highest value as it compares the same parameter using observed data. Depending on the location of the in situ observation, the WaPOR data with the highest resolution was used for the comparison.

Robustness analyses

Finally, the analyses focus on the consistency between the different WaPOR layers, in particular those that are independently developed.

The selection of data for comparison and robustness analyses were dependent on the availability of data products online and on willingness of our partners to share their data.

As can be seen from Table 2, the report provides a wide range of analyses to validate the WaPOR dataset. It combines comparative analyses at continental level, various analyses at country, basin and field scale to the highest resolution of comparison at pixel resolution. The report provides a first indication of the quality of the individual data layers. The following chapters will describe the results of the quality assessment in three different thematic areas, similar to the portal: climate, water, and land. Each chapter will contain an assessment of the data layers found in the specific theme (Table 1).

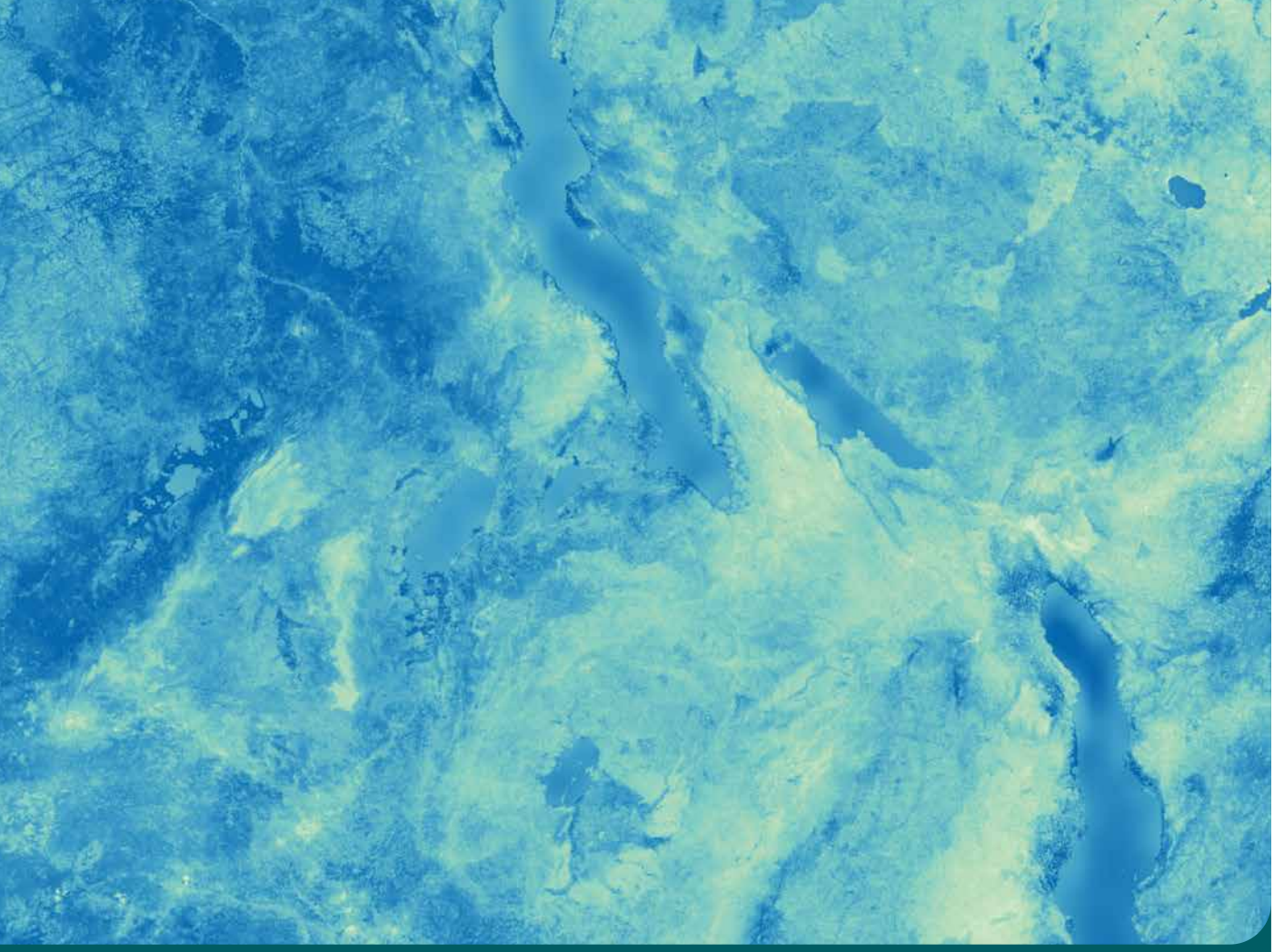

Detail of WaPOR Map "Actual EvapoTranspiration and Interception (ETIa) 2018 - Democratic Republic of the Congo, Tanzania and Zambia"

2. Climate

A. Precipitation

A.1 Introduction

There are various remote sensing products of precipitation (PCP) available in the open domain and in near-real-time for Africa (Table 3). Some started in the 1980s and are continuing into the present. Increasingly remote sensing data products have included bias-corrections using ground observations (e.g. Xie *et al.*, 2011). Various studies evaluated the performance of satellite-derived products. At continental scale, Awange *et al.* (2016) found that the various products performed better at different time scales and different geographical locations. There is not one product which outperforms the other products across temporal and spatial scales, although TRMM and CHIRPS are often found to be among the more reliable products (e.g. Cheema and Bastiaanssen, 2011; Simons *et al.*, 20016; Ha *et al.*, 2018). Generally, satellite remote sensing products that correct biases using ground observation performed better compared to those that use remote sensing alone (Awange *et al.*, 2016; Pomeon *et al.*, 2017).

The CHIRPS dataset, used for the WaPOR database, is an existing data product and has a spatial resolution of 5 km (Funk *et al.*, 2015). This database was modified for data gaps for WaPOR important agricultural areas (FAO,

Table 3
Example of available real time PCP data products over Africa

Satellite product	Temporal coverage	Spatial coverage	Spatial resolution	Temporal resolution	Reference
ARC Version 2.0	1983–present	Africa	0.1° (~10 km)	Daily	Xie and Arkin, 1995
CHIRPS Version 2.0	**1981–present**	Near global	0.05° (~5 km)	Daily	Funk *et al.*, 2015
CMORPH	1998-present	Africa	0.1° (~10 km)	3-hourly	Joyce *et al.*, 2004; Xie *et al.*, 2011
PERSIANN-CDR	1983–present	Near global	0.25°(~27 km)	Daily	Hsu *et al.*, 1997; Novella and Thiaw, 2013, 2010
RFE Version 2.0	2001–present	Africa	0.1° (~10 km)	Daily	Herman *et al.*, 1997
TAMSAT	1983–present	Africa	0.0375° (~4 km)	Decal	Maidment *et al.*, 2014; Tarnavsky *et al.*, 2014
TRMM 3B42 version 7	1998–present	Near global	0.25°(~27 km)	3-hourly	Maidment *et al.*, 2014

2018). The dataset combines remote sensing information with ground observations. In various studies, CHIRPS data has been compared to observed PCP and other similar satellite PCP products. For example, in Burkina Faso, daily products generally performed poorly compared to ground observations. Aggregated products at monthly and annual scale performed much better (>0.8) (Dembele and Zwart, 2016). Data with higher spatial resolution performed better at station to pixel level (Dembele and Zwart, 2016). For decadal scale, Dembele and Zwart (2016) found that RFE performed best, closely followed by ARC and CHIRPS. Similarly, Hessels (2015) compared various remotely sensed PCP products with weather station data from the Blue Nile region and found that the CHIRPS data product displays the best correlation with station data. For East Africa, Dinku et al (2018) found that CHIRPS performed better than ARC and slightly better than TAMSAT at decadal and monthly timescales (whereas TAMSAT performed better at daily time scales).

A.2. Data analyses

The average annual PCP for the African continent lies between 537 and 597 mm per year (Table 4). The standard deviation of the mean annual PCP is 18 mm per year, which shows at a continental scale a relatively constant annual PCP. However, locally large variations in PCP occur between years with far reaching consequences for rainfed cropping systems and flood risks. A few areas in the vicinity of steep mountain ranges show very high annual PCP amounts (>3 000 mm per year) throughout the entire period. This is around the coast of West Africa and Cameroon and the east coast of Madagascar (which are more visible when adjusting the legend) (Figure 1; right). The general spatial variation in PCP at the continental scale is consistent with known PCP trends, low values are found across the Sahel and the Middle East region. Also high amounts of PCP occur around the West Coast of Africa, around the equator and the inlands of the Democratic Republic of Congo and highlands in East Africa (Uganda, Rwanda, Ethiopia) and the east coast of Madagascar (Figure 1).

Table 4

Average annual WaPOR PCP statistics (mm/yr) for the African continent

	2009	2010	2011	2012	2013	2014	2015	2016	2017	Average
Min	0	0	0	0	0	0	0	0	0	0
Max	4 789	5 257	4 787	4 576	4 330	5 004	4 735	4 759	5 876	4 901
Mean	572	597	587	590	566	565	537	562	584	573
Sd	603	632	624	621	611	599	580	597	626	604

Figure 1

Average annual WaPOR PCP (2009-2017) using two different legends (based on quartiles, left and based on equal intervals, right).

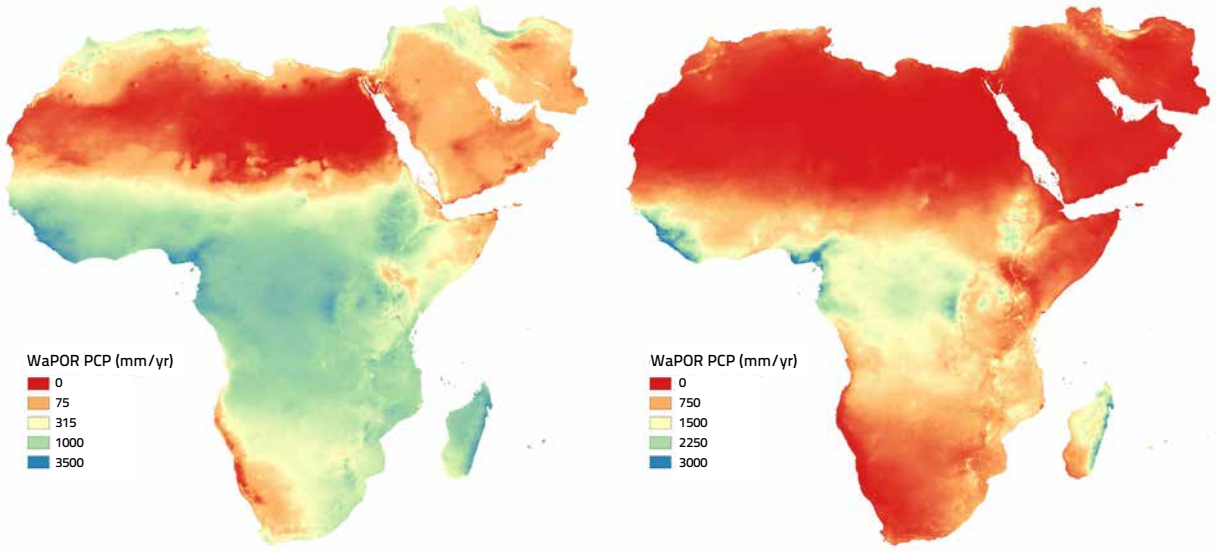

Comparison with other spatial data products

A comparison was made between the average annual PCP of Harvest Choice (HC) (Harvest Choice, 2011) and the average annual precipitation of the WaPOR database (Figure 2). The HC dataset is based on the reanalysis dataset from the University of East Anglia Climatic Research Unit (CRU) that essentially is interpolating and extrapolating between measured rainfall at gauges (New *et al.*, 2000). This dataset shows similar high PCP areas in West Africa and Madagascar (Figure 2 left). Considering the difference in the period of observation (1901-2005 vs 2009-2017), the general trend of PCP is similar between the two datasets, except for a few areas (Figure 2 right). These areas were found in Madagascar and Eastern part of the Democratic Republic of Congo. We have more trust in the CHIRPS data because many locations in Africa are not equipped with a rain gauge, and this affects the quality of the CRU-based PCP dataset.

Figure 2

Average annual PCP Harvest Choice (HC) and difference between the HC (1901-2005) and WaPOR data (2009-2017)

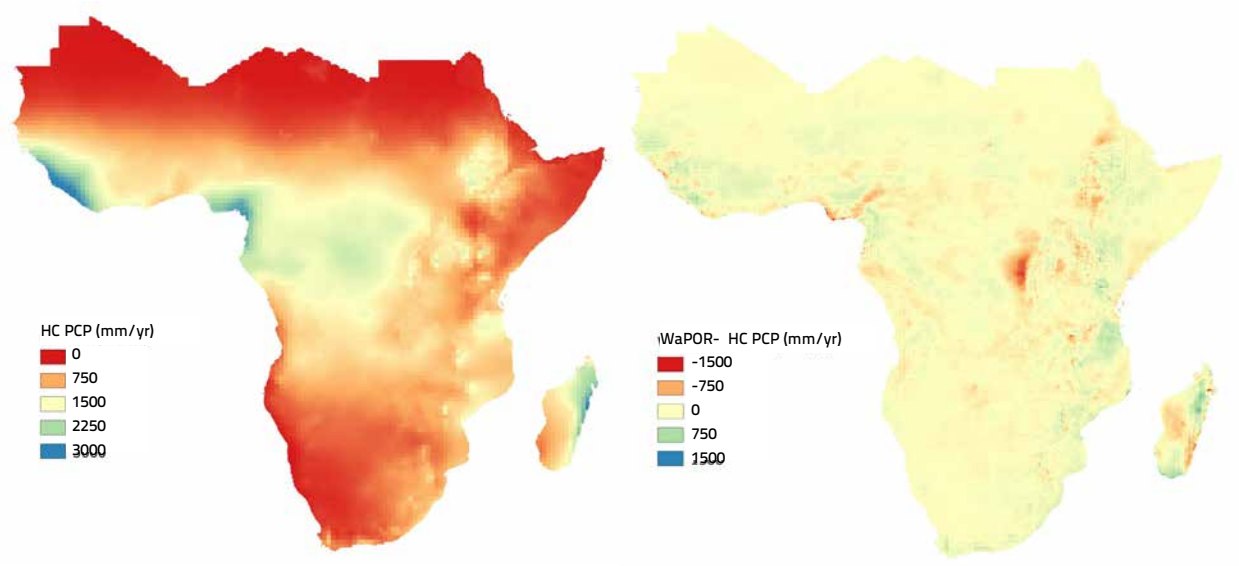

A.3 Conclusion

The PCP dataset posted on the WaPOR data portal is based on the CHIRPS dataset. This dataset from USGS has been validated and tested for many years by different independent science teams. The CHIRPS dataset is among the top PCP products available online and performs specifically well on decadal timescales as shown by Dembele and Zwart (2016).

B. Reference Evapotranspiration

B.1. Introduction

After the introduction by FAO of the global standard Reference evapotranspiration (RET) (Allen *et al.*, 1998), RET became a well-recognized concept to express the climatologic variability of crop ET. The attractive character of RET is that it is only affected by climatic factors, excluding other factors like for example crop and soil typology (Allen *et al.*, 1998). Over the past decades various approaches have been developed to calculate RET, often based on simpler input data (e.g. Hargreaves and Samani, 1985; de Bruin *et al.*, 2016). However, the Penman-Monteith equation (Allen *et al.*, 1998) is the most applied approach, after it was selected to be the best performing equation in a variety of climates by an FAO expert consultation in 1990. The drawback is that more detailed climatological information is required (radiation, humidity, temperature and wind speed), which is not always everywhere available in weather stations over the African continent.

Solar radiation is nowadays available with an unprecedented accuracy from Second Generation Meteosat (MSG) measurements over Africa and Near East. What remains is local prevailing humidity, temperature and wind speed, that are more commonly taken from numerical climatic and weather forecasting models to fill the voids of in situ

weather stations. The RET provided by WaPOR is based on the standardized FAO Penman-Monteith equation (Allen *et al.*, 1998) and input retrieved from MERRA, which utilizes MSG (solar radiation). The data is available at a spatial resolution of 20 km.

B.2. Data analysis

The average annual WaPOR RET ranges between 2 047 and 2 071 mm per year (see Table 5). The map shows large variations of average RET (Figure 3). The highest RET values (3 500 mm/yr) can be found across the Saharan desert and Middle East countries. These high values are controversial because due to the desert conditions, values for air humidity are low and the values for air temperature are high which at actual evaporation rates of 3 500 mm/yr would immediately result in a higher air humidity and lower air temperature and as such suppressing RET. This also the basis of Bouchet's complementary relationship in evaporation processes (Bouchet, 1963). This implies that the extremely high RET values will never be reached. The very high RET values in desert conditions are therefore a consequence of the chosen standard methodology (Allen *et al.*, 1998) and not an error of WaPOR. Lower RET values (825 mm/yr) are found in coastal areas, highlands of Ethiopia and the tropical forest in the Democratic Republic of Congo. Lower RET values occur due to low solar radiation (many clouds) and high humidity due to frequent rainfall events. Therefore, PCP and RET are inversely related (compare Figures 1 and 3).

Table 5

Mean annual WaPOR RET and standard deviations (for all regions)

Year	2009	2010	2011	2012	2013	2014	2015	2016	2017	Mean
Mean	2 068	2 071	2 051	2 050	2 058	2 060	2 047	2 062	2 057	2 059
Sd	518	514	518	497	512	535	521	510	519	511

Figure 3

3 WaPOR Average Annual RET for the years 2009-2017 and difference between average annual RET and RET 2009.WaPOR data (2009-2017)

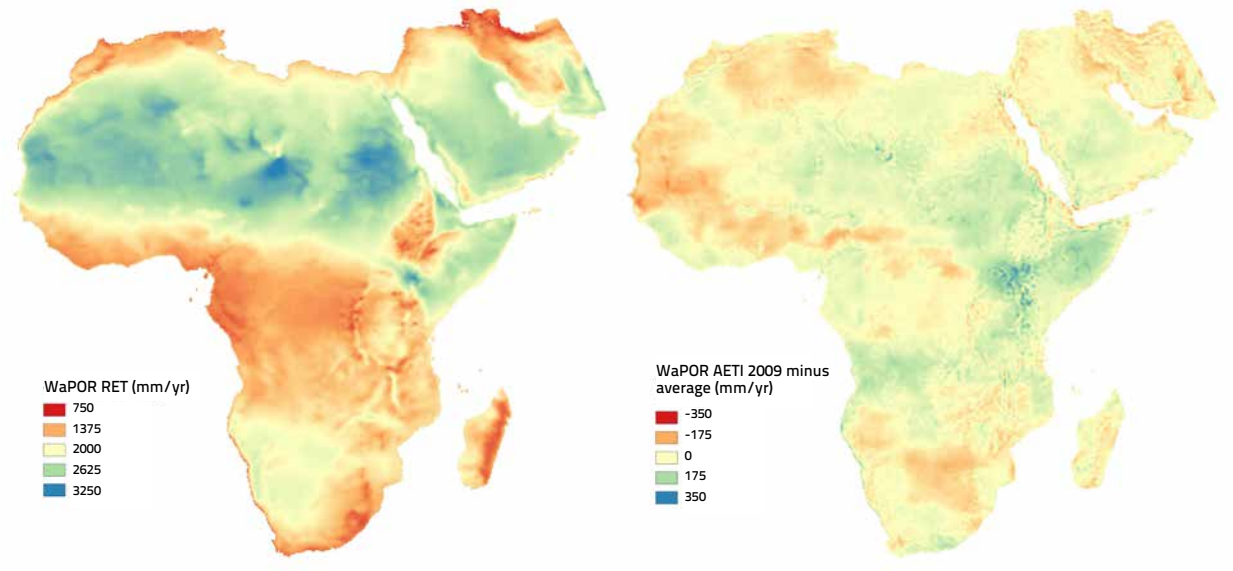

The annual WaPOR RET is very consistent and the inter-annual variability is very low because average climatic conditions hardly change. However, when comparing WaPOR RET in 2009 to the long-term average (Figure 3 right), large parts of southern Africa and West Africa show value well below average RET, while East Africa RET values are above average. This is consistent with 2009/10 being determined an El Nino year, which is often associated with drought conditions in Southern and West Africa and wet conditions in East Africa (Conway, 2009; Richard *et al.*, 2000; FAO, 2019). Even though the two periods do not overlap completely, the difference of WaPOR RET in 2009 compared to the overall average shows similar impacts as reported for El Nino events.

Comparison with other spatial data products

WaPOR RET was compared with the TerraClimate (TC) database (Abatzoglou *et al.*, 2018). TC RET is calculated by using FAO Penman Monteith using reanalysis data from the Climate Research Unit (CRU) time series data version 4.0 (Harris and Jones, 2017). TC RET values were validated using 50 FLUXNET stations, but these were mainly found in USA and Europe. The two datasets provide significantly different patterns and values (Figure 4). Especially the transition zone between the Sahel and humid tropics is underestimated by TC RET as compared to WaPOR RET. For some reason, there is a substantial disagreement for Algeria and Sudan. TC uses air temperature for the analyses, which could be the root cause for these type of differences, and this dispute could be solved by using satellite thermal measurements in future studies.

To complete the comparison, RET data directly downloadable on the GLDAS website has been consulted as well (Figure 5). The GLDAS RET values are substantially higher compared to WaPOR. This could be related to the GLDAS formulation of RET or the solar radiation that they use from atmospheric circulation models (instead of MSG). Considering the fact that these values are very high, more trust to WaPOR RET is given.

Figure 4

TerraClimate RET Comparison WaPOR RET and TerraClimate RET (average for 2009-2017)

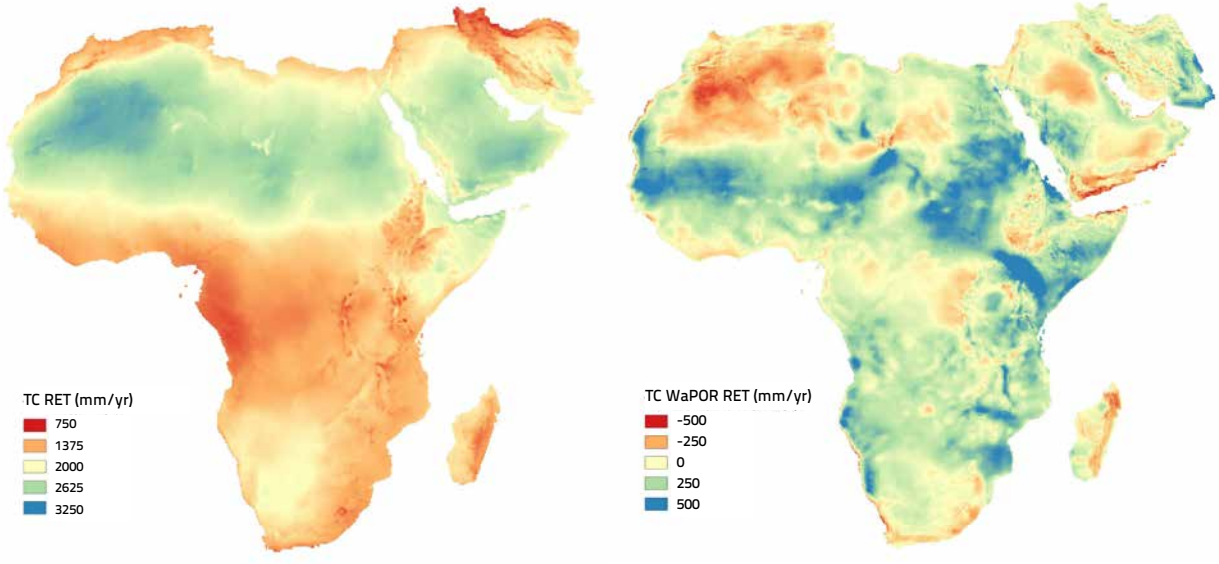

Figure 5

GLDAS RET and comparison with WaPOR RET for the year 2010

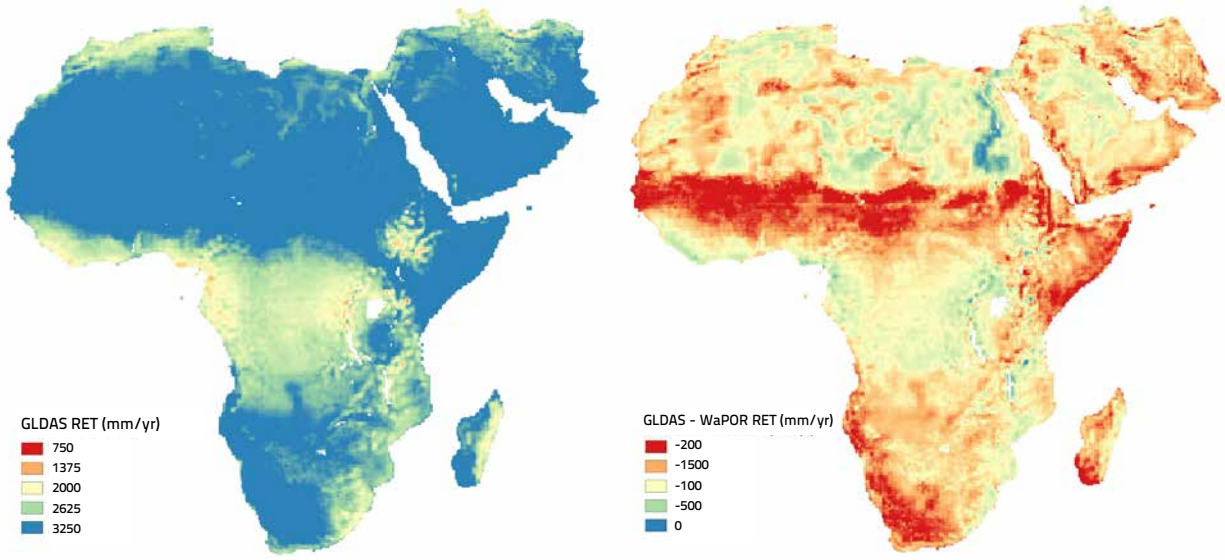

Point data comparison

Full-fledged weather stations generally measure all parameters required to calculate RET using the Penman-Monteith equation. Therefore, station RET was compared to WaPOR RET for a number of locations. Since the WaPOR RET data has a spatial resolution of 20 km following MERRA no perfect correlation with station data can be expected. The first comparison uses data from a weather station at Port Said, Egypt. Results are displayed in Figure 6. The linear regression indicates that the station data and WaPOR data have a good correlation with an R^2 of 0.94. In comparison with the 1:1 line the WaPOR RET data is consistently lower by 17 percent compared to the station data.

A second location is the Tal Amara weather station in the Bekaa Valley in Lebanon. For this station, surrounded by agricultural fields, a longer time series of data was available, but for some periods data was not recorded (e.g. radiation in early 2016) resulting in gaps (Figure 7). The WaPOR RET data follow the seasonality of the station data. The r^2 between the two datasets (2014-2016) is lower than for the Port Said station at 0.89, but is still relatively good. Tests with more weather stations should be done to improve the accuracy of the quality assessment.

B.3 Conclusions

On the continental level, variations in RET are low (varying less than 25 mm per year, 0.6%), due to similarity in climatology between consecutive years. The WaPOR RET data is able to identify the impacts of the 2009 El Nino event, with higher than average RET in Southern and Western Africa and lower RET values in East Africa. The station comparison (only two stations) gives high correlation with the WaPOR data. This suggests that MERRA is a good choice for computing RET, being an attractive solution for areas not being equipped with routine and complete weather stations.

Figure 6

RET from Egypt Port Said Station and WaPOR RET for 2014 – 2015

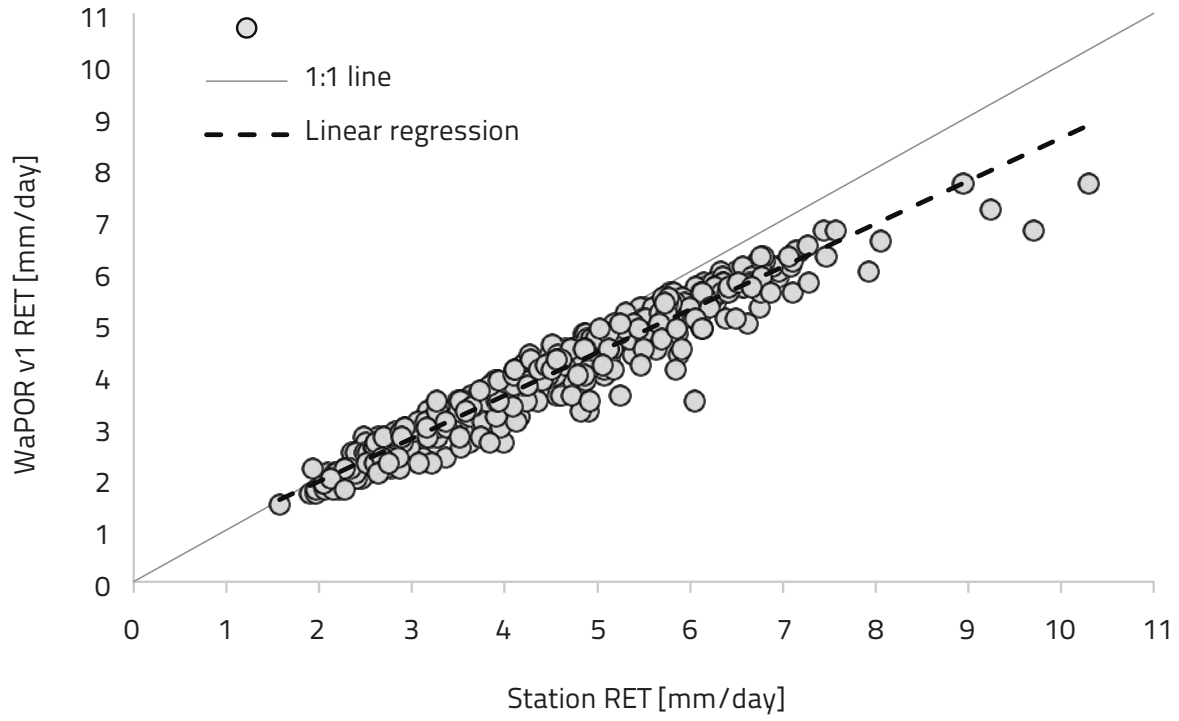

Figure 7

RET station data and WaPOR RET data for Tal Amara, Lebanon

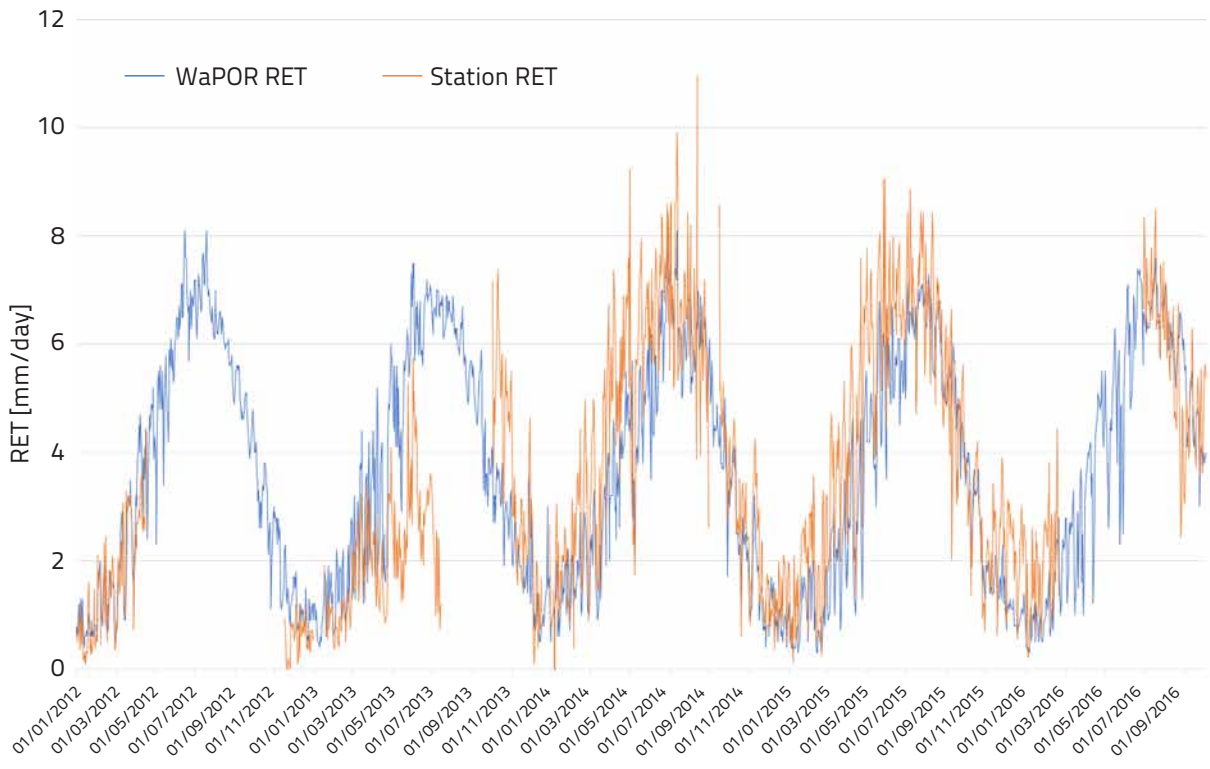

Detail of WaPOR Map "Actual EvapoTranspiration and Interception (ETIa) - 1-10 May 2019 - Central and sub Saharan Africa"

3. Water

A. Actual Evapotranspiration and Interception

A.1 Introduction

The Actual Evapotranspiration and Interception (AETI) flux is dependent on the availability of energy, the prevailing Leaf Area Index (LAI) and soil moisture. AETI is an important component in the water balance, accounting for up to 90 percent of the consumption of incoming precipitation in river basins such as the Nile system. It is of major importance for disciplines ranging from hydrology to agricultural and climate sciences (Łabędzki, 2011; Trambauer *et al.*, 2014). Scientists have struggled to measure AETI in the field and have resorted to calculating it indirectly through crop coefficients assuming conditions and crop development stages that follow certain specific standards not considering diseases nor nutrient status (Allen *et al.*, 1998). Direct measurements of AETI by for instance flux towers, surface renewal or scintillometers are scarce in Africa and only available for a few point locations (flux towers) or for small spatial extents (<5 km) for limited periods of time (scintilometer) as part of academic research (Trambauer *et al.*, 2014; Kongo *et al.*, 2011). For the AETI at field and river basin scale, it is customary to use remote sensing techniques to assess AETI because hydrological and crop growth models cannot capture the complex ecosystem and biophysical dynamics induced by humans (land use and soil moisture) and nature (diseases; fungi; salinity).

AETI is not directly measured by satellites. Instead, AETI can be determined from other terms of the surface energy balance, calculated through physical variables that can be observed from space. Therefore various types of remote sensing algorithms for the estimation of AETI have been developed. IHE Delft is making ensemble predictions of AETI using seven different standard models. In addition, there exist AETI data layers based on flux measurements, climate models and machine learning algorithms. A recent overview is provided by Pôcas *et al.* (2015) and Paca *et al.* (2019).

Various studies evaluate AETI at large scales using inter-comparison of AETI estimations derived from different types of models (Fisher *et al.*, 2017; Jiménez *et al.*, 2011; Kiptala *et al.*, 2013; Miralles *et al.*, 2016; Mu *et al.*, 2011; Schuol *et al.*, 2008; Trambauer *et al.*, 2014; Vinukollu *et al.*, 2011; Wartenburger *et al.*, 2018; Zhang *et al.*, 2016). The differences found between the models arise from inconsistencies in the use of forcing data, model conceptualization and user defined parameter estimations and in the calculation method for AETI. Thus, when comparing magnitudes and spread of AETI between the different approaches it is difficult to assess which model is more accurate than others, specifically since there is limited ground observations to validate the data.

The WaPOR AETI data estimates Transpiration (T), Evaporation (E) and Interception (I) individually and sums them up as AETI = T + E + I. WaPOR is based on the ETLook model (Bastiaanssen *et al.*, 2012; Samain *et al.*, 2012). ETLook is designed for automated processing, and is versatile as it allows for soil moisture as an input data layer. I is calculated independently using parameters for vegetation cover, leaf area index and precipitation. Most other multi-layer surface energy balance models require more input data that are either not available, or the model schematization is too simple so that the outputs are no longer reliable. The FRAME consortium has developed ETLook into an operational model.

A.2 Data analysis

WaPOR AETI shows similarities to the PCP dataset (Figure 8), the availability of water is clearly the constraining factor for AETI. Energy (RET) plays a key role in equatorial Africa with frequent cloud cover and moist atmosphere. Other areas with high AETI values are locations where water is available from surface runoff, flooding or groundwater presence for example the Inner Niger Delta in Mali, the Sudd wetland in Sudan, the Nile Delta and River in Egypt and the Okavango Delta in Botswana (Figure 8). At continental scale, average annual AETI shows little variation from 496-519 mm per year (Table 6).

Table 6
WaPOR AETI 2009-2017

	2009	2010	2011	2012	2013	2014	2015	2016	2017	Average
Min	0	0	0	0	0	0	0	0	0	0
Max	2 336	2 243	2 213	2 217	2 154	2 183	2 191	2 216	2 285	2 226
Mean	505	497	496	497	488	500	499	513	519	502
Sd	516	490	508	492	497	505	504	513	521	505

Figure 8
Average annual WaPOR AETI (2009-2017)

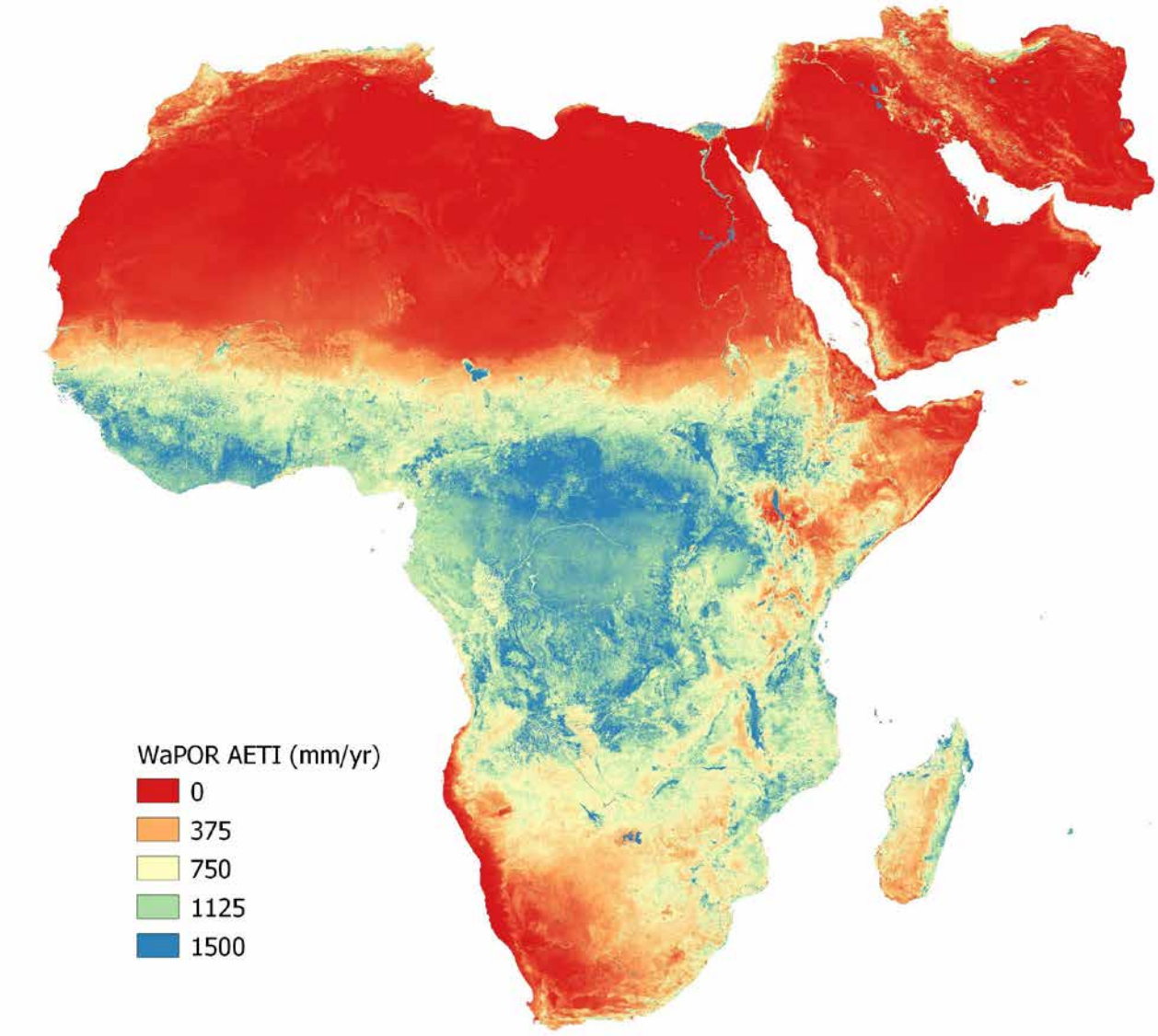

Comparison with other spatial data products

There are numerous spatially distributed AETI products available for Africa (Table 7). The products use different input data and different approaches and vary in quality and spatial resolution. The WAter Cycle Observation Multi-mission Strategy - EvapoTranspiration - WACMOS-ET (Michel *et al.*, 2016), LandFlux-EVAL (Mueller *et al.*, 2013), and Model Tree Ensemble (MTE) (Jung, 2009) should also be mentioned in this regard. The LandFlux-EVAL covers the period of 1989 to 2005, with a spatial resolution of $1^{o} \times 1^{o}$ (Mueller *et al.*, 2013)[1]. The MTE product is upscaled from the database of the FLUXNET. The MTE ran for a longer period, from 1982 until 2011, spatially distributed on a $0.5^{o} \times 0.5^{o}$ grid (Jung *et al.*, 2010)[2]. The WACMOS-ET Project has a better spatial resolution of $0.25^{o} \times 0.25^{o}$, for the period 2005 to 2007 (Michel *et al.*, 2016). The WACMOS-ET product is a combination of LandFlux-EVAL and MTE,

[1] https://data.iac.ethz.ch/landflux/

[2] https://www.bgc-jena.mpg.de/geodb/projects/Home.php

and thus expected to be superior. The development of each product has been peer reviewed, however with limited observed AETI data to validate the accuracy over Africa and the Middle East.

Table 7

Statistics of AETI products over Africa 2010

Satellite product	AETI estimation approach	Source of input data	Reference
ETMonitor	Process based model implementing processes of energy balance, plant physiology, and Soil water balance	MODIS, Microwave data	Hu and Jia, 2015
CMRSET	Based on Priestley-Taylor Equation and relation between EVI and GVMI	MODIS	Guerschman *et al.*, 2009
SEBS	Calculates the energy balance, by calculating the sensible heat flux based on local maxima and minima of surface temperature	MODIS	Su, Z. 2002
GLEAM v3.2	Based on Priestley-Taylor Equation (ETpot) multiplied by soil stress factors based on soil properties and interception is added based on CMORPH and TRMM	AMSR-E, LPRM, CMORPH, TRMM	Miralles *et al.*, 2011a and b
SSEBop v4	Combines ET fractions generated from RS LST with reference ET using a thermal index approach.	MODIS	Senay *et al.* 2014
ALEXI	Calculates the evaporative fraction based on the morning and evening overpass of MODIS. Based on this fraction the ETa is determined.	MODIS, GOES	Anderson *et al.*, 2007
MODIS16	Combines the Penman Monteith equation and the surface conductance model.	MODIS	Mu *et al.*, 2007; 2011b
LandFlux-EVAL	The LandFlux-EVAL covers the period of 1989 to 2005, with a spatial resolution of 1o × 1o (https://data.iac.ethz.ch/landflux/)	-	Mueller *et al.*, 2013
WACMOS-ET	The WACMOS-ET product is a combination of LandFlux-EVAL and MTE, and thus expected to be superior	Various	Michel *et al.*, 2016
Model Tree Ensemble	The MTE product is upscaled from the database of the FLUXNET	Various	Jung *et al.*, 2009
GLDAS	NOAH land surface models with remote sensing data assimilation	MODIS and ASCAT	Rodell *et al.*, 2004
TerraClimate	Water Balance Model outlined by Dobrowski *et al.* 2013	WorldClim version 2	Abatzoglou *et al.*, 2018
WECANN	Artificial Neural Network	MODIS	Alemohammad *et al.*, 2017

Table 8 shows the general statistical values of 11 remote sensing AETI products and Figure 9 shows the annual AETI for WaPOR and ten similar databases for the year 2010. All products have similar spatial variabilities, identifying the arid regions (Sahel and Middle East) and the majority can pick up high AETI values in the Nile Delta and the irrigated agriculture along the Nile River. The average AETI of ten non-WaPOR product is 442 mm/yr with a minimum of 323 mm/yr (GLEAM) and a maximum of 570 mm/yr (CMRSET). The WaPOR estimate is 497 mm/yr, and this is a rather average value, being 12 percent different from the average value.

Table 8

Statistics of AETI products over Africa 2010

	WaPOR	ETMonitor	CMRSET	SEBS	GLEAM	SSEBop	ALEXI	MODIS16	MTE	GLDAS	WECANN
Min	0	0	0	0	0	0	0	0	0	0	0
Max	2 243	2 414	2 567	1 730	1 953	2 808	2 010	1 828	1 407	1 689	1 177
Mean	497	402	570	376	323	497	519	402	418	468	434
Sd	490	423	466	396	1425	498	492	279	407	415	359

Figure 9

Comparison of the spatial distribution of AETI for 2010 from different products

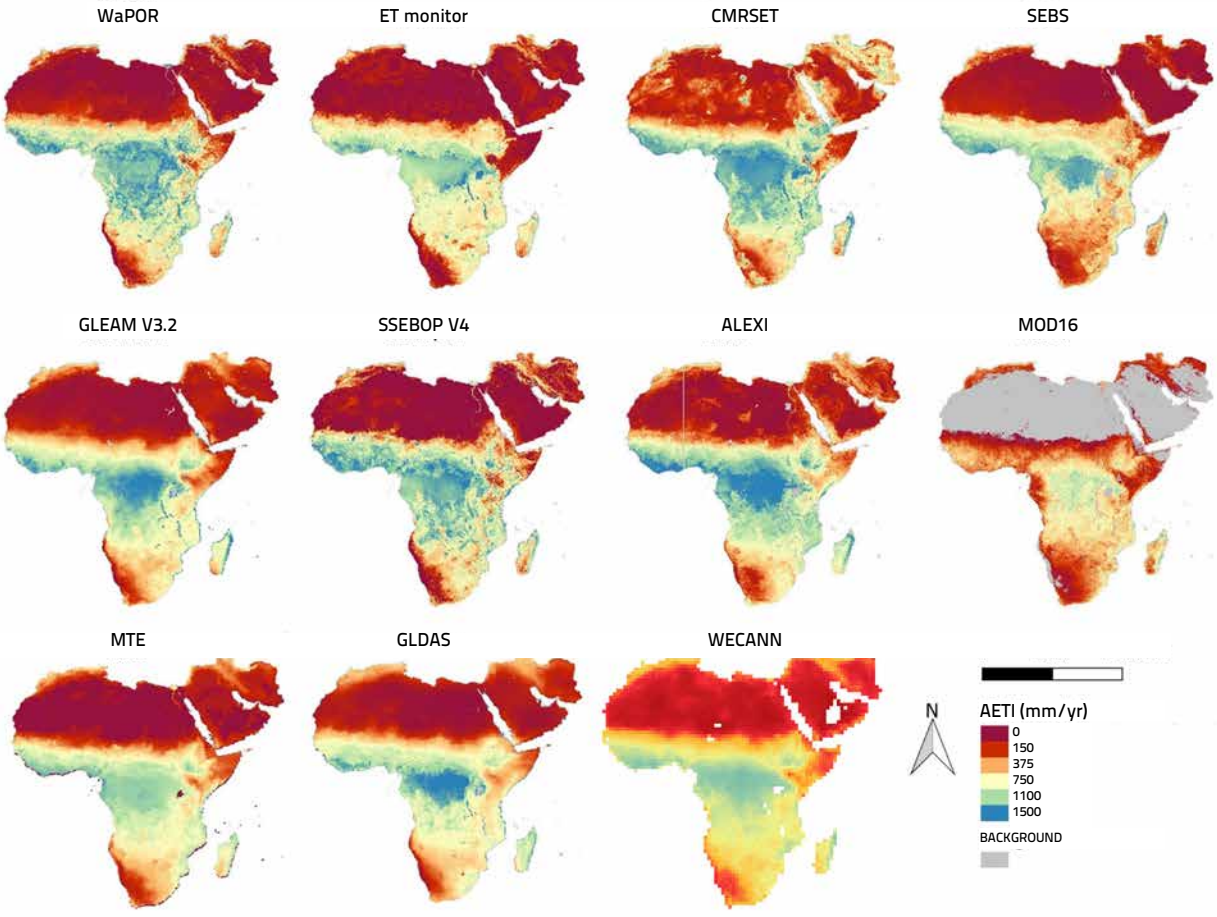

Comparing the AETI products, the following observations can be made. The spatial resolution of GLEAM, WECANN, MTE and GLDAS is too low to pick up detailed spatial variations, such as the irrigated areas around the Nile River. The MODIS16 product compared to the other products generally underestimates AETI, and does not provide data for the arid regions. From the other six products, the main differences occur in the central part of the African continent. ETmonitor and SEBS underestimate AETI in central Africa compared to the other four products. This area has a high percentage of cloud cover, which affects also the WaPOR AETI data. ETmonitor combines optical and microwave sensors and as such being capable of calculating AETI during cloudy periods. Similarly, CMRSET and ALEXI seem to overestimate AETI in the arid areas, with some unrealistic values observed in Libya and Chad. The spatial distribution of AETI in WaPOR and SSEBop are remarkably similar. This can be attributed to the fact that both algorithms are based on the surface energy balance principles and make use of an internal calibration of hot and cold edges.

It can be concluded that the WaPOR AETI data does not contain obvious flaws such as it is witnessed for some of the other AETI databases. At continental level WaPOR AETI provides data that is at par with the other high quality products. It also provides it at very high spatial and temporal resolution.

Comparison of AETI product based on water balance model (TerraClimate)

The WaPOR AETI was compared with the TerraClimate AETI product (Figure 10). This product is derived using the water balance approach (Abatzoglou *et al.*, 2018). The overall trend between the two products is very similar; the major differences are found in irrigated areas, such as the Nile Delta, and in the Sudd Wetland in Sudan. TerraClimate AETI is not able to pick up the increase in AETI due to irrigation and flooding in those areas, which WaPOR does.

Figure 10
TerraClimate AETI product compared to WaPOR AETI

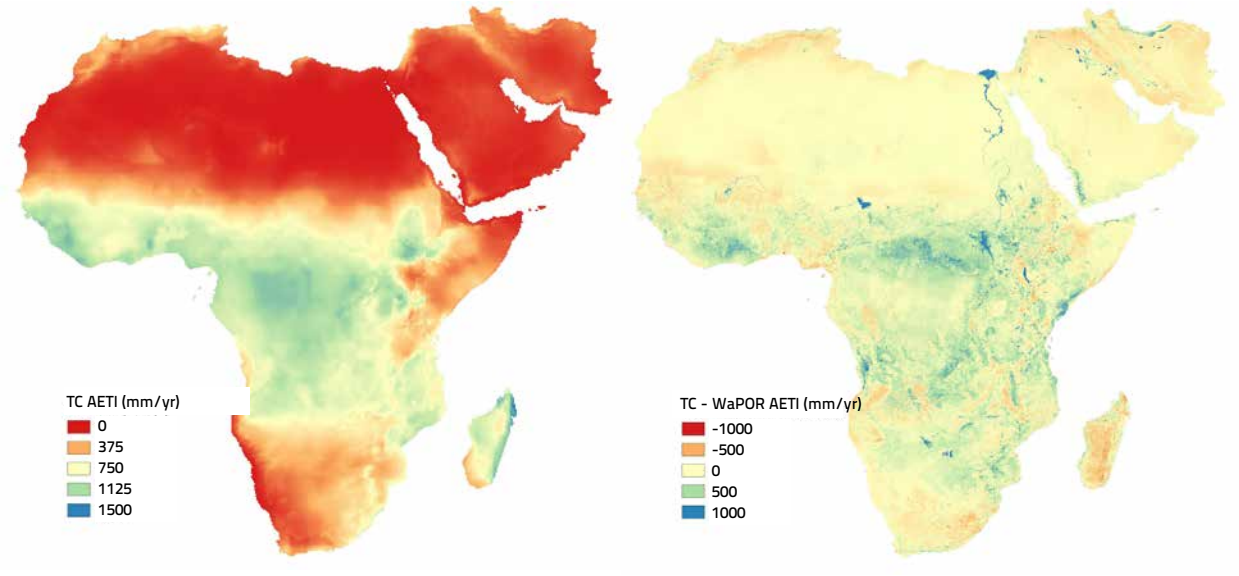

Comparison using continental scale water balance

The WaPOR AETI was evaluated at river basin level using the classical water balance approach (WB). The long term WB assumes a negligible change in storage, and therefore the total inflow (PCP) should be equal to the total outflow (AETI and discharge (Q)) and therefore AETI should be equal to PCP minus Q (equation 1):

$$AETI = PCP - Q \qquad \text{eq 1}$$

The information on Q and PCP was obtained from external datasets. WB AETI was compared to WaPOR AETI. For the comparison in Figure 11, the observed Q was obtained from the Global Runoff Data Centre (GRDC)[3] (see Annex A for locations of the data points) and for PCP we used the EWEMBI reanalysis PCP data (Dee *et al.*, 2011). Figure 11 shows the value of AETI inferred from the WB for three key river basins in Africa (Congo, Niger and Nile basin), as well as for two sub-basins in the Nile basin (inset of Figure 11). The Nile basin covers an area of 3.17 M km^2, which represents some 10 percent of the African continent. With 6 825 km, the Nile is the longest river in the world. It has two main tributaries: (i) the White Nile originating from the Equatorial plateau of East Africa and (ii) the Blue Nile, with its sources in the Ethiopian highlands. WB AETI for Congo, Niger and Nile are 1 206, 607 and 667 mm/yr respectively. The corresponding WaPOR AETI estimates are 1 266 mm/yr (5.0% difference), 591 mm/yr (2.6% difference) and 668 mm/yr (0.0% difference) which is very encouraging.

Figure 11

GRDC stations in Africa and the spatially averaged AETI determined from the water balance of the Congo, Niger and Nile basins

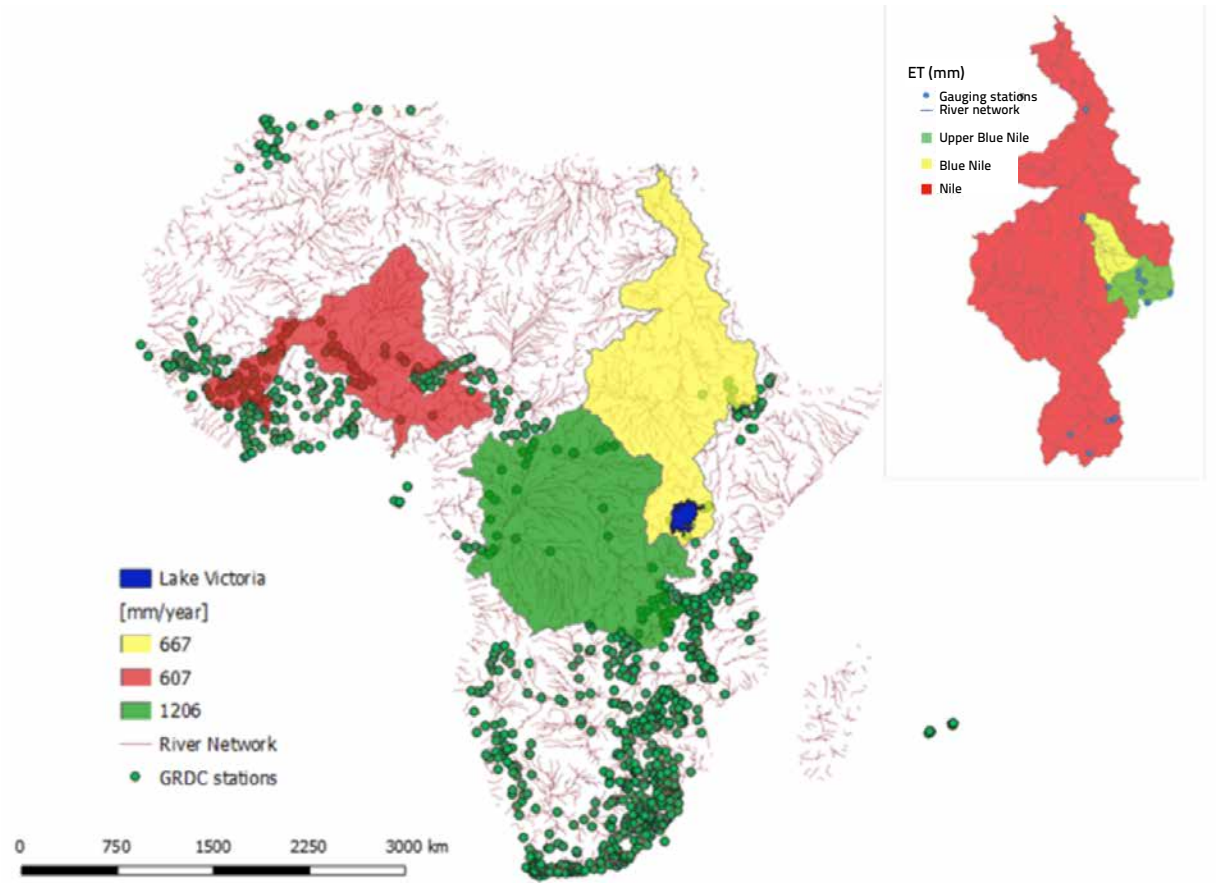

Source: GRDC

[3] The Global Runoff Data Centre, 56068 Koblenz, Germany

A similar WB approach has been executed for an additional 28 basins in Africa (Figure 12). The average absolute difference between the two datasets is 14 percent (ranging between 0 and 58%); combining all river basins the difference is 0.2 percent (the over- and underestimation for individual basins is evened out at the continental level). The largest difference occurs in smaller river basins. It can be noticed that WaPOR AETI is systematically under-estimated in the in semi-arid climate zones such as Groot, Olifants and Orange. These South African basins are all containing sparse vegetation areas, likely the cause factor for low basin-wide AETI values. Considering that the method did not consider longer-term water storage changes in the water balance analysis, the difference of 14 percent is remarkably good.

Five other AETI data layers have been consulted for a comparative analysis in the same 28 river basins (with varying periods of available data) (Table 9). While WaPOR AETI was 846 mm/yr, PCP-Q for the same basins was 847 mm/yr. This is a very good agreement and shows congruency of WaPOR AETI with basin scale water balances. Next to WaPOR, SSEBop provided a good match with 811 mm/yr. WaPOR and WECANN (Alemohammad *et al.*, 2017) have the highest correlation, but on overall, WaPOR AETI performs best.

Figure 12

Comparison of WaPOR and WB AETI for 28 selected river basins covering the period 2009 to 2017

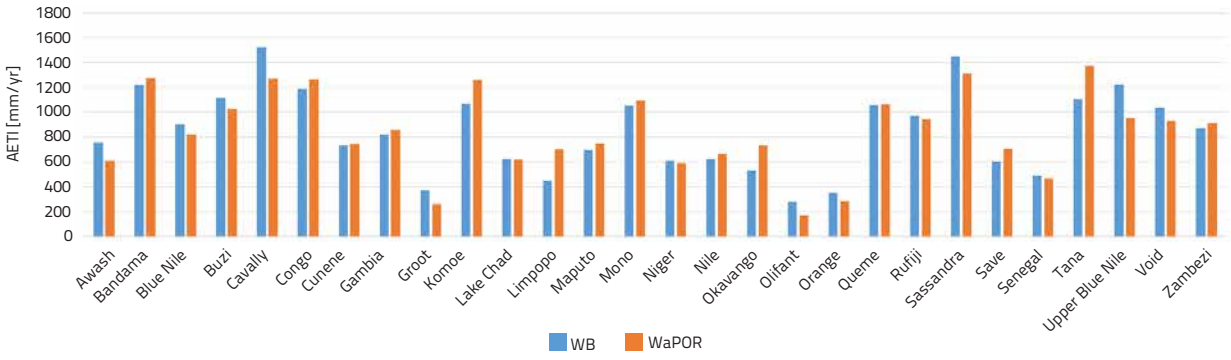

Table 9

Comparison of various AETI products for the 28 river basins specified in Figure 12 (See Annex B for details per basin)

	PCP-Q (observed)*	WaPOR (2009-2017)	GLEAM (1980-2013)	MOD16 (2000-2014)	SSEBop (2003-2017)	WECANN (2007-2015)	MTE (1983-2012)
Average [mm/yr]	847.21	845.64	550.39	676.75	810.54	697.71	694.18
Average [mm/yr]	787.45	822.3	550.10	575.90	760.99	636.77	661.23
Correlation		0.92	0.89	0.90	0.89	0.92	0.89
Difference [mm/yr]		34.83	237.34	211.55	26.45	150.67	126.22

* Different time periods

Comparison with SWAT+ for Africa

A hydrological SWAT+ model was set up for Africa to compare the WaPOR AETI layers with AETI outputs from the SWAT+ model. SWAT+ has been widely used to support water resources and agricultural management at river basin scale (Arnold *et al.*, 1998). A detailed description of the model setup is provided in Annex A. The comparison of WaPOR and SWAT+ AETI shows areas where SWAT+ AETI is significantly lower than WaPOR AETI (green areas in Figure 13). These areas correspond with irrigation areas and wetlands (e.g. Lake Chad and Inner Niger Delta in arid zones), which are not implemented in SWAT+ and which are known to have high evapotranspiration. Global irrigation maps also indicate these areas as irrigation areas. For that reason, we conclude that the values of WaPOR are more realistic than SWAT outputs.

Figure 13

Long-term annual average AETI estimates by (left) WaPOR (2009-2017) and (right) SWAT+ (2010-2016) and difference between WaPOR and SWAT+ AETI for Africa (below)

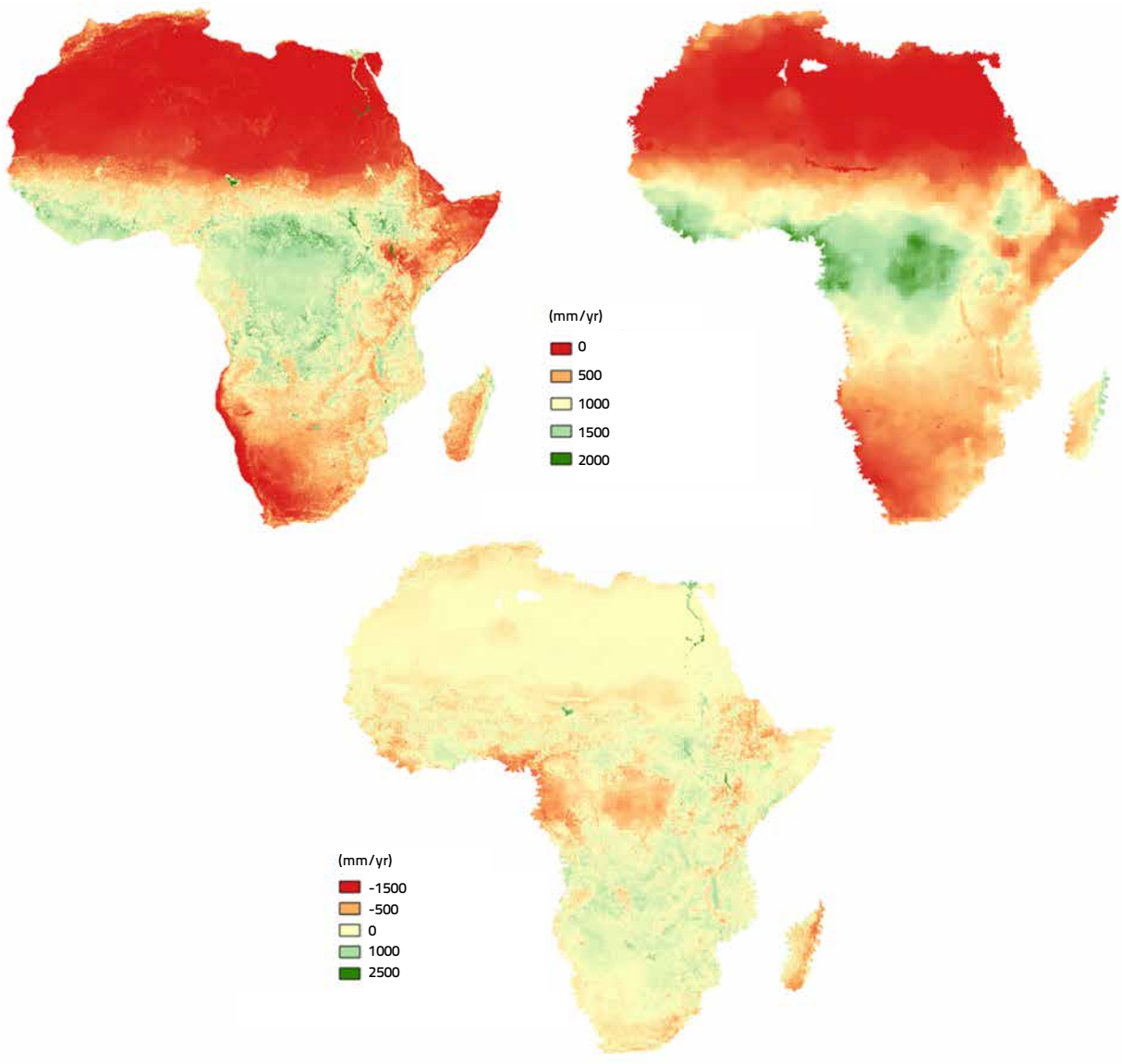

In some areas, we see that the SWAT+ AETI is significantly higher compared to WaPOR AETI (in red in Figure 13). These areas are predominantly located in forested areas (Annex A) where high evaporation can be expected. One of these areas is located in the Congo basin. We compared WaPOR and SWAT+ AETI with a mass balance analysis (PCP-Q) for the three major basins in Africa and a selected number of sub-basins (Table 10). The results suggest that the WaPOR AETI results are more realistic. It is however advised to further explore and evaluate the WaPOR AETI results of forested areas.

As a general conclusion, the comparison of SWAT+ and WaPOR leads to a confirmation of the WaPOR results. In most areas, the difference between the two methods is small and within the range of uncertainties of both methods. At locations with large differences, the WaPOR results seem to be more realistic. This confirms the advantage of using indirect earth observations of the AETI process.

Basin comparison – Litani River Basin

The Litani River Basin is located in Lebanon and covers an area of 2 170 km^2. The basin is the focus of a Water Accounting study using WaPOR data inputs (Tran *et al.*, 2019). This section validates the overall water balance using WaPOR data. Table 11 has been compiled to evaluate WaPOR PCP and AETI data for the entire basin. The average WaPOR PCP-AETI value is 624 - 436 being 188 mm/yr, or 408 Mm^3/yr.

The Litani River Authority (LRA) provided outflow data at the Qasmiye (Sea Mouth) gauging station to support the analysis of this project. During the wet year 2012, the total outflow was 360 Mm^3/yr, but the flow into the sea reduced to 60 Mm^3/yr during 2014, a dry year. The 5-year average outflow between 2011 and 2015 is 193 Mm^3/yr. For an area of 2 170 km^2, this represents a water yield of 89 mm/yr. This is equivalent to 14 percent of the gross rainfall.

Table 10

Comparison of AETI estimates using PCP-Q, WAPOR and SWAT+ for basins in Africa

	PCP-Q		WAPOR		SWAT+	
Basin Name	AETI [mm/yr]	Period	AETI [mm/yr]	Period	AETI [mm/yr]	Period
Nile	667	1912-1984	668	2009-2017	578	2010-2016
Blue Nile	937	1960-1982	822		911	
Upper Blue Nile	1 135	1980-1982 1999-2002	955		1 114	
Niger	607	1970-2006	591		630	
Congo	1 206	1903-2010	1 266		1 276	
Lake Victoria	1 091	1950-2005	1 035		976	
Lake Victoria (lake surface)	1 539*	1993-2014	1 138		893	

* based on study by Vanderkelen *et al.*, 2018

Table 11

Comparison of annual P and ET values for the entire Litani Basin based on the original WaPOR data.

Year	PCP (mm/yr)	PCP (Mm^3/yr)	AETI (mm/yr)	AETI (Mm^3/yr)	PCP - AETI (mm/yr)	PCP – AETI (Mm^3/yr)
2009	746	1 619	484	1 050	262	569
2010	638	1 384	496	1 076	142	308
2011	633	1 374	439	953	194	421
2012	816	1 772	441	957	375	815
2013	741	1 608	491	1 066	250	542
2014	456	990	361	784	95	206
2015	530	1 150	424	921	106	229
2016	594	1 290	399	865	196	425
2017	461	1 000	387	839	74	161
Average	**624**	**1 354**	**436**	**946**	**188**	**408**

Next to the river discharge into the ocean, the Litani Basin also has a significant interbasin transfers. The main interbasin transfer is the water drawn from Qaraoun Lake after hydropower production at the Abd el Al station. Through Markaba and Awali tunnels water is delivered to the urban settlements of Beirut and irrigated land outside the watershed of the Litani. The discharge capacity of the tunnels is 22 m^3/s[4]. However, the actual discharge in this tunnel varies greatly between years (Figure 14), with an average discharge of 200 Mm^3/yr from 2012-2016. Litani water is also transferred into the Hasbani River, that lies in southern Lebanon and flows to Israel. There is also water conveyed to Marjayoun, which is in the middle of the basin boundaries. The Qasimiya and Ras Al Ain irrigation project, which is one of the most important irrigation projects in Lebanon, draws water from the river before the basin outlet at sea mouth with discharge capacity of approximately 5 m^3/s. The water is conveyed to villages in Sidon and Maachouk, both are outside of the basin[5]. Since monthly discharge by these several inter-basin water allocation projects are not reported, it is infeasible to quantify the total inter-basin transfer on a monthly basis.

The uncertainty in inter-basin transfer makes it difficult to estimate actual water availability. In the Litani Basin, the long-term water storage trend should be considered in the analyses. This information was obtained from the GRACE satellite, which shows a negative trend in storage (JS) (Figure 15). The trend of water storage for a single GRACE pixel that covers central Lebanon from 2009 to 2016 is -21mm/yr, which is translated into -43.5 Mm^3/yr in the Litani Basin.

4 The Litani River Authority - Power Stations and Tunnels (http://www.litani.gov.lb/en/?page_id=95)

5 The Litani River Authority - Qasimiya and Ras Al Ain Irrigation Project (http://www.litani.gov.lb/en/?page_id=117)

Figure 14

Discharge in Markaba tunnel after hydropower turbines at Abd el Al station

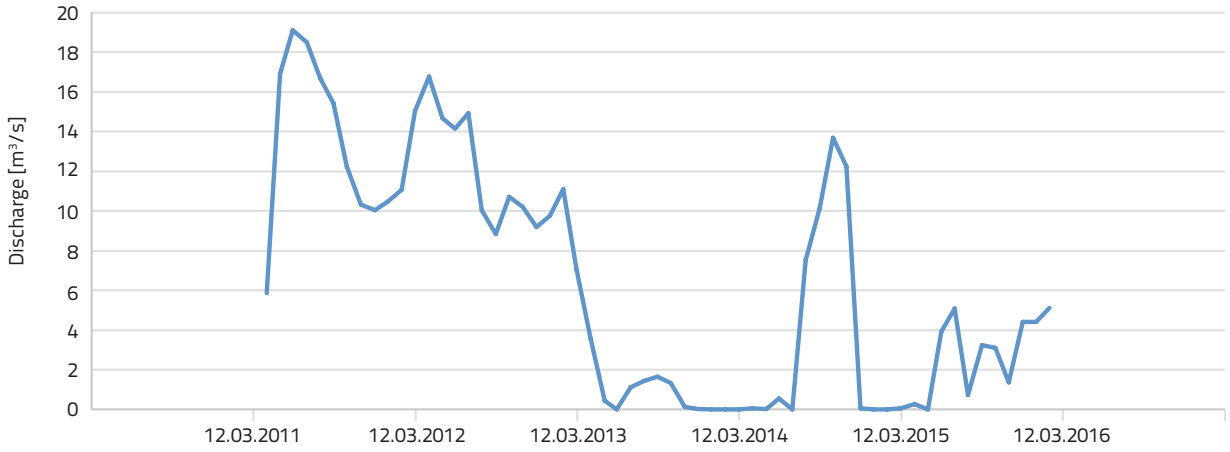

The uncertainty in inter-basin transfer makes it difficult to estimate actual water availability. Nevertheless, total discharge measured at the sea mouth outlet and Markaba tunnel is approximately equal to PCP – AETI - JS for the year 2012 and 2013 (Figure 16; Table 12), which means that the total WaPOR AETI for the basin covering heterogeneous land use is reasonable.

Figure 15

Longer-term trend of declining water storage in Lebanon based on GRACE gravity measurements

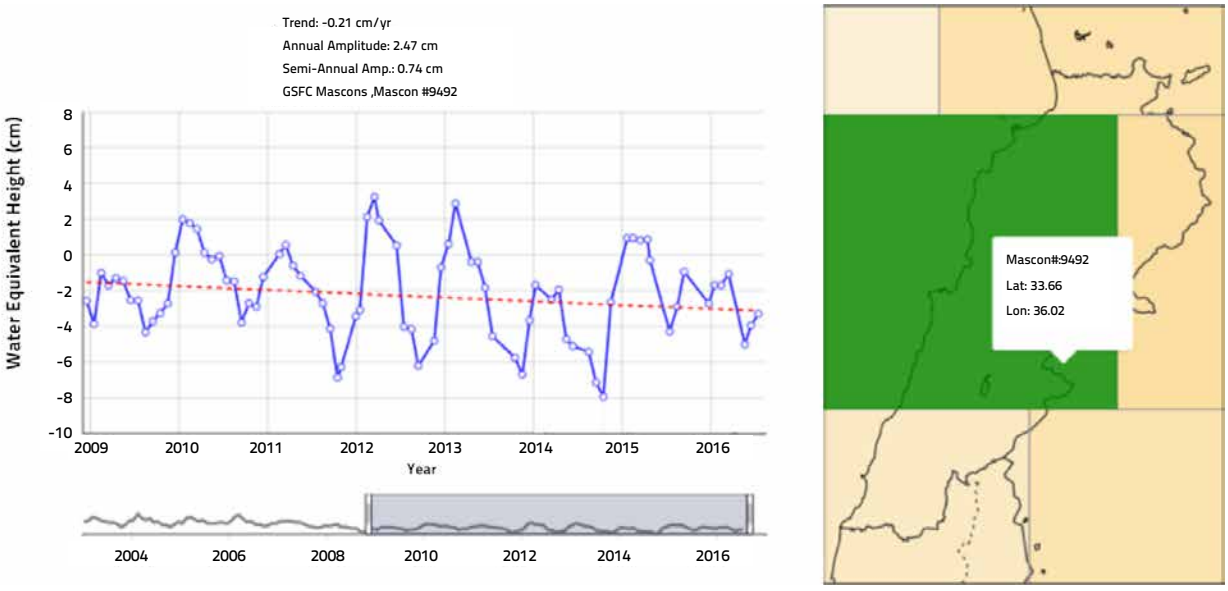

Source: https://ccar.colorado.edu/grace/gsfc.html

Figure 16

Total discharge from Litani outlet at sea mouth and Markaba tunnel compared with PCP – AETI – ΔS, based on remote sensing data

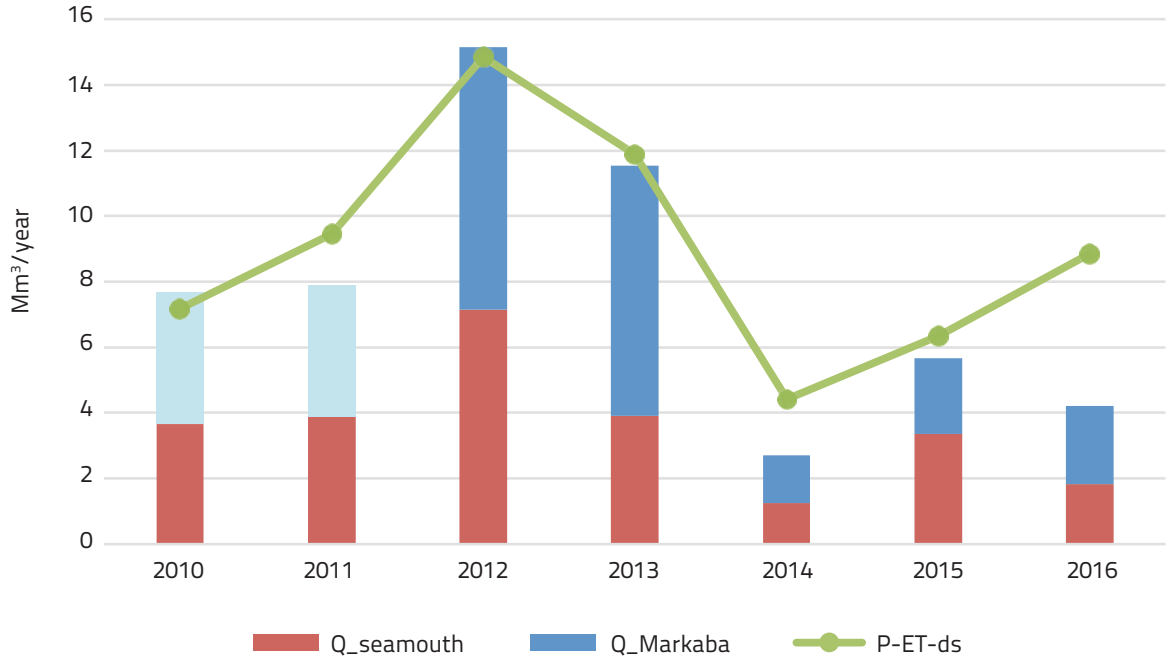

Table 12

Average annual water balance components of the Litani River Basin using WaPOR data inputs

Year	$Q_{seamouth}$	$Q_{Markaba}$	PCP	ΔS	PCP-ΔS-Q	WaPOR AETI
2010	183.0	200	1,319	-65	1,001	1,026
2011	194.3	200	1,310	-72	988	908
2012	357.2	400	1,689	35	897	912
2013	196.1	381	1,533	-77	1,033	1,016
2014	62.6	73	943	-25	832	747
2015	167.9	116	1,096	-99	911	878
2016	91.2	120	1,229	-38	1,056	825
Average	**178.9**	**213**	**1,303**	**-49**	**960**	**902**

Sub-basin comparison – Nile Basin

The AETI in the Nile basin has been estimated by various authors using various methods (NBI, 2014; Belete *et al.*, 2018; Bastiaanssen *et al.*, 2014; Hilhorst *et al.*, 2011; Senay *et al.*, 2009; Jung *et al.*, 2017). The WaPOR AETI values (entire basin, Blue Nile and Upper Blue Nile) were compared to the estimates of the other studies and compared to the Water Balance using observed data (Table 13).

Even-though the AETI estimates refer to different time periods, the WaPOR AETI values (688 mm/yr) are similar to the WB AETI values (667 mm/yr). Bastiaanssen *et al.* (2014) used a calibrated version of the SSEBop model and concluded that the total AETI was 633 mm/yr for the period 2005 to 2010. Karimi *et al.* (2012) for a single year (2017) estimated the basin-wide AETI to be 622 mm/yr. Senay *et al.* (2014) estimated the average AETI to be 702 mm/yr and the volume 2 056*10^9 m^3/yr. The WaPOR AETI estimates of 668 mm/yr are within the expected range (545 to 700 mm/yr; average 638 mm/yr). Considering that WaPOR AETI is within 5 percent of the other estimates, it is believed that the AETI volume for the Nile Basin by WaPOR is highly accurate. This is in agreement with the other finding of the Congo, Niger, Litani and the 28 basins presented in Figure 12.

A more detailed breakdown comparison of the Nile System could be achieved from comparison against the FAO Nile study (Hilhorst *et al.*, 2011). The program for the hydrology and water resources management of the Nile Basin ran between 2004 and 2009. The main project objective was to contribute to the establishment of a common knowledge base at the Nile Basin level. The AETI under FAO Nile was computed by a combined approach of water balance (rainfall, discharge) and crop water requirements. There are thus no direct measurements of AETI, yet this will be considered as "ground truth". For the climatic inputs of this study, the average observation period between 1960 to 1990 has been used in FAO Nile.

Table 13

Comparison of AETI estimates using the water balance, WaPOR and past studies in the Nile Basin

Basin Name	WaPOR		Water Balance (WB)		Other Studies			
	AETI [mm/yr]	Period	AETI [mm/yr]	Period	Model	AETI [mm/yr]	Period	reference
Nile	668	2009-2017	667	1912-1984	Improved MOD16 algorithm	545	2000-2012	Nile Basin Initiative, 2014
					InVEST	700	1950-2000	Belete *et al.* 2018
					Nile-DST	628	1960-1990	Hilhorst *et al.* 2011
					Adjusted SSEBop	633	2005-2010	Bastiaanssen *et al.* 2014
					ETLook	622	2017	Karimi *et al.*, 2014
					SSEBop	702	2000-2012	Senay *et al.* 2014
Blue Nile	822		937	1960-1982	Adjusted SSEBop	737	2005-2010	Bastiaanssen *et al.* 2014
					Nile-DST	863	1960-1990	Hilhorst *et al.* 2011
Upper Blue Nile	955		1 135	1980-1982 1999-2002	VegET	500	2001-2007	Senay *et al.*, 2009
					Noah3.3-M2	909	2007-2010	Jung *et al.* 2017
					CLSMF2-M2	1 010		
					ALEXI	979		
					GLEAM	675		

Table 21 of the FAO Nile synthesis report describes the (i) AETI over land, (ii) AETI over open water and the (iii) AETI over wetlands. The total AETI is also provided and used for the validation of WaPOR. The FAO-Nile team has defined 11 sub-basins of the Nile. Since we did not have access to digital boundaries, the shape file provided by the Nile Basin Initiative has been used instead. The sub-basins between FAO Nile and NBI are not matching exactly as can be observed from the area statistics presented in Table 14. FAO Nile covers a total area of 3.17 million km² while NBI adds up to 3.24 million km². For these reasons, the AETI data was compared per unit of land instead of considering a bulk volume.

Figure 17
Geographical location of the sub-basins according to NBI

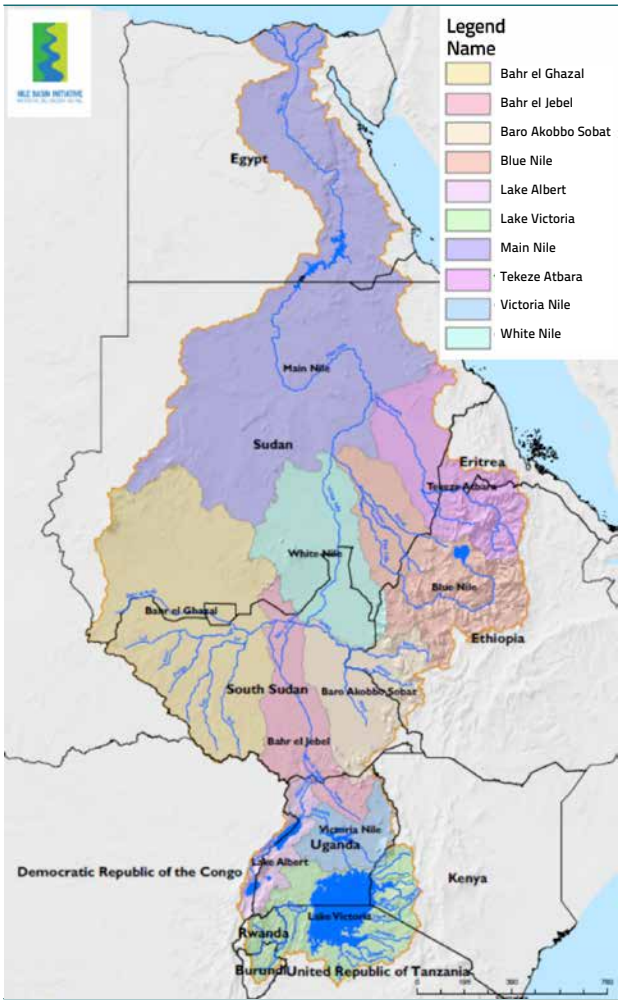

Source: Nile Basin Initiative - http://www.nilebasin.org/

The total annual AETI for the Nile according to FAO Nile – here considered as ground truth – is 1 991*10^9 m^3/yr (i.e. 628 mm/yr). WaPOR AETI shows 2 052*10^9 m^3 for a 2.2 percent larger area. The difference in volumetric AETI of 61 10^{9}m^3/yr is 3 percent, hence after correction for area the two values are remarkably similar.

The correlation coefficient for all the sub-basins is with R^2 of 0.93 very encouraging. The lower AETI rates of the lower Nile in Northern Sudan and Egypt is very accurate. More deviations arise in the tropical sub-basins of the Baro – Akobo – Sobat and Lake Victoria, which is most likely related to cloud cover as a disturbing factor on the determination of the land surface evapotranspiration. Overestimations and under-estimations are in perfect balance (Figure 18), which can also be related to the inaccuracy of the "ground truth" and ascribed to different study periods. This shows that the total WaPOR AETI for large sub-basins of typically 300 000 km² with rather diverging climates and land use is accurate.

Table 14

AETI statistics per sub-basin according to FAO-Nile and WaPOR

	FAO Nile			WaPOR		
	Area	AETI		Area	AETI	
	(km^2)	(mm/yr)	($10^9 m^3$/yr)	(km^2)	(mm/yr)	($10^9 m^3$/yr)
Main Nile d/s Atbara	877 866	124	109	986 111	120	119
Atbara	237 044	397	94	232 321	416	97
Main Nile d/s Khartoum	34 523	211	7	35 458	179	6
Blue Nile	308 198	863	266	308 474	792	244
White Nile	260 943	554	145	238 349	575	137
Bahr el Ghazal & el Arab	606 428	749	454	720 012	885	637
Pibor-Akabo-Sobat	246 779	907	224	231 352	1 147	265
Bahr el Jebel	136 400	1 196	163	80 789	1 196	97
Kyoga-Albert	197 253	1 124	222	157 541	1 250	197
Lake Victoria basin	264 985	1 160	307	250 549	1 013	254
Total	**3 170 419**	**628**	**1 991**	**3 240 957**	**633**	**2 052**

*slight difference in area is a result of the delineation of the sub-basins

Figure 18

Relationship between the longer-term total FAO-Nile and WaPOR AETI per sub-basin of the Nile

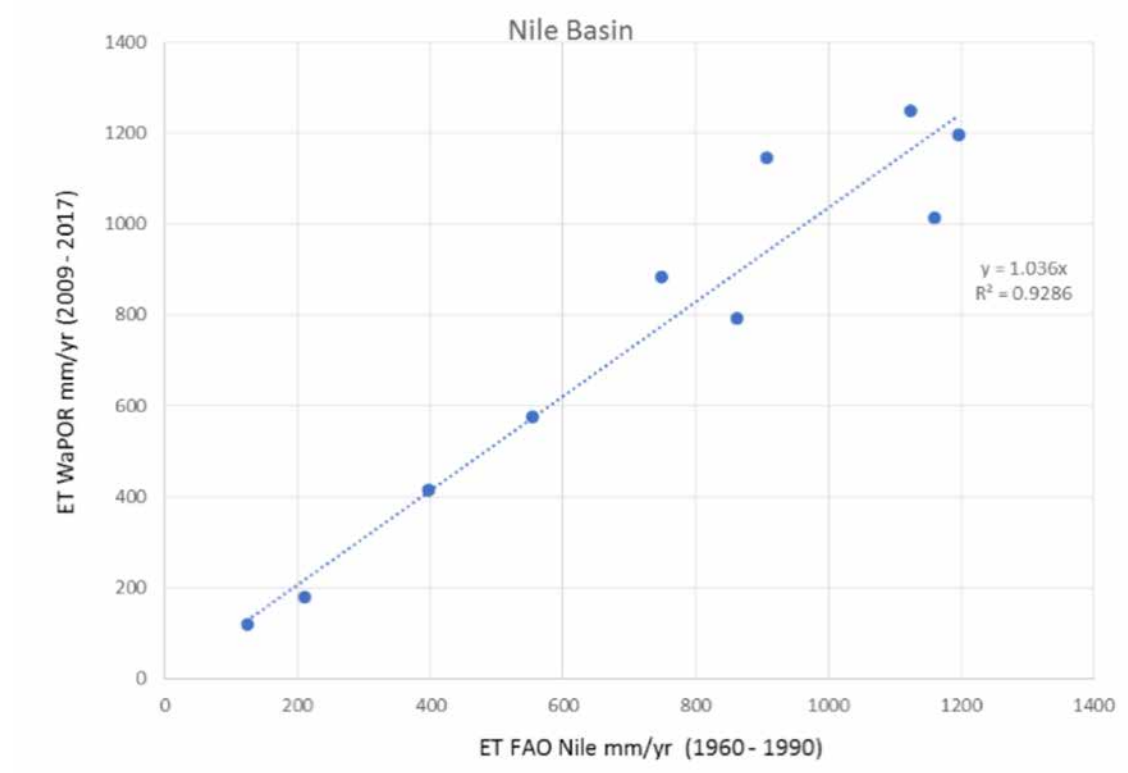

Sub-basin comparison - Fayoum Depression

The Fayoum Depression in Egypt has a well established water balance due to its depression character and irrigation supply through one single main canal, and was therefore explored for validation purposes. Following Salvadore *et al.* (2019) - who summarized the water balance from various sources- the water balance for the gross area including Lake Qarun reads as:

AETI = PCP + Q - q
With
PCP = 20 Mm^3/yr
Irrigation supply Q = 2 900 Mm^3/yr
Return flow q = 250 Mm^3/yr

Over a year, the change in storage was assumed zero and the recharge to groundwater assumed negligible (Salvadore, 2019). The resulting AETI from the total oasis then becomes 2 670 Mm^3/yr, equivalent to 882 mm/yr (Table 15). This is much lower than the potential AETI of 1 420 mm/yr as suggested by Ramadan *et al.* (1989). The irrigation supply of 2 900 Mm^3/yr per unit of land is 1 827 mm/yr being equivalent to a planned irrigation efficiency of 78 percent to meet the crop water requirements (1,420/1,827 x 100%). It is likely that AETI is lower than 1 420 mm/yr because salinity persists and crops in Fayoum are not expected to evaporate at their potential rate. Wolters *et al.* (1989) approximated the AETI to be 1 100 mm/yr, and this seems more realistic than the 882 mm/yr found for WaPOR.

For the irrigated area of 158 734 ha displayed in Figure 19, the total AETI from WaPOR is 1 400 Mm^3/yr. Ramadan *et al.* (1989) estimated the total crop water consumption to be 1 460 Mm^3/yr, being very close to WaPOR AETI. We believe however, that different areas are considered, which could explain the fact that the volumetric AETI values are similar, and the water depths are not. The irrigation efficiency becomes 48 percent (1.4/2.9 x 100%), which seems low for a classical flood irrigation scheme with reuse of drainage water. Even though WaPOR AETI estimates are about 20 percent lower than expected, other remote sensing products show even lower estimates for AETI (Table 15). Salvadore (2019) created an ETensemble product using ETMonitor and SSEBop with a bias correction factor to be able to create an AETI product which resembles the actual situation.

Table 15

Annual AETI (mm/yr) of the land use class irrigated land in Fayoum Depression

	2009	2010	2011	2012	2013	2014	2015	2016	2017	Average
WaPOR	802	877	759	846	850	941	965	941	961	882
ALEXI	726	735	748	742	751	742	759			743
CMRSET	604	663	640	636						636
ETMonitor	423	430	458	435	466					441
MODIS	312	285	334	306	331	333				317
SSEBop	822	802	876	844	883	837	888	855	861	852
SEBS	194	216	149	198	187	159	191	147		180
ETensemble*	1 110	1 099	1 155	1 122						1 122

* Ensemble created using ETMonitor and SSEBop by Salvadore (2019)

Figure 19

Location of the Fayoum Depression in Egypt. The polygons indicate irrigated areas

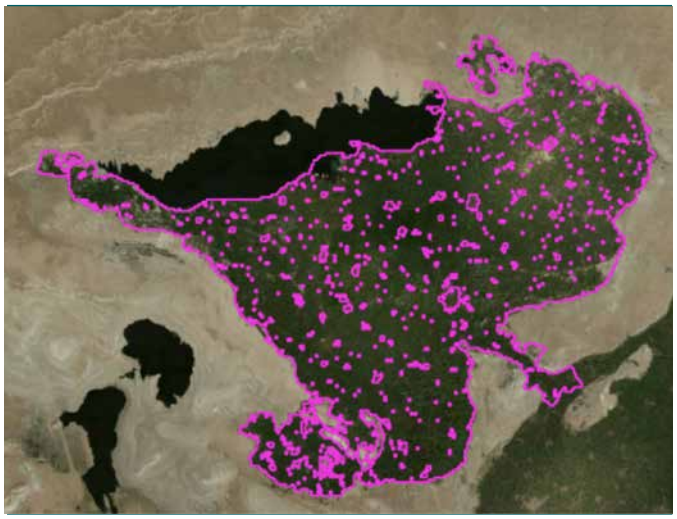

Field scale flux measurements

Observed AETI data in Africa is very limited, as flux towers are very expensive. Eddy covariance flux data is often considered the "gold" standard for the estimation of AETI, however, even these measurements can have up to 15-20 percent error. The eddy covariance data is compared with WaPOR data using the pixel available at the coordinates of the flux tower. The assumption is that the point data measured by the flux tower captures the average value of the grid cell (Marshall *et al.*, 2013). This assumption is more likely when the station lies within homogeneous and flat terrain. If this is not the case, eddy covariance may vary significantly and may not be representative for the grid cell value (Baldocchi *et al.*, 1988).

We obtained data from seven stations. The FLUXNET database [6] provided data for three stations in Africa, in Ghana, Senegal and South Africa. The three sites have distinctive differences in land use. The site in Ghana is located in the Ankasa national park, which is located in a primary tropical forest (Chiti *et al.*, 2010; Marchesini *et al.*, 2011; Valentini *et al.*, 2016). The site in Senegal is located in Dahra, a village at the verge of the Sahel (Tagesson *et al.*, 2015; doi: 10.18140/FLX/1440188). The third site is located in the Kruger national park (Skukuza), with shrubs and other low vegetation (Archibald *et al.*, 2009; doi: 10.18140/FLX/1440246). In addition, we got access to flux data from three stations in South Africa over irrigated crops from the Universities of KwaZulu Natal (grapes and sugarcane) and one station in Egypt from the University of Tsukuba (various crops typically found in Egypt).

A 250 m (WaPOR Level 1) or 100 m (WaPOR Level 2 – only available for Ghana and Egypt) footprint is in fact too large for properly representing the footprint of flux towers because most contribution on the measured atmospheric water vapor originates nearer to the location of the flux tower (this within a single pixel). The pixel value is in that case always a systematic underestimation, and this aspect needs to be considered in the analysis followed hereafter. The data is provided at daily time steps, whilst the WaPOR AETI data is available at decadal (10 days) time steps. For this reason, the eddy covariance data is first averaged per decadal and then compared with the WaPOR AETI time series.

The WaPOR AETI decadal data is plotted against the FLUXNET data in Figure 20 (time series comparison are found in Annex C). For each station there are periods where the station AETI values are not consistent with observed trends, and these periods were removed from the analyses (Annex C). Only one of the stations show good correlation between the station data and WaPOR data (Senegal WaPOR Level 1 – r^2 equals 0.7), for the other stations r^2 ranges between 0.1 and -1.1. The bias for the flux station in Senegal and South Africa are -3 percent and 4 percent, respectively. For the station in Ghana, WaPOR AETI is systematically overestimated by 21 percent and 67 percent for Level 1 and Level 2 respectively. Even though there is a large scatter between the flux tower and WaPOR AETI data (Figure 20), the WaPOR AETI data is within the same ballpark as the flux tower data. There is an exception for the flux tower in Ghana, compared with both the Level 1 and Level 2 data.

[6] https://fluxnet.fluxdata.org/

Figure 20
Comparison Fluxnet tower and WaPOR AETI

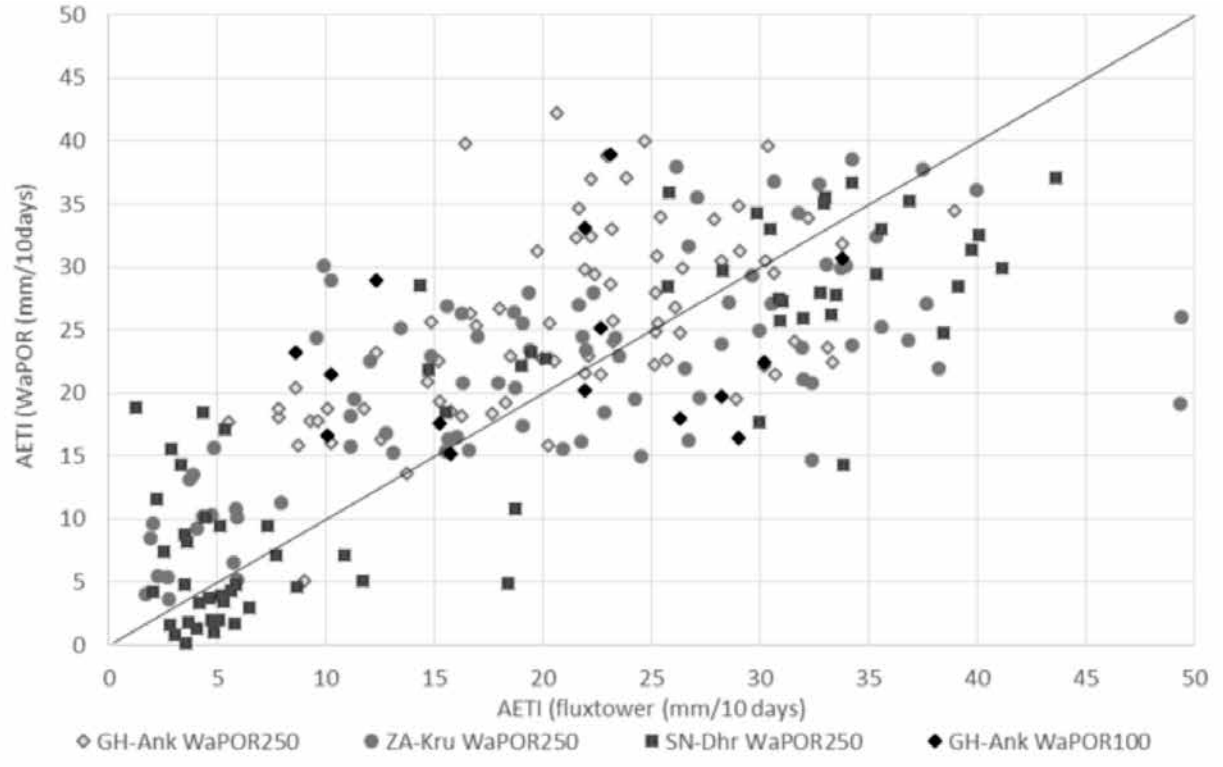

Three other eddy covariance datasets were made available by the University of Kwazulu Natal. The three flux towers are located in agricultural areas: one in sugarcane and the other two in vineyards. Results of the comparison are shown in Figure 21. The dataset of Komati (sugarcane) is for 2011 – 2012; for Vergelegen and Kapel (vineyard) it is 2013 – 2016. The dataset of Komati is a Surface Renewal system as described in Bastidas-Obando *et al.* (2017). The dataset of Kapel and Vergelegen are based on one-sensor eddy covariance systems.

Figure 21 shows that for the sugar cane (Komati) dataset the WaPOR AETI layer compares reasonably well with the flux tower results. Despite a good correlation, the WaPOR AETI estimates are higher than AETI values of the flux tower by 23 percent. The comparison for vineyard data (Vergelegen and Kapel) indicates essential differences. The values from WaPOR AETI are significantly lower than those found at the flux tower. Results show that the AETI ranges from 0 to 2 mm/day, whereas the observations range from 0 to 5 mm/day with an overall bias of 60 percent.

In addition to cropland, the University of KwaZulu Natal installed a flux tower in the natural grasslands at Cathedral Peak in South Africa. The station data shows good correlation with the WaPOR AETI data for pastures (Figure 22). The largest outliers also have the highest number of missing days and potential error in the observations. During this period, WaPOR AETI estimates are lower compared to the flux tower observations (Figure 22). Excluding this period, the overall correlation between the WaPOR and observed AETI data is 0.66 with a bias of -33 percent, The general trend of WaPOR AETI for pastures is very similar to the flux tower observations, however there is a significant underestimation of the WaPOR AETI.

Figure 21

Comparison flux tower and WaPOR AETI in South Africa

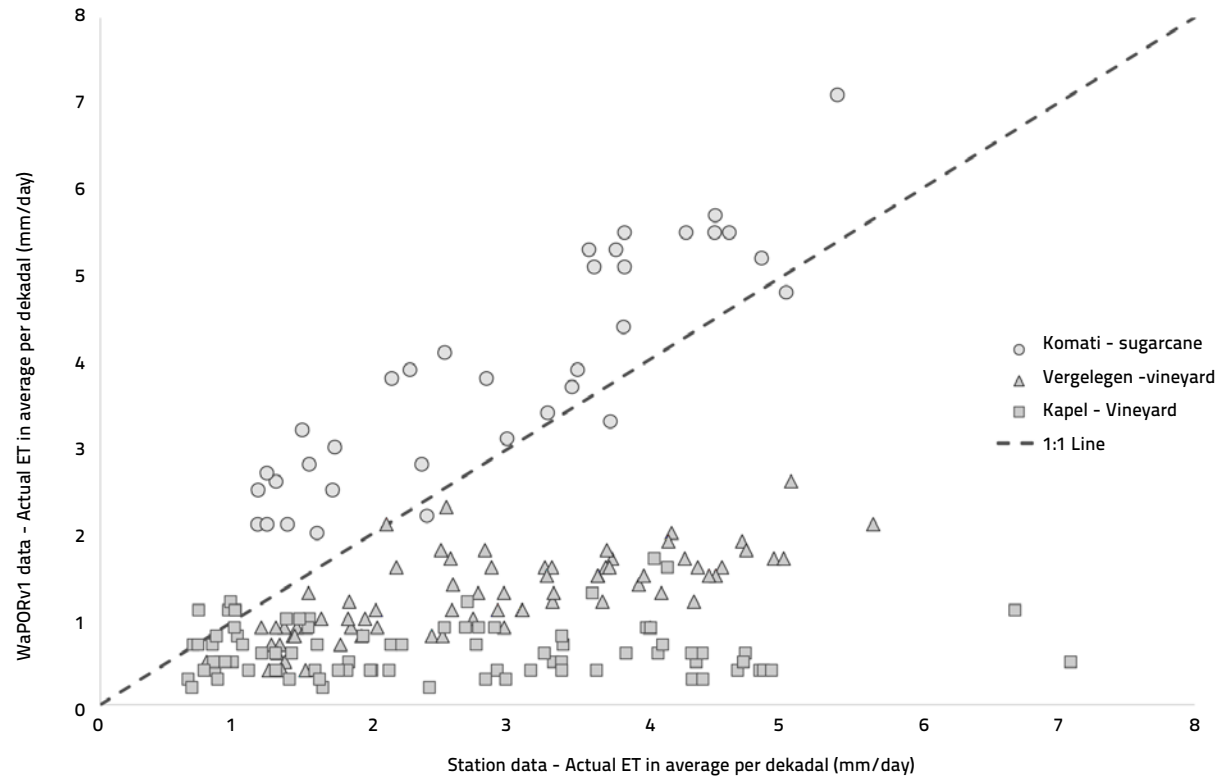

Figure 22

Comparison flux tower AETI data and WaPOR AETI at Cathedral Peak, South Africa

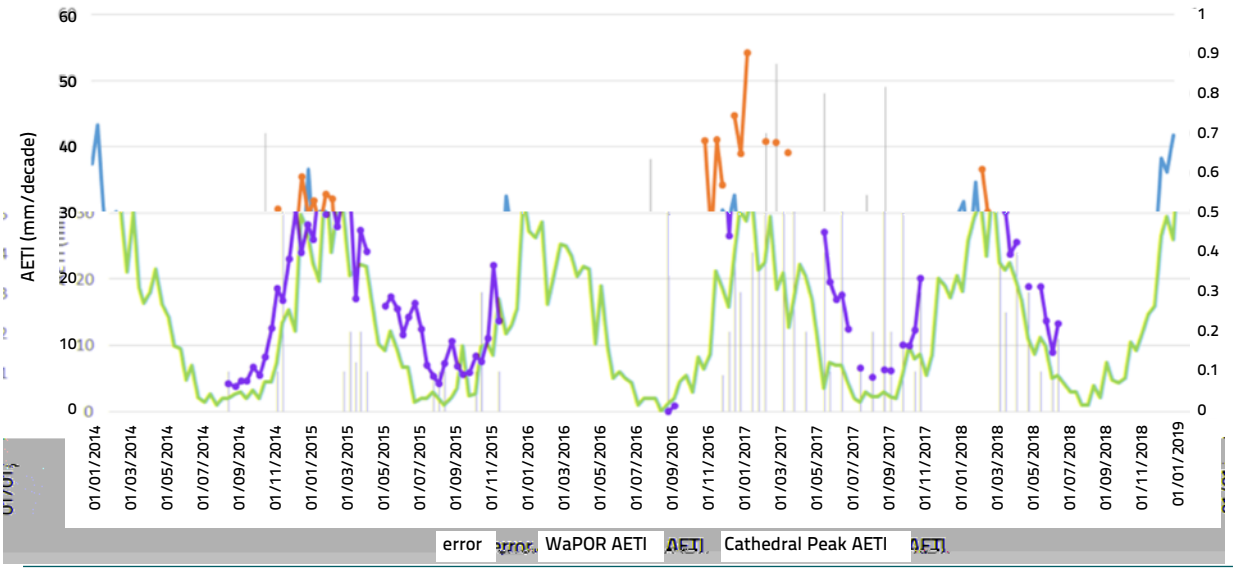

Although not presented here, a similar comparison with ten-day interval eddy covariance measurements was conducted for an unpublished flux dataset from Morocco, revealing an R^2 of 0.58 and bias of +12 percent between WaPOR AETI and flux tower AETI, using the surface energy balance residual closure method. Using the direct latent heat flux measurements, R^2 increased to 0.70 with a bias of 19 percent.

The comparisons between the observed flux tower data and WaPOR shows two different trends, a number of stations show very good correlation or small bias despite the challenges between the pixel size and footprint of the flux tower (e.g. Senegal, Skukuza, Komati and Cathedral Peak, South Africa). On the other hand, a number of stations do not show good correlation or large biases. There are a number of possible reasons related to the spatial uniformity of the land use. For example, sugarcane plantations have a more spatial uniform AETI behavior, which eliminates the disturbing role of footprints in the validation exercise. However, the Level 2 data for Ghana did not improve the correlation between the two datasets; in this case errors in the observed data could be an issue, and Twine *et al.* (2000) indicated that AETI can be underestimated from 10 up to 30 percent. The comparative analyses to point observations show that vineyards cannot be validated, but that sugarcane, grasslands and shrubs lay all within the range of 0 to 30 percent uncertainty.

The University of Tsukuba (Japan) has installed various eddy covariance system in the Nile Delta of Egypt to measure the complete energy balance under actual growing conditions of irrigated fields (Sugita *et al.*, 2017). While they have measured the energy balance under both traditionally irrigation methods and water savings using different schedules and drip irrigation, this section of the report only deals with the flux measurements conducted in the traditional irrigation treatments. The in situ fluxes were measured in the period 2010 to 2014, and we used the values reported in Sugita *et al.* (2017) for comparison with the WaPOR AETI. Maize and rice are the summer crops and fava beans and wheat the winter crops. Three different sites were installed with eddy covariance sensors, and these sites are referred to as Sakha-A, Sakha-B and Zankalon. The Sakha-B site was used mainly for adjusted irrigation schedules, so the analysis in this section mainly deals with Sakha-A. The annual AETI values measured vary between 875 to 1 225 mm/yr, with an average value of 972 mm/yr (see Table 16). Matching WaPOR pixels have been identified and a 3x3 window was selected for excluding the effect of geometrically inaccuracy. WaPOR suggest the average value for Sakha-A in the period 2010 to 2014 to be 1 000 mm/yr. For Sakha-B the average value is 1 011 mm/yr and for Zankalon 1,295 mm/yr (Table 16). The ten-day data is presented in Figure 23. El-Quosy and El-Guindy (1989) reported a typical AETI range of 1 056 to 1 275 mm/yr, depending on the climatic zone in the Nile Delta and the associated cropping pattern in each of their four climate zones. The AETI of a single crop varies between 370 mm (wheat) to 880 mm (cotton), so the actual cropping pattern determines the total AETI of a certain pixel or group of pixels. This short synopsis reveals that the annual AETI totals of WaPOR are very close to the field measurements. The ten day WaPOR AETI values are compared to the in situ flux measurements for crop development stages (Sugita *et al.*, 2017) and are presented in Figure 23. The peak flux measurements during summer are exceeding the WaPOR AETI estimates; the WaPOR AETI values do not exceed 5.5 mm/d during ten-day periods, while the in situ measurements suggest this can be as high as 6.5 mm/d for periods of ten days and longer (Sugita *et al.*, 2017).

Table 16

Comparison of annual WaPOR and measured AETI on traditionally irrigated crops in the Nile Delta

Location	Crop rotation	Irrigation	Measured AETI (mm/yr)	WaPOR AETI (mm/yr)
Sakha-A	Maize & Fava beans	Flood	875	1 000
Sakha-B	Rice & Wheat	Basin	1 225	1 011
Zankalon	Rice & Berseem	Basin	816	1 295
Average			**972**	**1 102**

Figure 23

Temporal variability of flux measurements and WaPOR AETI for the flux site Sakha-A

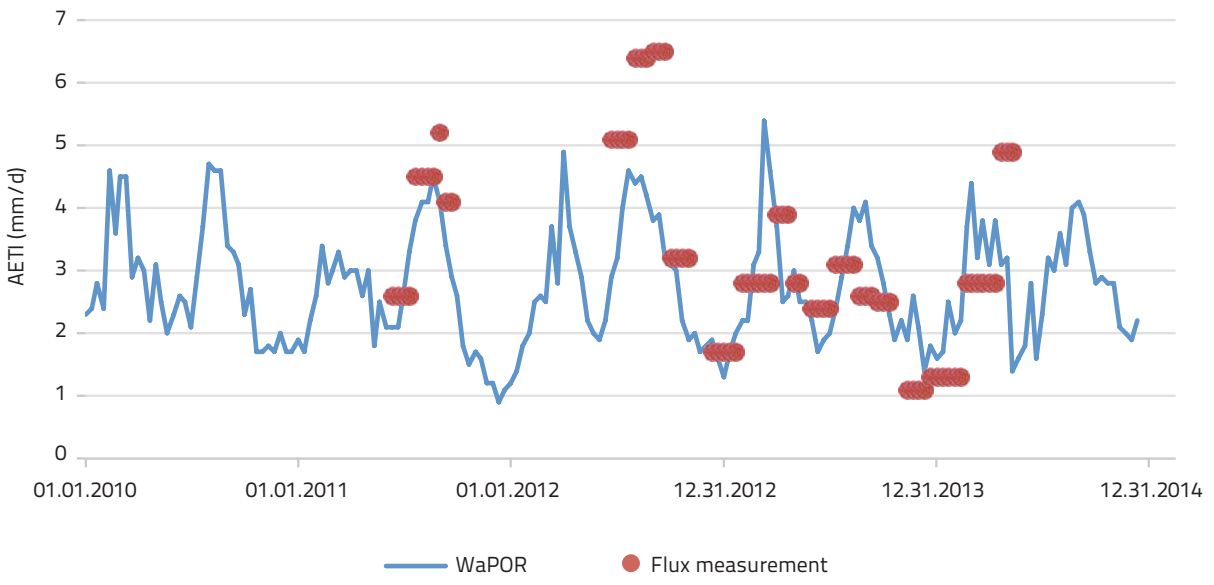

A further breakdown of the annual AETI values is to evaluate the AETI fluxes per type of crop and per growing season (see Table 17). Flooded maize in Sakha-A should typically evaporate 680-720 mm/season (Sugita *et al.*, 2017), whereas WaPOR AETI estimates 327-360 mm/season, typically 50 percent lower. The evaporation of the winter crops (wheat and berseem) in Sakha-A is 511-608 mm/season, whereas WaPOR AETI values lay in the range of 391-487 mm/season, 9-26 percent lower. For Zankalon, the agreement for winter crops is much better with less than 3 percent deviation (AETI measured is 446-549 mm/season and WaPOR AETI is approximately 448-561 mm/season). The interim conclusion is that AETI of WaPOR during winter period is reasonable but that during the summer it is significantly underestimated. Interestingly, at annual timescales, WaPOR AETI values are higher than the observed AETI (1 102 mm/yr compared to 972 mm/yr), this difference originates from the fallow periods. This is a point of attention, WaPOR AETI underestimates crop AETI (which is mainly T), and overestimates fallow land AETI (which is mainly E).

Field soil water balance measurements

The University of Oxford is conducting a special program in Jordan, Israel and Palestine on Water and Food Security in the Middle East[7]. As part of this program, field measurements and farm interviews on different irrigated crops in the Jordan Valley took place. Various field sites in Jordan and Israel were covered. Different vegetables are included in the analysis, namely onions, bananas, berhis, citrus, madjoul, lemons, grapefruits and oranges. Additional information can be found in Gilmont *et al.* (2018). Because of the wide variability in irrigation water supply gathered from the field campaigns, we used average values for the nine different fields in Jordan and ten fields in Israel.

In the field sites in Jordan, the average PCP is 389 mm/yr and the irrigation supply (Irr) based on interviews and measurements is 957 mm/yr (Table 18). The average WaPOR AETI is 728 mm/yr. The rest term of the soil water balance represents the total runoff and drainage (assuming storage changes over the year is small). This yields in a

[7] http://wanainstitute.org/en/publication/decoupling-national-water-needs-national-water-supplies-insights-and-potential-countries

Table 17

Seasonal measured and WaPOR AETI fluxes

Site	Irr	Crop	Season				AETI (mm/season)	
				Start	End	Duration	Observed*	WaPOR
Sakha-A	Flood	Maize	Summer	20-06-2010	01-10-2010	103	680	360
Sakha-A	Flood	Maize	Summer	14-06-2011	17-09-2011	95	632	335
Sakha-A	Flood	Maize	Summer	01-07-2013	10-10-2013	102	720	327
Sakha-A	Basin	Wheat	Winter	25-11-2011	08-05-2012	164	511	391
Sakha-A	Basin	Wheat	Winter	11-12-2012	13-05-2013	153	608	446
Sakha-A	Flood	Sugarbeet	Winter	07-11-2013	09-05-2014	182	538	487
Zankalon	Basin	Berseem	Winter	26-10-2011	25-05-2012	211	549	561
Zankalon	Flood	Fava beans	Winter	08-11-2012	18-04-2013	177	446	448

* Sugita *et al.*, 2017

large total runoff of 618 mm/yr. When assuming that 70 percent of PCP is available for AETI (runoff coefficient of 30%), the average AETI from irrigation ($AETI_{irr}$) becomes 455 mm/yr, resulting in an on-farm irrigation efficiency (I_{eff}) of 48 percent (455/957 x 100%). In reality, runoff is lower and efficiency higher. Because the calibration of the Fayoum Depression indicated a bias correction of 1.2, the data was analyzed again with 1.2 x WaPOR AETI. The result is a revised estimate of $AETI_{irr\_1.2}$ being 473 mm/yr and an associated $I_{eff\_1.2}$ of 83 percent (Table 18). This seems to be realistic values for micro-irrigation in Jordan. Hence, a bias correction of 1.2 on WaPOR AETI is required for irrigated areas in Jordan.

For Israel, the amounts of applied water were acquired mainly from interviews and carefully verified in the field. Lemons, grapefruit and oranges are included in the dataset. PCP is with 283 mm/yr lower than for Jordan, and the irrigation supplies are higher 1 115 mm/yr. WaPOR AETI is with 549 mm/yr and derived irrigation efficiency of 32 percent unrealistically low and not in agreement with the significant water supplies of 1 115 mm/yr, and in the presence of micro-irrigation (Table 19). Because a bias factor of 1.2 was insufficient, a correction factor 1.6 was used. The runoff and drainage reduces then from 849 mm/yr to 520 mm/yr and the efficiency doubles from 32 to 63 percent. This is still a relatively low irrigation efficiency.

For both analyses (Jordan and Israel), the WaPOR AETI required a bias correction to obtain realistic results for the field soil water balance analyses. This bias correction is meant for relatively small corrections, and not as calibration coefficient. It must be noted that other components of the field soil water balance (PCP, Irr and runoff) are estimated and not measured. There is also a discrepancy between the small-scale agricultural features of the Jordan Valley and the spectral resolution of 100 m and 250 m pixels, this may be fixed if the

Table 18

Components of the field scale soil water balance in irrigated vegetables in the Jordan Valley (in mm/yr); the Jordan component

Country	Crop	PCP	Irr	WaPOR AETI	Runoff	AETIpcp	$AETI_{irr}$	Ieff	$AETI_{irr\_1.2}$	$I_{eff\_1.2}$
Jordan	Onion	400	567	937	30	280	657	116	844	149
Jordan	Banana	400	856	909	347	280	629	74	811	95
Jordan	Banana	400	1 433	683	1 150	280	403	28	540	38
Jordan	Berhi	400	821	559	662	280	279	34	391	48
Jordan	Citrus	350	881	780	451	245	535	61	691	78
Jordan	Citrus	350	409	586	173	245	341	83	458	112
Jordan	Berhi	400	2 022	686	1 736	280	406	20	543	27
Jordan	Madjoul	400	374	734	40	280	454	121	601	161
Jordan	Madjoul	400	1 248	674	974	280	394	32	529	42
Average		**389**	**957**	**728**	**618**	**272**	**455**	**48**	**601**	**83**

Source: Gilmont *et al.*, 2019

Table 19

Components of the field scale soil water balance in irrigated vegetables in the Jordan Valley (in mm/yr); the Israel component

Country	Crop	PCP	Irr	WaPOR AETI	Runoff	$AETI_{irr}$	Ieff	$AETI_{irr\_1.6}$	$I_{eff\_1.6}$
Israel	Onion	300	700	468	532	258	37	539	77
Israel	Lemon	350	1 100	496	954	251	23	549	50
Israel	Majool	215	1 600	650	1 165	500	31	890	56
Israel	Barhi	215	1 400	740	875	590	42	1 034	74
Israel	Banana	350	1 200	589	961	344	29	697	58
Israel	Grapefruit	250	1 000	500	750	325	33	625	63
Israel	Orange	250	1 000	505	745	330	33	633	63
Israel	Madjoul	300	1 200	516	984	306	26	616	51
Israel	Barhi	300	1 200	448	1 052	238	20	507	42
Israel	Onion	300	750	578	472	368	49	715	95
Average		**283**	**1 115**	**549**	**849**	**351**	**32**	**680**	**63**

Source: Gilmont *et al.*, 2019

WaPOR Level 3 (30 m resolution) is available in the area. We also believe that the high aridity may play an additional role in underestimating WaPOR AETI.

A.3 Conclusion

Compared to similar remote sensing databases, the WaPOR AETI database is among the ones with the most realistic signatures at larger scale and for time-integrated values. The comparison with the water balance of 28 river basins is encouraging, and these findings were consistent with the basin analysis of the Congo, Niger and Nile system. The results of the Litani Basin shows proper concurrency with the measured outflows to the Mediterranean Sea and interbasin transfers. More uncertainty arises for smaller areas such as Fayoum Depression and Jordan Valley where WAPOR AETI seems systematically underestimated by 20 percent and more. However, analyses of comparative remote sensing products for the Fayoum area shows that WaPOR AETI preforms better than the other products, with only SSEBop performing in similar fashion. Both Fayoum and Jordan Valley are located in semi-arid and arid climates, and WaPOR AETI appears to underperform under arid conditions.

The advantage of flux towers is that shorter periods can be evaluated as well. The validation with individual flux tower data suggests that peak fluxes during hot Egyptian summers are not met. Rarely WaPOR estimates fluxes more than 5 mm/d during decadal time increments. The correlation with flux data for stations in South Africa varies by location and land use. The more arid Western Cape has a lower performance than Cathedral Peak that is lush green for the majority of the year. We conclude also that the performance of field measurements (flux towers and soil water balances) are not free from substantial errors, both related to methodology and second to the footprint mismatch with 100 m and 250 m pixels (Table 20). It remains to be a scientific challenge to collect reliable AETI data from field observations, which are representative for WaPOR pixel resolution. At continental and basin scale level, WaPOR AETI data is among the best AETI products available, and even better performance can be expected as the influence of seasons and vegetation can be improved for the version 2.0.

Table 20

Synthesis of in situ comparison of WaPOR AETI data

Country	Methodology	Land use	Climate	Deviation (%)
Ghana	Eddy covariance	Primary tropical forest	Humid	+22
Senegal	Eddy covariance	Sahel	Arid	-3
South Africa	Eddy covariance	Nature Park	Semi-arid	+4
South Africa	Surface renewal	Agriculture (sugarcane)	Semi-arid	+23
South Africa	Eddy covariance	Agriculture (grapes)	Arid	-60
South Africa	Eddy covariance	Pastures	Humid	+20
Egypt	Eddy covariance	Agriculture (cereals)	Hyper-arid	-20
Jordan	Soil water balance	Agriculture (vegetables and fruit trees)	Arid	-20
Israel	Soil water balance	Agriculture (vegetables and fruit trees)	Arid	-60

B. Separation of Evaporation-Transpiration-Interception

B.1 Introduction

WaPOR AETI recognizes three evaporation components, transpiration (T) through the plants contributing to photosynthesis and biomass production, evaporation from soil, water bodies and built up areas (E) and interception (I). Each component is calculated separately, using the ETLook approach and added up to AETI (FAO, 2018). ETLook is based on a two-layer Penman-Monteith equation (Bastiaanssen *et al.*, 2012). T is often considered to represent the productive component of AETI, whereas E and I are considered unproductive. Changing agricultural water management practices to increase T over E and I can increase agricultural productivity without increasing water use (Rockström *et al.*, 2003) and this is also referred to as "the vapour shift". The availability of having T, E and I data is thus very attractive to support analysis in the agricultural water consumption debate. Similar to AETI, there are relative few datasets that collect data on T, E and I on a long term and at a relatively large spatial resolution. It is therefore difficult to validate the individual WaPOR datasets of T, E and I with observed data. Validating AETI at field scale is difficult already, and validating the individual components is an even harder challenge.

B.2 Data analysis

The WaPOR T, E and I values for the year 2010 are presented in Figure 24 and Table 21. The maps show that for water bodies and the Sahara and Kalahari desert surfaces, WaPOR T is very low (see Lake Victoria), WaPOR T is high where there is abundant biologically active vegetation (such as Congo). The WaPOR E, T and I data layers show trends that are consistent with what is expected. The high values of I in the inland of the Democratic Republic of Congo are directly related to the high PCP values in the same area.

Partitioning of annual AETI over the land area by WaPOR for 2018 is estimated to be 71 percent transpiration, 21 percent soil evaporation and 7 percent interception (Table 21).

Figure 24
WaPOR T, E and I for the year 2010

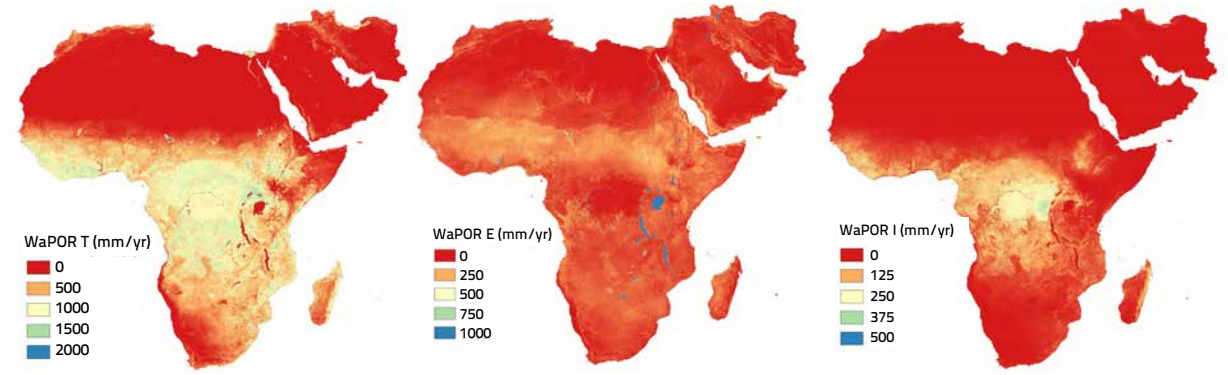

Table 21

Overview of continental values of WaPOR AETI, T, E and I per land use class in mm/yr for year 2010

Land use class	Area	AETI	T	E	I
Natural vegetation	12 585 800	795	626	107	73
Rainfed agriculture	1 566 131	477	346	120	19
Irrigated agriculture	336 983	496	376	119	15
Urban	101 619	229	111	145	11
Bare soil and sparse vegetation	16 012 249	48	7	43	0
Water	211 623	1 033	25	1 049	2
Total	**30 814 405**	**517**	**368 (71.1%)**	**111 (21.5%)**	**38 (7.4%)**

Spatial data products

Three different spatial data products are used to compare the WaPOR split, ETMonitor, GLDAS and Budyko approach by Mianabadi *et al.* (2019). An overview of the continental values for each product is provided in Table 22. For the Budyko approach E and I are combined in the Budyko I values. The high ratio of T/AETI obtained using the Budyko approach is more realistic that the values for ETMonitor and GLDAS. WaPOR comes closes to this value of the remote sensing data products. Detailed comparison between WaPOR and the other AETI split products is provided below.

The first comparative data product of E, T and I is the ETMonitor remote sensing model (Hu and Jia, 2015), using a process-based approach (Zheng *et al.*, 2016). In this section we only present the comparison of T (Figure 25). The maps of E, I and AETI are provided in Annex D. The general trends for the different maps are similar for the two products, however WaPOR T is significantly higher than ETMonitor T (Figure 25) and this is also reflected in the AETI comparison (Annex D). At the same time, ETMonitor E is higher around the tropics of Cancer and Capricorn compared the WaPOR E. The split between E and T for ETMonitor seems to favour E over T and vice versa for the WaPOR data. Choudhury *et al.* (1998) computed also T, E and I globally using a land surface model being calibrated with remote sensing data. This lead publication suggests that T is the dominant component of AETI in 20 out of the 28 latitude bands. WaPOR I is also higher than ETMonitor I in central Africa and the inlands of the Democratic Republic of Congo.

Table 22

Overview of continental values of WaPOR AETI, T, E and I per land use class in mm/yr for year 2010

	AETI	T	E	I	T/AETI
WaPOR	495	355	104	34	0.72
ETMonitor	402	226	149	27	0.56
GLDAS	468	180	182	118	0.38
Budyko	350	271	77		0.77

Figure 25
WaPOR and ETMonitor comparison of annual T values

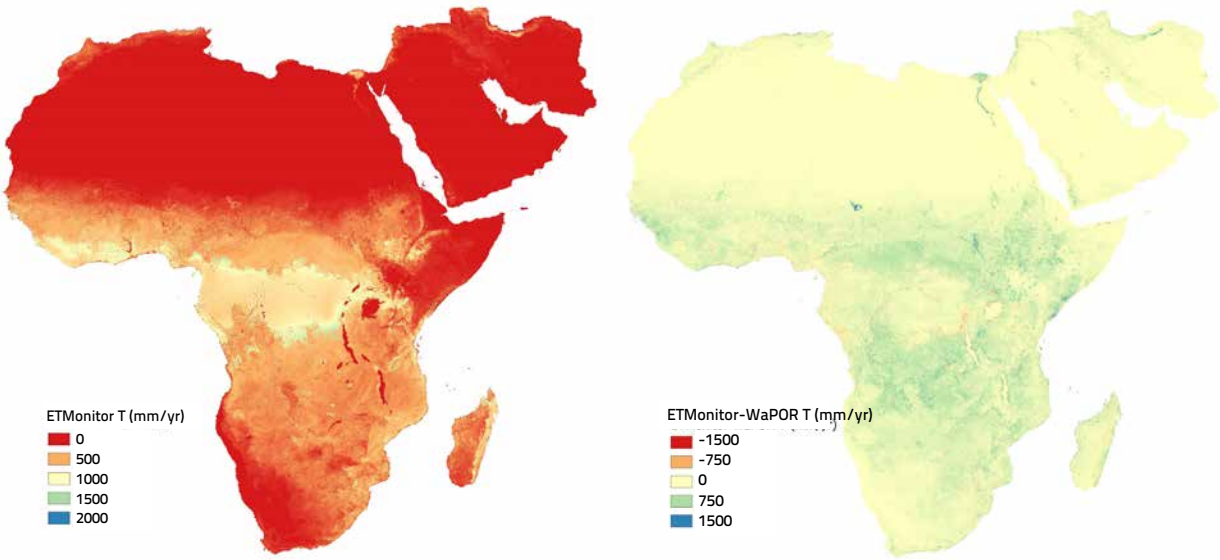

The second remote sensing product to compare WaPOR T is the GLDAS T (Figure 26). Similar trends are found between the two products, T for the rain forest in Congo are very similar, whereas the area around it shows large deviations. In addition, GLDAS T is not able to capture the high T for irrigated areas (e.g. in the Nile Delta and along the Nile River in Egypt), flood plains, shallow groundwater table areas and for deeper rooting groundwater dependent ecosystems. The main reason is that the Land Surface Models of GLDAS consider rainfall as the only source of water. Seepage, capillary rise, flooding and irrigation processes are still ignored in Land Surface Models.

GLDAS E is very similar to WaPOR E (see Annex D), however GLDAS I and WaPOR I differ significantly, with GLDAS estimating very high I across the coastal areas in West Africa and generally between latitude of +10° to –20°. GLDAS utilizes a canopy surface water storage (Rodell *et al.*, 2004), this storage seems to be on the high side, thereby overestimating I compared to WaPOR I.

Another just very recently published independent data source describing T comes from Mianabadi *et al.* (2019). These authors used a well-known approach to separate T from I using the Budyko curve (Figure 27). Even though the periods and the resolution differ (Budyko approach is an average over long time period for 0.250), the values are quite comparable. The Budyko method is overestimating T compared to WaPOR T in the Congo Basin, as well as in the humid tropics of Ghana and Ivory Coast. The Budyko estimation of I, shows high values for areas in the Lake Victoria basin in East Africa, and coastal zones such as the east coast of Madagascar and the coastal zones in West Africa (see Annex D), which are also the same areas where WaPOR estimates very high PCP values. We therefore believe that the larger picture of annual and absolute WaPOR T values for vast areas are good.

Mianabadi *et al.* (2019) compared their T and I products to two other products, GLEAM v3.0a (Martens *et al.*, 2017; Miralles *et al.*, 2011a) and Simple Terrestrial Evaporation to Atmosphere Model (STEAM) (Wang-Erlandsson *et al.*, 2014, Wang-Erlandsson *et al.*, 2016). The Budyko approach as presented here is in line with the two complex land surface models (Mianabadi *et al.*, 2019). WaPOR provides not only T and I values for each decade, it also provides it at much higher resolution than the Budyko approach.

Figure 26

GLDAS T comparison with WaPOR T for the year 2010

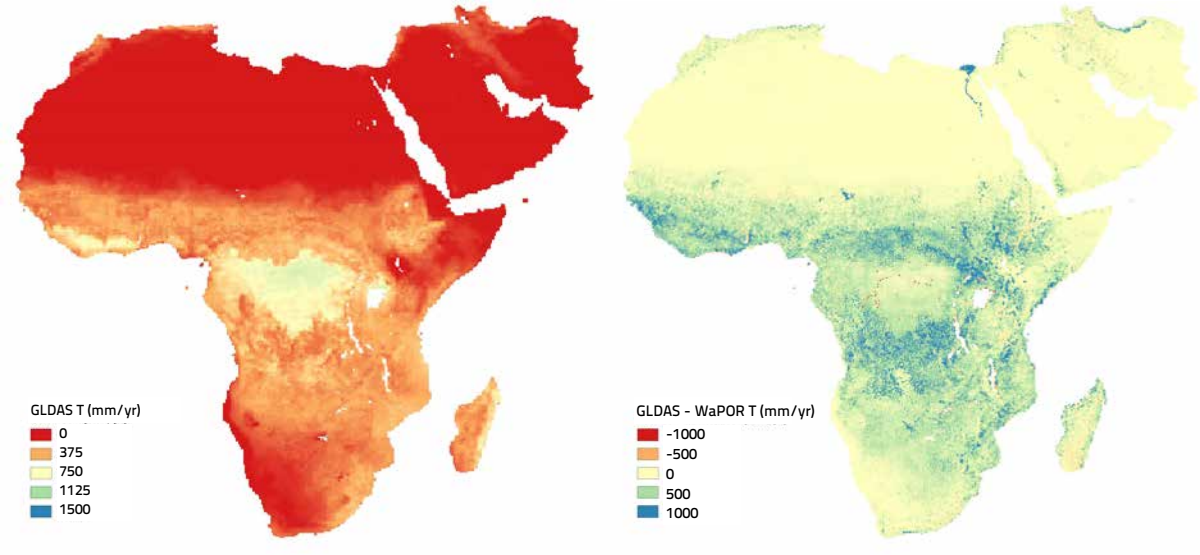

Figure 27

Budyko T and comparison with WaPOR T

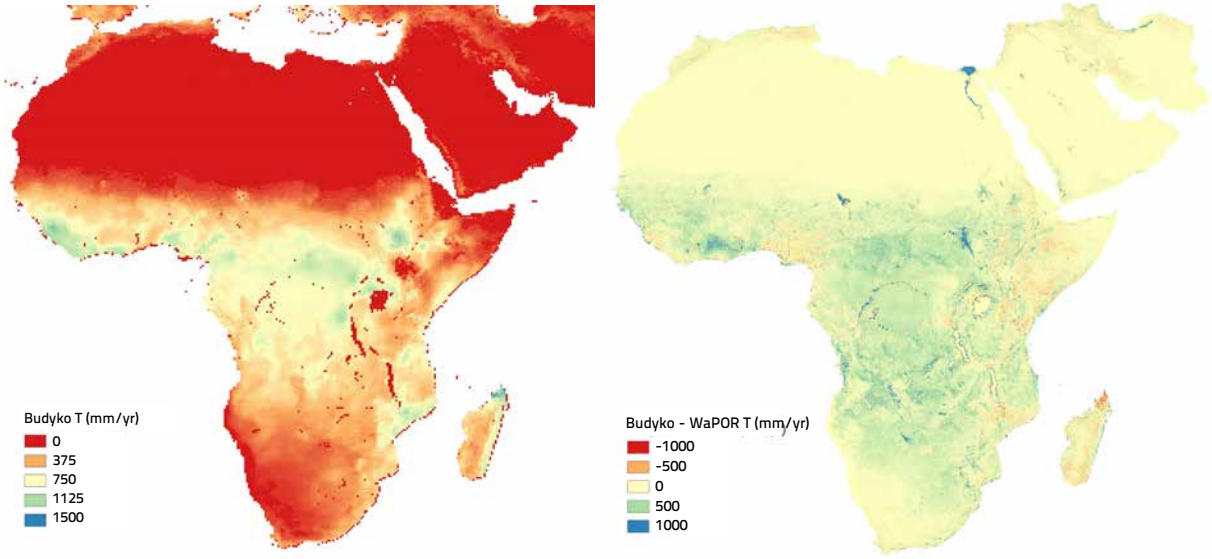

Field measurements of T fluxes

A field site near Bir Marwa in the Takelsa Valley of northeast Tunisia (36.783055N, 10.624166E) was equipped with sap flow instruments in a Michele Palieri table grape plantation during 2015 (Figure 28). Sap flow measures directly the transpiration rate T, and is therefore a valuable asset for directly validating the T flux of WaPOR without any indirect interpretations. The flow rates for each position are calculated as product of cross sectional areas of the surrounding ring and the sap velocity (cm/hr). Measurements were taken at 15 min time interval and

resulting sap flow is the sum of sap flow rates for inner and outer thermistors. The in situ measurements covers the period May to December 2015.

The measured sapflow is approximately 1 mm/d during May when the *LAI* of the plantation is low (0.2 m^2/m^2). The *LAI* increase to 1.5 m^2/m^2 by the end of June. The relatively low value of *LAI* is caused by the row crop character of grapevines where the average *LAI* of canopies and underground reduces the total *LAI* for a field. The associated sapflow during the summer is typically 4 to 5 mm/d, a value that is according to the expectations, so there is no doubt on the accuracy of the field measurements. At the end of December, the sapflow is again 1 mm/d, and it expected to be even lower when the grapevines go dorment between December and May (Figure 29).

Figure 29 shows the disagreement with WaPOR T values. While at low T fluxes the performance of WaPOR is at least realistic, the agreement disappears when the sapflow exceeds 2 mm/d. The T fluxes from WaPOR are in general only 43 percent of the field measurements, hence a serious under-estimation in T is occuring. From the entire period between 1 January 2009 and 11 January 2019, the maximum decadal T flux from WaPOR is 3.2 mm/d only (October 2018). The maximum decadal AETI flux is 3.9 mm/d (August 2018). Clearly, peak T-fluxes are not determined properly by WaPOR.

The accumulated T-flux from WaPOR for an average year is 503 mm/yr, the associated AETI-flux is 593 mm/yr (hence T/AETI is 85% being a rather high value). The annual PCP is approximately 465 mm/yr. Indeed, the grapevines are irrigated, and AETI values seem low. Hence, at local fields during the irrigation season, T values from WaPOR are too low. The overall conclusion is that T from WaPOR is under-estimated at higher sapflow values.

Figure 28
Location of the sap flow measurements in Tunisia

Figure 29

Measurement of actual transpiration fluxes with sapflow devices in a grape plantation in northeastern Tunisia

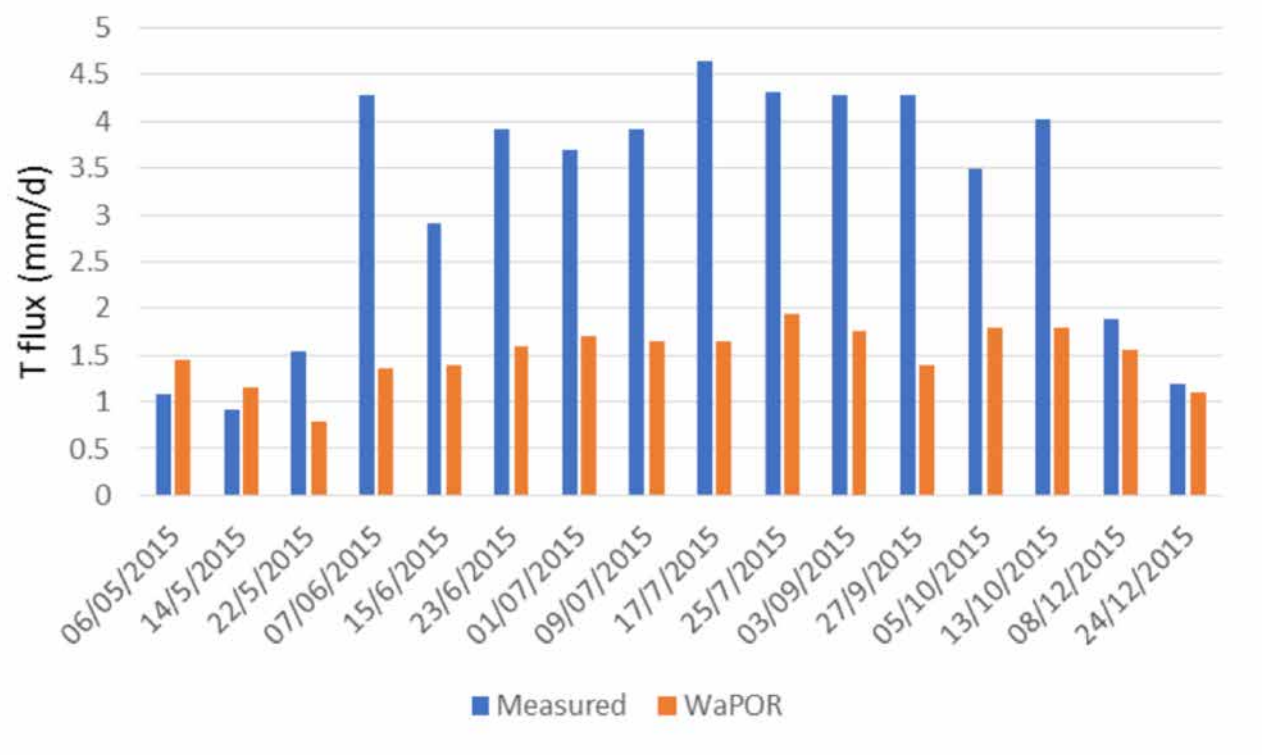

B.3 Conclusion

With limited available data to compare E, T and I, we focused on comparing the WaPOR data with alternative sources (ETMonitor, GLDAS, Budyko). All three T, E and I layers individually showed reasonable ranges in values and spatial variability. Compared to ETMonitor, WaPOR estimates of T are more realistic. With limited in situ observations available, the one comparison we did manage to do indicates that the T is underestimated during the cropping season. For cropland with lower *LAI* (LAI~2), there are signals from the field scale analysis that WaPOR T values are underestimated. Also, AETI was found to be at the lower side for several semi-arid and arid test sites which can also be ascribed to low E values. Because *LAI* and rainfall have both distinct intra-annual variabilities (that are not always related), it is recommended that T, E and I partitioning should be investigated in more detail on a monthly basis.

The ETLook model applied in WaPOR separates the available energy into T and E depending on the factor α*LAI (equation 7 and 8 in FAO, 2018), where α is the light extinction factor for net radiation [-] and *LAI* is the leaf area index. As explained in FAO (2018), *LAI* is derived from a large number of similar functions compiled from literature, however the value of α seems to be a calibration factor, which needs to be critically reviewed. Zhang *et al.* (2014) identified different values for α based on a comprehensive analyses of different datasets. They found variations between different land use classes and within land use classes (Table 23).

As the total bulk AETI is accurate (previous section), improving WaPOR T estimates can be achieved by refining α, the sensitivity of this parameter should therefore be evaluated. If less available energy will go to T, then more

Table 23
Light extinction factor for net radiation

Plant functional type/ land use class	α_{mean}
Grassland	0.50± 0.15
Cropland	0.62± 0.17
Shrubland	0.56± 0.13
Broadleaf forest	0.59± 0.12
Needleleaf forest	0.40± 0.11
Average	**0.56± 0.16**

will go to E for maintaining conservation of partitioning. That will immediately modify the T fraction in the right direction. However, a warning should be given that T should not be reduced much during full crop development as various analyses suggested T to be at the low side when crops are matured (Senegal, Sakha-A, Zankalon, Jordan Valley). Again, more detailed analyses are needed where the sensitivity to α is included for assessing potential T fluxes, as well as the regulating role of soil moisture on actual E and T fluxes. For now, we conclude that T for most ecosystems is rather good and in harmony with the most recent insights on T fluxes, except for cropland where some improvements are needed.

C. Robustness

C.1 Introduction

The WaPOR water layers (AETI, T, E and I) and RET are calculated independently and at different resolutions (250 m, 100 m or 30 m vs 20 km), comparing them therefore provides interesting validation of the WaPOR water layers at continental scale. The coefficient between AETI and RET is also known as the crop coefficient (kc). The coefficient is known to be high over water bodies, because there water is not a limiting factor. Over vegetated areas, kc should reflect a curve depending on the crop stages during the growing season. The coefficient will be low for bare land areas and similar dryland surfaces. A similar comparison was done to evaluate the ratio of T over AETI, indicating the contribution of AETI towards biomass production (T) compared to non-productive evaporation in the form of E and I. Low values of T/AETI are expected for water and bare soil, whereas for natural vegetation and agriculture the values are expected in the range of 0.7 to 0.8.

For selected irrigation systems further analyses were done (see Figure 30 for locations of these irrigation schemes). The Wonji irrigation scheme is located in Ethiopia in the Awash Basin and it is a sugarcane estate in a semi-arid area. The Kpong irrigation schemes is located along the Lower Volta River in southern Ghana. The Kpong includes mainly smallholders with rice, besides commercial farmers growing bananas. The area has a humid climate. The Bekaa Valley is located in the Litani Basin in Lebanon, growing various crops, including wheat, grapes and potatoes as well as other vegetables. The area is semi-arid. The forth area is the Fayoum irrigation scheme in Egypt. The farmers of Fayoum grow maize (summer) and wheat (winter) on a rotational basis. The irrigation schemes were selected based on the availability of auxiliary data and local knowledge of the authors. IHE Delft has sent students for fieldwork to these regions as part of the WaPOR project. The MSc thesis on the Wonji irrigation scheme was written by Yilma (2017). The MSc thesis dealing with the Bekaa Valley was prepared by Alvarez-Carrion (2018). A study by Salvadore (2019) provided data for the Fayoum irrigation scheme. The Kpong irrigation scheme in Ghana was added even though there was less data available, as it allowed for a comparison of an irrigation scheme in a more humid climate.

The analyses include the robustness checks between AETI and RET and T and RET. The dual crop coefficient approach of FAO56 describes the ratio of T/RET to be equal to k_{cb} (basal coefficient) for crop transpiration (Allen *et al.*, 1998). The coefficient k_{cb} describes the potential transpiration rate without experiencing soil moisture stress (the factor k_s represents the stress reduction coefficient). Together with k_e for soil evaporation, it makes crop coefficient k_c (Allen *et al.*, 1998; 2005):

$$AETI = k_{cb} * k_s * RET + k_e * RET + I$$

Note that I is not recognized in the dual crop coefficient framework. Numerous literature has proven that k_{cb} is linearly related to green fractional cover (for example, Calera *et al.*, 2001), which is in turn linearly related to NDVI (for example, Sellers *et al.*, 1997). In other words, the T/RET findings should have a strong relationship with the NDVI value, and this could be another independent check in further studies.

C.2 Data analysis

Continental analyses

The overall continental trend is according to expectations (Figure 30). High values are found around the coast of West Africa, large areas of the Democratic Republic of Congo, highlands of Ethiopia and east coast of Madagascar. In these areas, there is limited water shortage and vigorous vegetation. Under these circumstances, AETI equals RET. On the other hand, low values are found around the west coast of southern Africa, the Sahel region and Middle East. Here water and vegetation are constraining factors for AETI. It is worth noting that vegetated areas have higher AETI/RET values than open water bodies such as Lake Victoria (Table 24). The histogram (Figure 30, right) shows that there are pixels with AETI being higher than RET, which could be true for certain vegetation physical features (tall or dark plants, high LAI), or may be due to the different resolutions of RET and AETI.

Figure 31 shows ther T/AETI fraction. The fraction is unexpectedly high (>0.75) for the majority of the study area, leading to the average T/AETI value of 0.45. For the ETMonitor, GLDAS and Budyko the T/AETI fractions are 0.31, 0.22 and 0.46 respectively. Studies estimate the contribution of T to AETI globally to vary between 52 and 57 percent (Choudhury *et al.*, 1998; Wei *et al.*, 2017), but this also includes the tundras at northern latitudes. Upon closer inspection, we found that Choudhury *et al.* (1998) predict T/AETI for our study area between +35^{o}N and -35^{o}S to be 0.52. Both Budyko and WaPOR provide similar estimates for the continent. For bare soil and water the fraction of T of AETI is very small, whereas for vegetation, T as a fraction of AETI varies between 0.71 to 0.79, with the highest continental value being for natural vegetation (Table 24). A high T/RET fraction holds true for tropical forests with very high *LAI* (LAI>5).

Figure 30

Average WaPOR AETI over RET (2009-2017), with locations of selected irrigation schemes (next section)

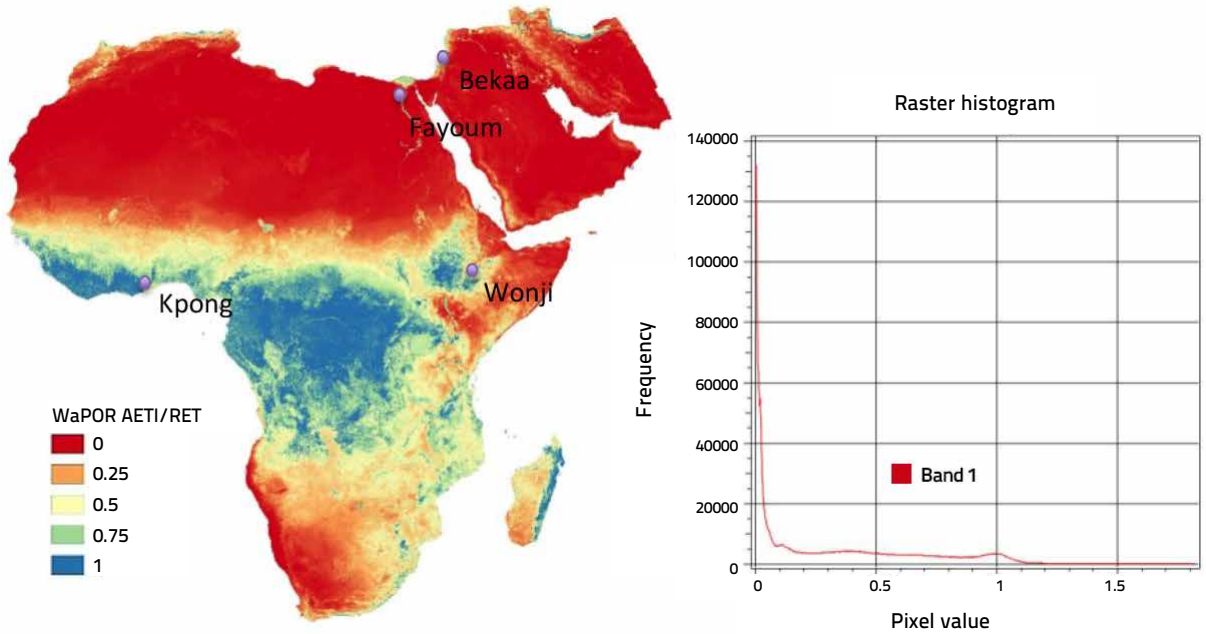

Table 24

Overview of continental values of WaPOR robustness

Land use class	Area	AETI	T	RET	AETI/RET	T/AETI	T/RET
Natural vegetation	12 585 800	795	626	1 412	0.56	0.79	0.44
Rainfed agriculture	1 566 131	477	346	1 484	0.32	0.73	0.23
Irrigated agriculture	336 983	496	376	1 556	0.32	0.76	0.24
Urban	101 619	229	111	1 699	0.13	0.49	0.07
Bare soil and sparse vegetation	16 012 249	48	7	2 036	0.02	0.14	0.00
Water	211 623	1 033	25	1 490	0.69	0.02	0.02
Total	**30 814 405**	**503**	**368**	**1 742**	**0.22**	**0.73**	**0.16**

Irrigation scheme comparison

Figure 32 overleaf shows the AETI/RET ratio (i.e. kc) and on the right the T/RET ratio (i.e. k_{cb}) for the selected irrigation schemes for one calendar year (2015). Except for the area in Ghana, the maps clearly show the distinction between the irrigated and surrounding landscapes. In Wonji, Fayoum and Bekaa, the surrounding area is water constrained. The availability of water is clearly a distinguishing factor in the development of vegetation. For the area in southern Ghana, the irrigated area cannot be distinguished as easily as in the arid and semi-arid areas.

Figure 31
Fraction of T over AETI (2009-2017)

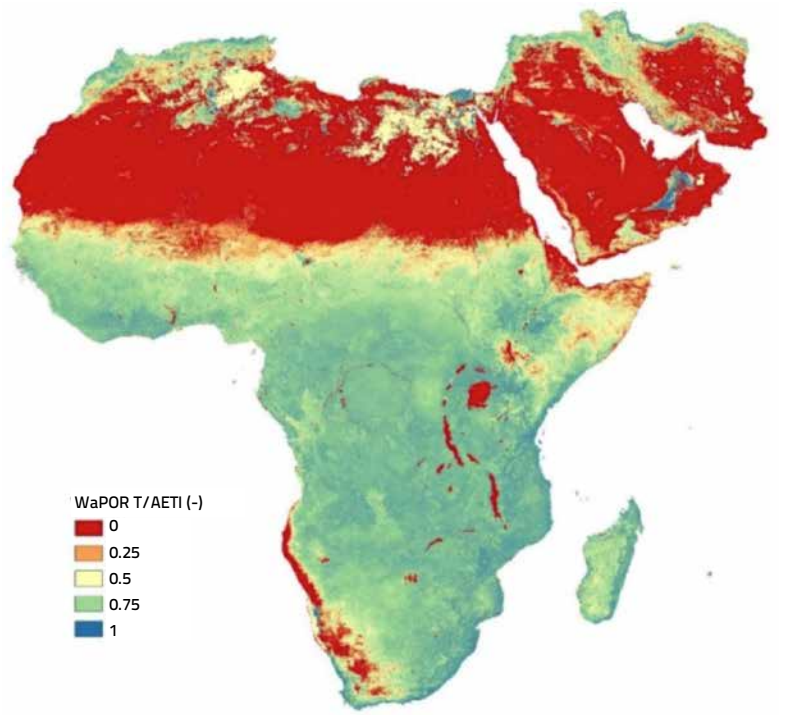

The average AETI, T, E and I for the selected irrigation schemes are provided in Table 25. Since the analyses include not only the cropping season, fallow periods will reduce kc and the period of fully developed crops will increase the average kc value. Because sugarcane is a perennial crop, it produces much higher kc value (0.67) than what is observed for Fayoum (0.22) and Bekaa (0.5) exhibiting crop rotation systems (Table 25). In addition, for the Fayoum system, not all fields are cultivated with wheat during the winter season, as indicated in the blue areas (Salvadore, 2019). The bright red area in the Fayoum system is the Qarun Lake, where Kc is close to 1. The productive component of AETI (T) varies per irrigation scheme. Fayoum in Egypt has the lowest value of productive AETI of 0.69 and Wonji the highest of 0.85 (Table 25).

The basal crop coefficient (k_{cb}) of the selected irrigation schemes ranges between 0.15 for the Fayoum system to 0.57 for Wonji. The season variation of AETI/RET and T/RET are presented in Figure 33 and 34. The theoretical k_c of sugar cane is 1.25 (Allen *et al.*, 1998) however, based on the WaPOR data, the annual kc value for Wonji is much lower at 0.67. This value is lower than the theoretical one, as various areas within the defined shapefile are not cropped, either they are fallow or consist of paths, buildings etc.

Table 25
Overview of WaPOR AETI, T, E and I per selected irrigation scheme for 2015

Name	Country	Main crop type	AETI	T	E	I	k_c (AETI/RET)	T/AETI	k_{cb} (T/RET)
Wonji	Ethiopia	Sugarcane	1,317	1,125	182	18	0.67	0.85	0.57
Fayoum	Egypt	Wheat, maize*	485	333	153	0	0.22	0.69	0.15
Bekaa	Lebanon	Wheat, potatoes, grapes	622	494	131	6	0.50	0.79	0.40
Kpong	Ghana	Rice	1,196	875	302	30	0.75	0.73	0.55
		Bananas	1,022	793	201	40	0.63	0.78	0.49

* rotational cropping

Figure 32

The AETI/RET ratio (left) and T/RET ratio (right) for selected irrigation schemes for year 2015 (from top to bottom: Wonji - Level 3, Fayoum - Level 2, Bekaa - Level 3, Kpong - Level 2)

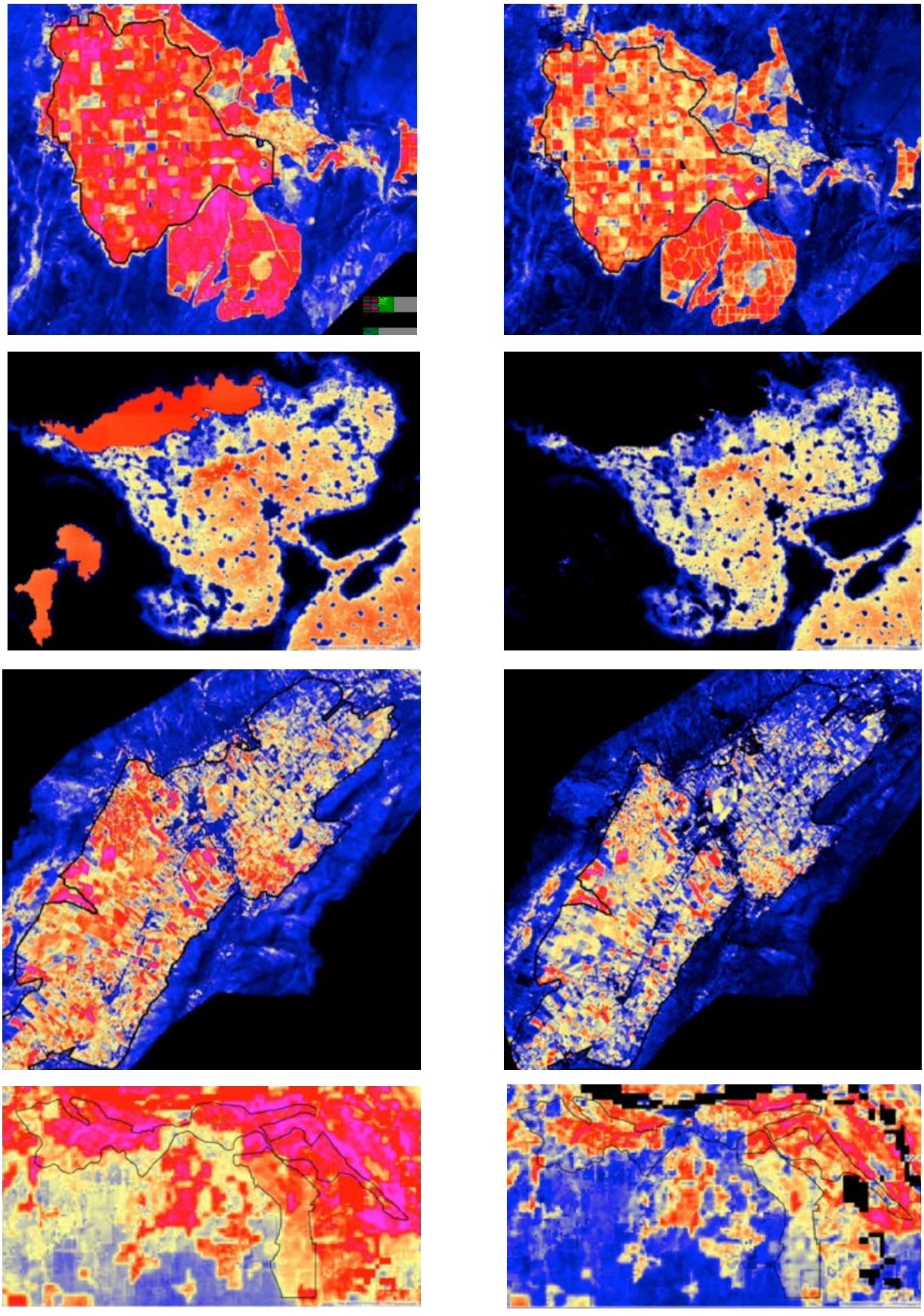

Figure 33

Monthly AETI/RET ratio for selected irrigation schemes

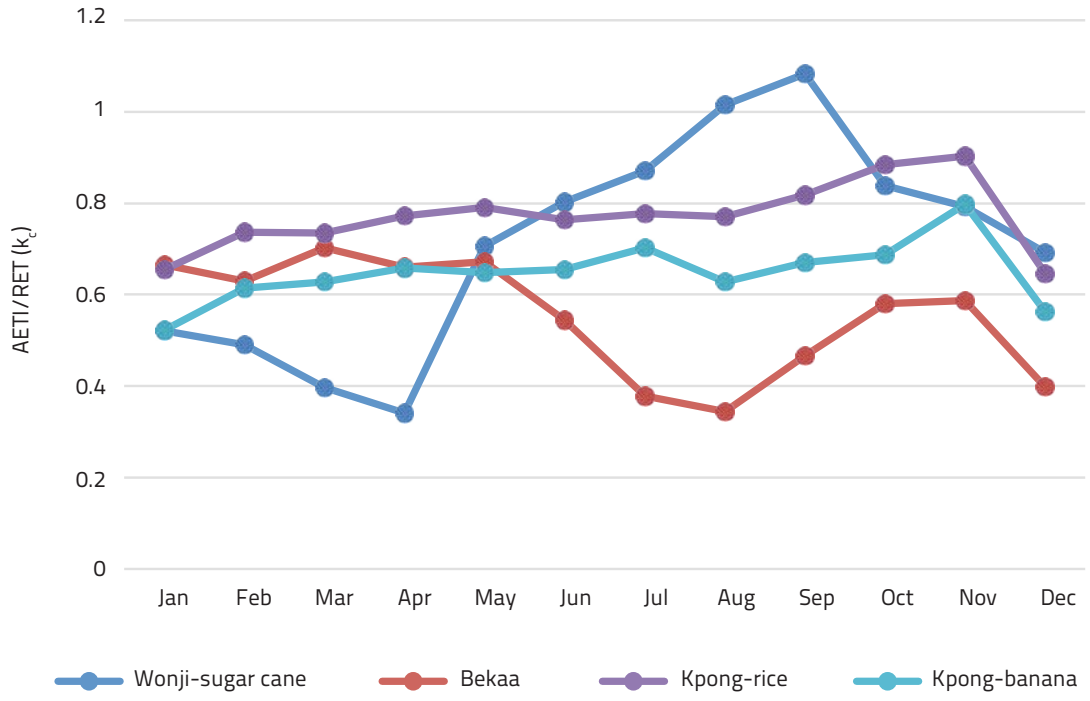

Figure 34

Monthly T/RET ratio for selected irrigation schemes

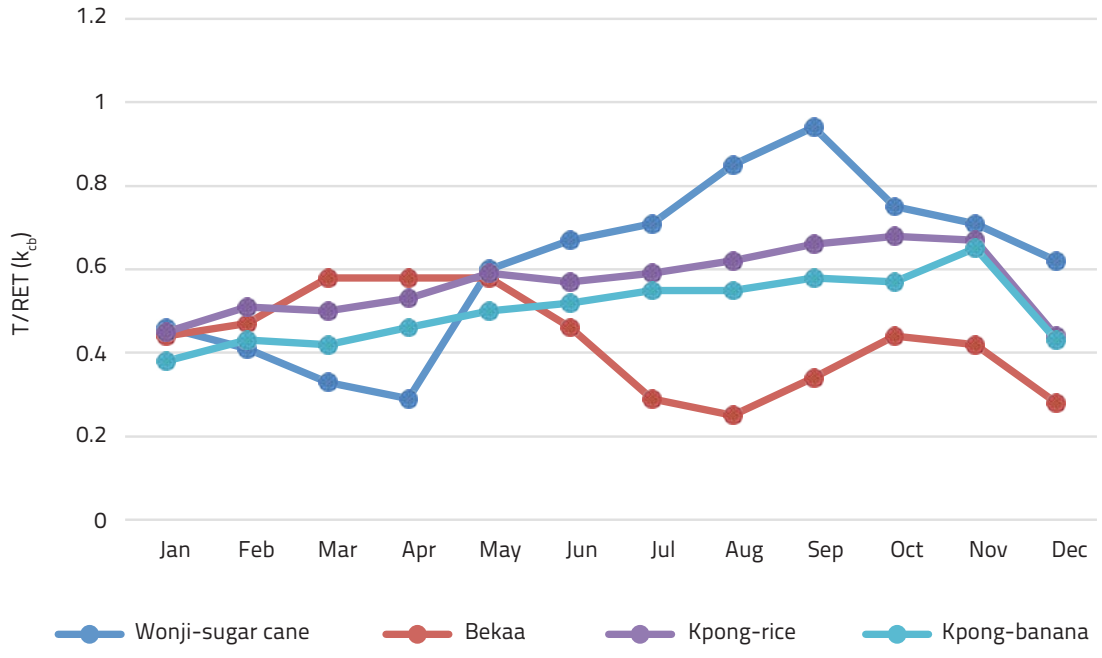

C.3 Conclusion

WaPOR AETI/RET ratio (k_c) at continental scale is 0.22, which at first glance seems low, but includes large areas in the Sahara and the Sahel regions where little or no evaporation is taking place. WaPOR AETI/RET ratio for the different land use classes confirms the accuracy of the WaPOR AETI layer compared to WaPOR RET, where high values are obtained in densely vegetated areas and for water bodies. WaPOR T/RET ratio (k_{cb}) at continental scale is 0.16, with higher values for vegetated areas (agriculture and natural vegetation) and low values for bare soil and water. Similarly, WaPOR T/AETI ratio at the continental scale exceeds 0.7. These high T/AETI fractions are supported by the Budyko analysis (Mianabadi *et al.*, 2019), and they are certainly reasonable for permanently lush green ecosystems. The general trends are consistent with expected values.

At irrigation system level, the comparative analyses show lower value for the AETI/RET and T/RET for the Fayoum and Bekaa irrigation schemes than expected for cropped areas. This could be due to parts of the area being fallow (e.g. Fayoum), or parts of the year being fallow, thereby lowering the ratios. The schemes in Ghana and Ethiopia are cropped for most of the year and return values that are more in the expected range for cropped areas. In these areas, productive evaporation (T) is significantly higher than unproductive evaporation (E and I). For systems with a significant fallow area (Fayoum), the T/AETI ratio is low.

To confirm the accuracy of the values additional comparison with NDVI is necessary (NDVI at the moment is not available from WaPOR). One issue of concern is that T/AETI fractions vary strongly with LAI, PCP and the soil moisture regulation of E and T fluxes. The underlaying processes can be judged much better if in the next round of quality assesment decadal values are going to be investigated. Hence, it is not unlikely that WaPOR T provides some new evidence that T/AETI should be higher than previously assumed.

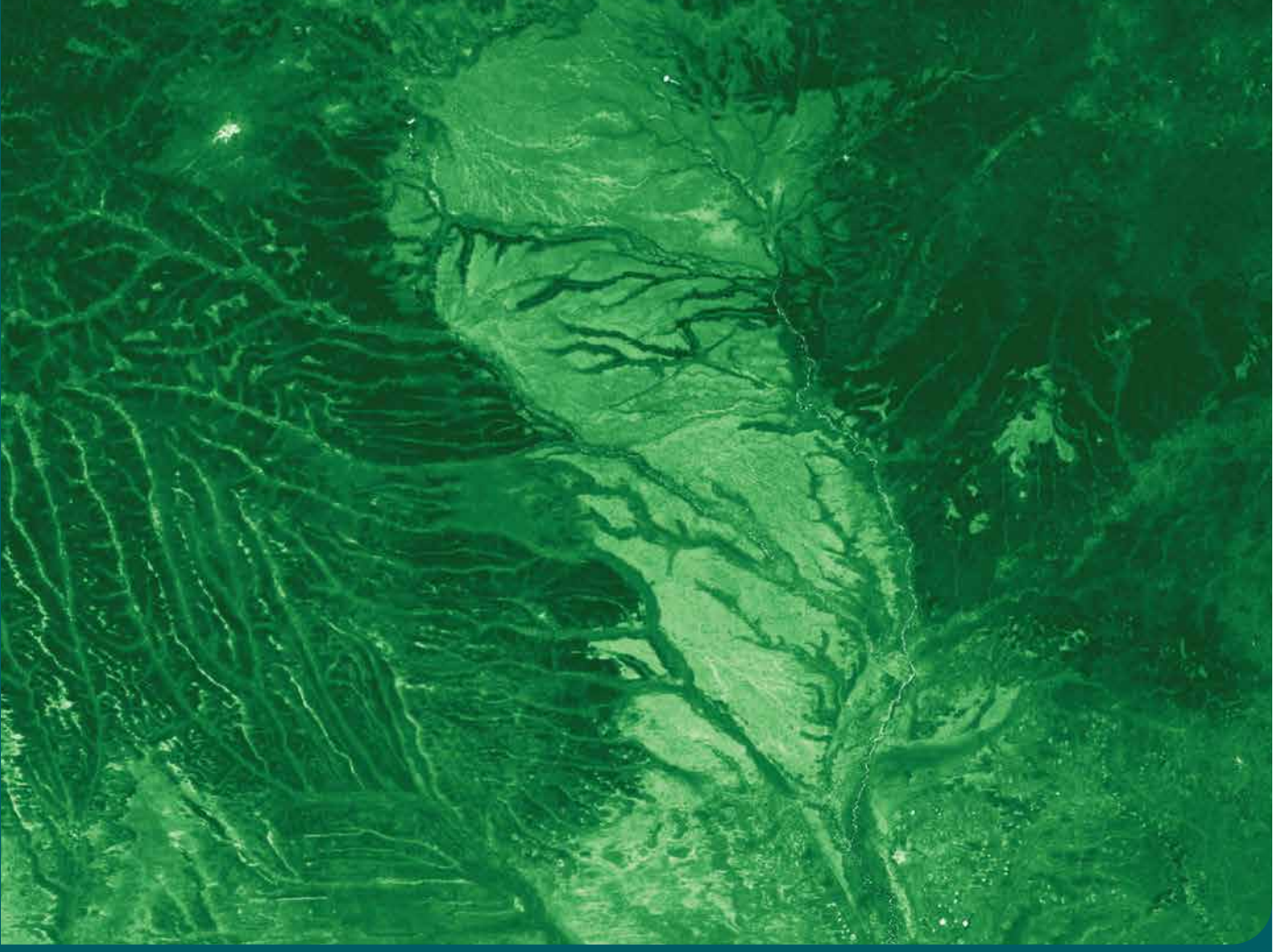

Detail of WaPOR Map "Above Ground Biomass Production 2018 - Eastern Angola and Western Zambia"

4. Land

A. Above Ground Biomass Production

A.1 Introduction

Producing more food per unit of land (kg/ha) and per unit of water (kg/m^3) is a major objective for increasing sustainable production in agriculture. FAO has shown in various studies that more food needs to be produced for meeting growing global food demand, and that will increase pressure on water resources. Most global data on crop yield and water resources are based on FAOSTAT and AQUASTAT. This data is based on secondary statistical datasets from the member countries. FAO launched the WaPOR program to complement such statisticswith spatially distributed information a on the local variability and trends in time, using cost-effective technologies.

The Above Ground Biomass Production (AGBP) is the ultimate indicator to express food production. The WaPOR database contains information on Above Ground Biomass Production (AGBP) based on the Net Primary Production (NPP). NPP reflect the daily net carbon exchange between land and atmosphere. During sunlight hours, crops intake carbon along with the release of water vapor into the atmosphere. During nighttime, part of the carbon is respired back into the atmosphere. The net result is the NPP. NPP is calculated in WaPOR using a remote sensing light use efficiency model (Ruimy *et al.*, 1999). NPP is expressed in gC/m^2/day. It is converted from gC to kg of dry mass (DM) per ha using a conversion factor of 22.22 (FAO, 2018). An additional conversion factor

to account for the percentage of biomass produced above ground is introduced. This conversion factor expresses the total weight of stems, branches, leaves, flowers, grains and lints above ground, versus the total weights of stubbles, bulbs, roots and tubers. In WaPOR, an average factor of 0.65 is applied throughout all pixels across the continent (FAO, 2018). The calculated continental AGBP considers C3 crop types and currently doesn't account for variations in land use and crop types to adjust the fraction of AGBP to total biomass and correct for different crop types. The database provides data on AGBP, which makes sense for cereals and most other crops. For potatoes, sugar beet and other tuber, root and bulb crops, it is better to revert back to the Total Biomass Production (TBP). This can be achieved as TBP = AGBP/0.65.

These constant factors are described in the methodology (FAO, 2018) but the implications associated with the simplifications should be well explained to users of the WaPOR database and instructions given on how to correct them when using the WaPOR database. For example, the ratio of the above and below ground biomass production varies across landscapes, and if users have (literature) information on this shoot – root ratio, a correction can be easily made. It should be made clearer to users that the default shoot – root ratio is 0.65.

C4 crops have a different biochemical system that converts the available solar radiation with a higher light use efficiency into dry matter or biomass production. On average, their extra efficiency is 80 percent higher as compared to C3 crops (being most crops). The most common C4 crops are sugarcane, maize and various oil seeds. To be able to estimate biomass and yield correctly for C4 crops, the WaPOR data thus needs to be corrected for areas where these crops grow.

A.2 Data analysis

The average WaPOR AGBP and NPP values for 2009-2017 are presented in Table 26 and Figure 35. As AGBP is linearly related to NPP, the two maps show the same variation across the continent. Variations between years at the continental scale are very small. The continental map is dominated by the close to zero values in the Sahel and large part of the Middle East. Larger inter-annual variations exist in the areas dominated by rainfall. In both maps, irrigated areas around the Nile river (Egypt) and the Office du Niger and Inner Niger Delta (Mali) appear clearly as bright spots in otherwise dry, low biomass producing areas.

Spatial data products

To the authors knowledge, only one comparative remote sensing product of NPP exists with a similar grid size (MOD17) (Heinsch *et al.*, 2003; Running and Zhao, 2015; Running *et al.*, 2015), besides several other assessments from global ecological production models. For this assessment a comparison is made with the MOD17 Terra and Aqua NPP products. There are discrepancies between the MOD17 Aqua and Terra products resulting from differences in overpass time, therefore we compared WaPOR NPP with the averages of the MODIS Terra and Aqua NPP products for 2011 (Figure 36).

The spatial patterns are similar for both data products even though MODIS does not estimate values for the Sahel region. The absolute difference between the two products shows large discrepancies between the two products in the Central African Republic (underestimation of MODIS compared to WaPOR), whereas the eastern part of Southern Africa and eastern Madagascar is generally overestimated by MODIS (Figure 37).

Table 26

Average continental values of WaPOR ABGP and NPP

	2009	2010	2011	2012	2013	2014	2015	2016	2017	Average
NPP in kgC/m^2/yr										
Max	1.42	1.41	1.48	1.54	1.61	1.65	1.61	1.60	1.49	1.53
Mean	0.20	0.19	0.21	0.20	0.17	0.19	0.17	0.17	0.20	0.19
Min	0	0	0	0	0	0	0	0	0	0
Stdev	0.63	0.63	0.64	0.63	0.62	0.63	0.63	0.63	0.64	0.51
AGBP in tonnes/ha/yr										
Max	27.3	26.7	26.6	28.4	24.2	27.4	27.8	27.0	26.9	26.9
Mean	4.6	4.6	4.7	4.7	4.7	4.6	4.5	4.4	4.5	4.6
Min	0	0	0	0	0	0	0	0	0	0
Stdev	5.6	5.6	5.6	5.7	5.7	5.7	5.7	5.6	5.6	5.6

Figure 35

Annual Above Ground Biomass Production (AGBP) and Net Primary Production (NPP) values averaged for 2009-2017 period

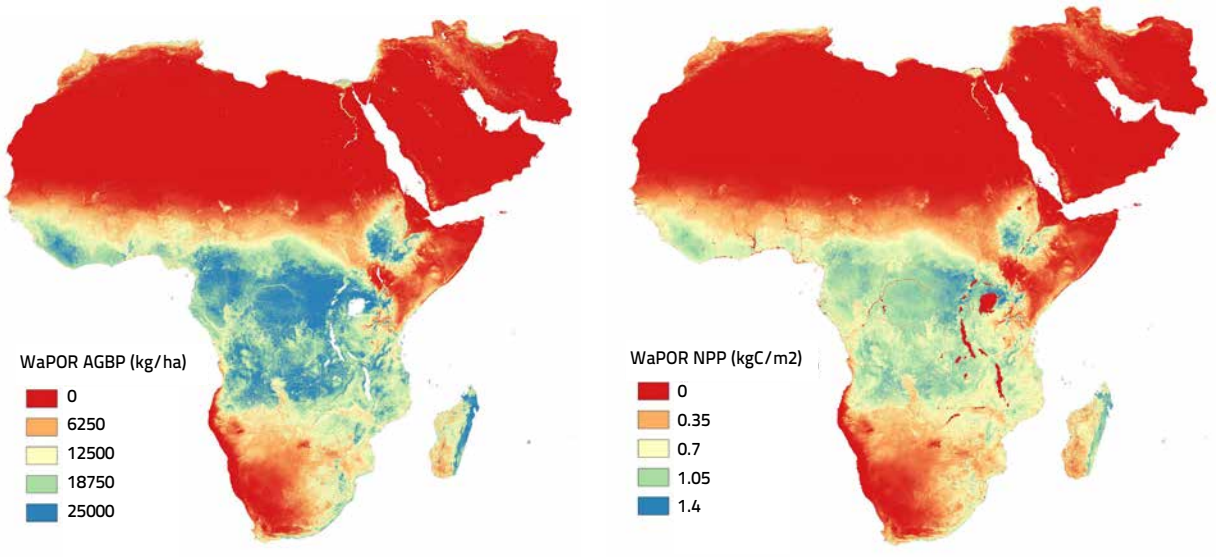

Figure 36

WaPOR NPP and average of MODIS Terra and Aqua NPP for 2011 (kgC/m^2)

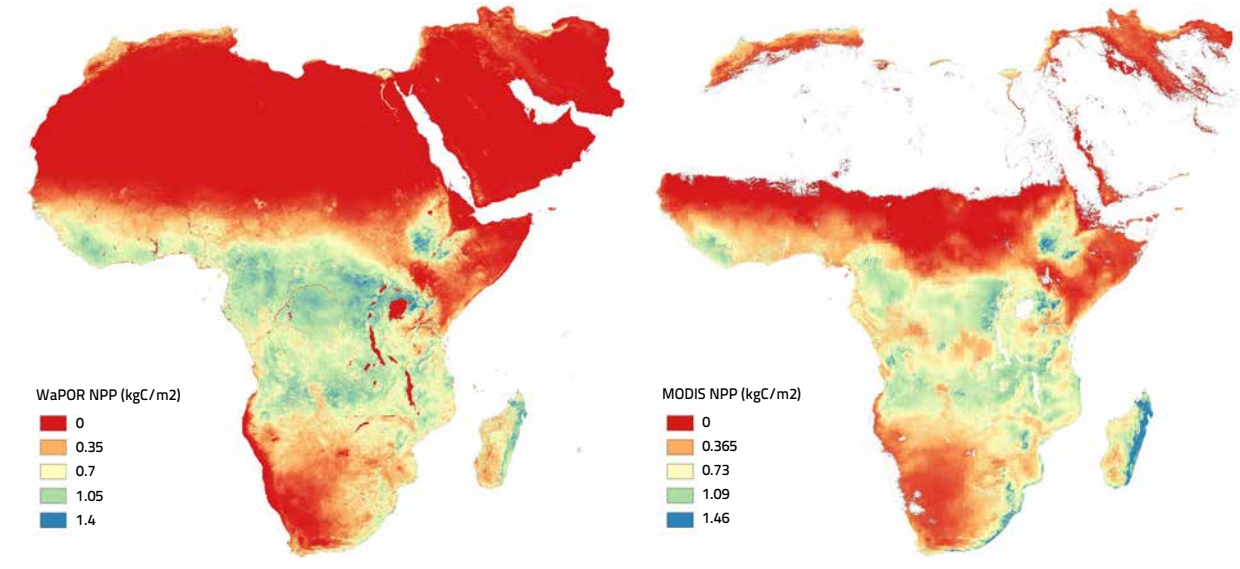

Figure 37

Difference NPP WaPOR and MODISAv as a fraction of MODISAv (left) and as absolute value (right) for 2011

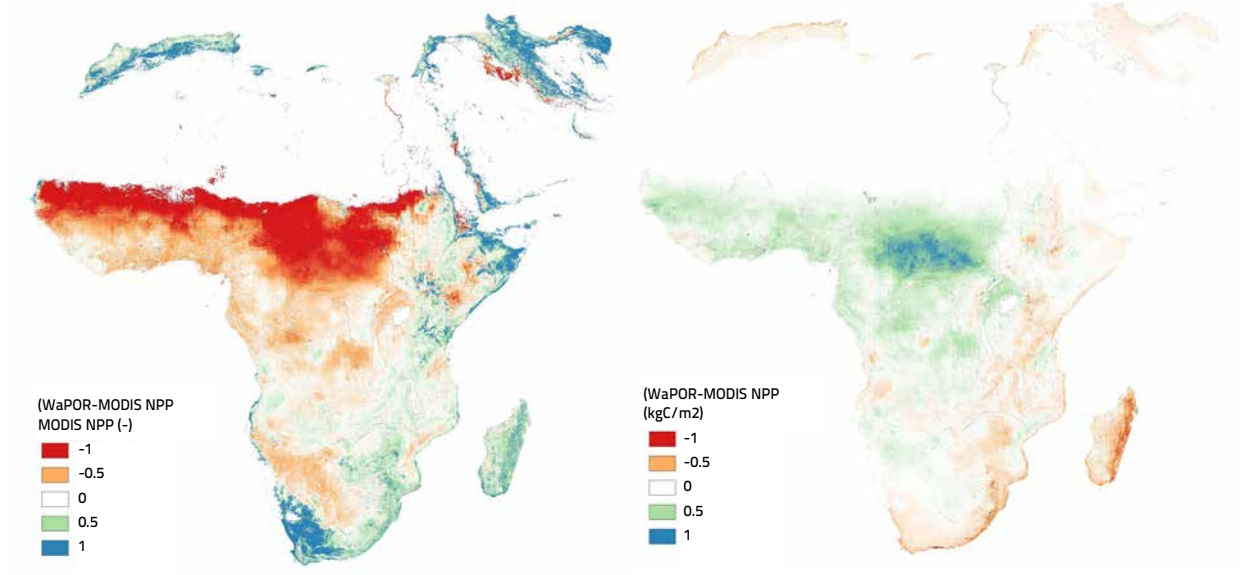

Even though it is difficult to say which data layer provides better NPP quality, the AETI comparison showed that WaPOR comes out with much better quality product than the MOD16 AETI product. Both products are using light use efficiency based approaches, but the choice of parameters, especially light use efficiency can create large deviations in the products.

Another independent check can be achieved from comparisons against global ecological production models. Figure 38 shows the result of NPP simulations done by the Center of Sustainability and the Global Environment

under the aegis of the University of Wisconsin. This IBIS model[8] shows NPP to vary between 0 and 1.3 kg C/m²/yr (Foley *et al.*, 2005; Kucharik *et al.*, 2000). The spatial trend for Africa is rather similar to WaPOR NPP, but with much lower resolution. Clearly, WaPOR NPP is able to differentiate water bodies and irrigated areas much better than the IBIS model (Figure 38).

WaPOR NPP is derived using light use efficiency value for different land use classes, for cropped areas it applies one value of 2.49 MJ/gr across the continent (FAO, 2018). This value corresponds to above and below ground biomass production (total biomass production (TBP)) and C3 crops. The light use efficiency values applied for trees, savannah and pastures are not provided in FAO (2018) and should be lower than for C3 crops (Foley *et al.*, 2005; Madini *et al.*, 2017). More information should be provided on the light use efficiency applied for the various agro-ecosystems and compared to other literature (e.g. Li *et al.*, 2012; Madani *et al.*, 2017).

Biomass estimates for selected irrigation schemes

Point measurements of AGBP are classically validated using crop yield data, which involve crop specific conversion parameters (harvest index, moisture content in the harvested fresh crop). A comparison was made to evaluate biomass production and yield to known values for the four selected irrigation schemes. For Wonji and Bekaa Valley, Yilma (2017) and Alvarez-Carrion (2018) used the pySEBAL script developed by IHE Delft and collected field data from the two areas. For Fayoum, Salvadore (2019) worked with the Ministry of Water and Irrigation in Egypt to develop a water account for the area, this included validation data on yield. For the area in Ghana, two reports from the Ghana Irrigation Development Authority were used to validate the results (GIDA, 2010). These datasets were used to compare the WaPOR AGBP layer. The total biomass production (TBP) was derived from NPP using the same conversion factors as the WaPOR database, without using the ratio of 0.65 of above ground

Figure 38

Global and annual NPP values simulated with the IBIS model (Foley *et al.*, 2005) and difference with WaPOR NPP

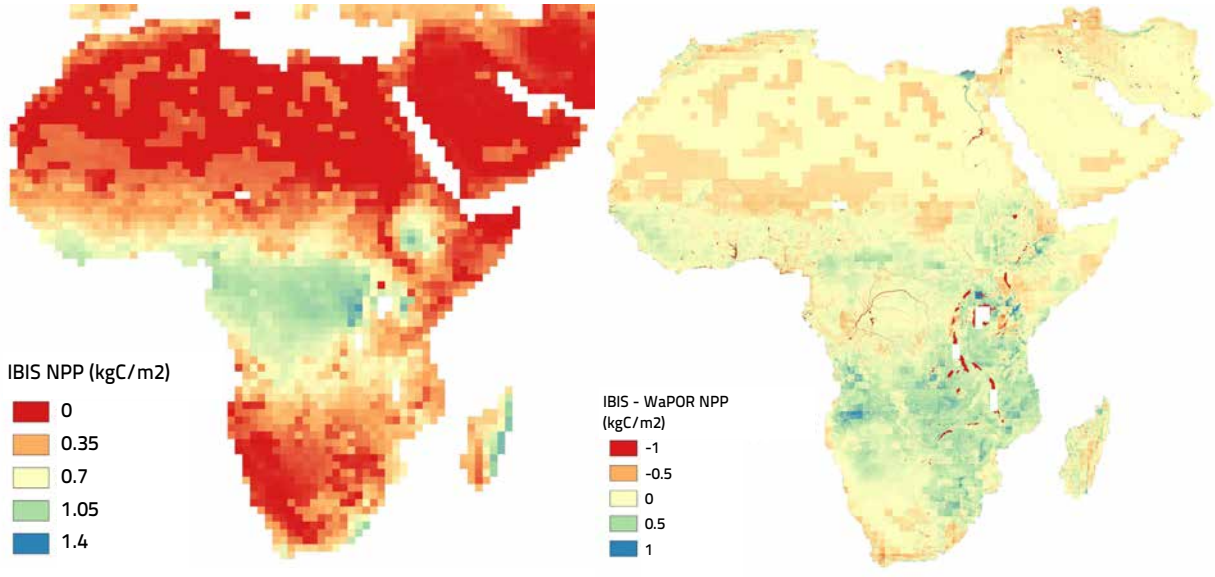

[8] https://daac.ornl.gov/cgi-bin/dsviewer.pl?ds_id=808

biomass production over total biomass production (FAO, 2018). The crop yield (Y) was then multiplied by a harvest index (h_i), for C4 crops multiplied by a factor of 1.8 (C_4). The final conversion is dividing by one minus the moisture content of the crop yield (m_c):

$$Y = \frac{TBP * h_i * C_4}{1 - m_c}$$

The harvest index and moisture content are crop (and location) specific parameters. For Bekaa and Wonji the WaPOR Level 3 (30 m resolution) is available, whereas for Fayoum and Kpong the 100 m resolution data was used.
Wonji irrigation scheme

The Wonji irrigation scheme is located in the Awash Basin, the area selected for comparison is an area cultivated with sugarcane. The cropping season of sugar cane in this area is 12-24 months on a rotational basis. We compared WaPOR yield to the yield observations, taking into account that the cropping season extends beyond one year. Even though, the AGBP layer for 30 m from the WaPOR portal is compiled based on the WaPOR determined cropping season (see section C), we decided to use our own predefined cropping season. We decided to estimate annual values for AGBP from January 2015 to June 2016 (18 months crop rotation), which is a similar period as Yilma (2017) used for the pySEBAL analyses.

WaPOR AGBP was converted back to Total Biomass Production (TBP) by dividing it by 0.65 (the ratio used by WaPOR). This TBP was multiplied by a crop specific ratio of AGBP and TBP (in this case set at 1.0 as root development for rotational sugar cane was assumed to be low). This was then multiplied by a harvest index (for sugar cane this was set at 1.0 as all harvested sugar cane ends up at the factory)[9]. An additional conversion was made to convert from C3 to C4 crops (factor 1.8). Finally the dry yield was converted to wet yield by dividing the value by the moisture content of the crop (set at 0.59, as estimated by Yilma (2017)).

Figure 39 and 40 show the maps of AGBP and yield for the area (the whole map was converted using the conversion factors as describe before).

Figure 41 show the yield distribution within the Wonji irrigation scheme. The average yield for 2015 a calculated is 100 tonnes/ha (Table 27). This value is similar to Yilma (2017) observed of 100 tonnes/ha. Steduto et al (2012) gives an average cane yield of 70 tonnes/ha and FAO gives ranges between 50-150 tonnes/ha being in perfect agreement with our check. Hence, WaPOR yield based on WaPOR AGBP seems rather realistic for sugarcane crops.

[9] Note that this harvest index is higher than reported in literature (0.65-0.85) and 0.65 estimated by Yilma (2017)

Figure 39

WaPOR Above Ground Biomass Production for 2015 for the Wonji irrigation scheme

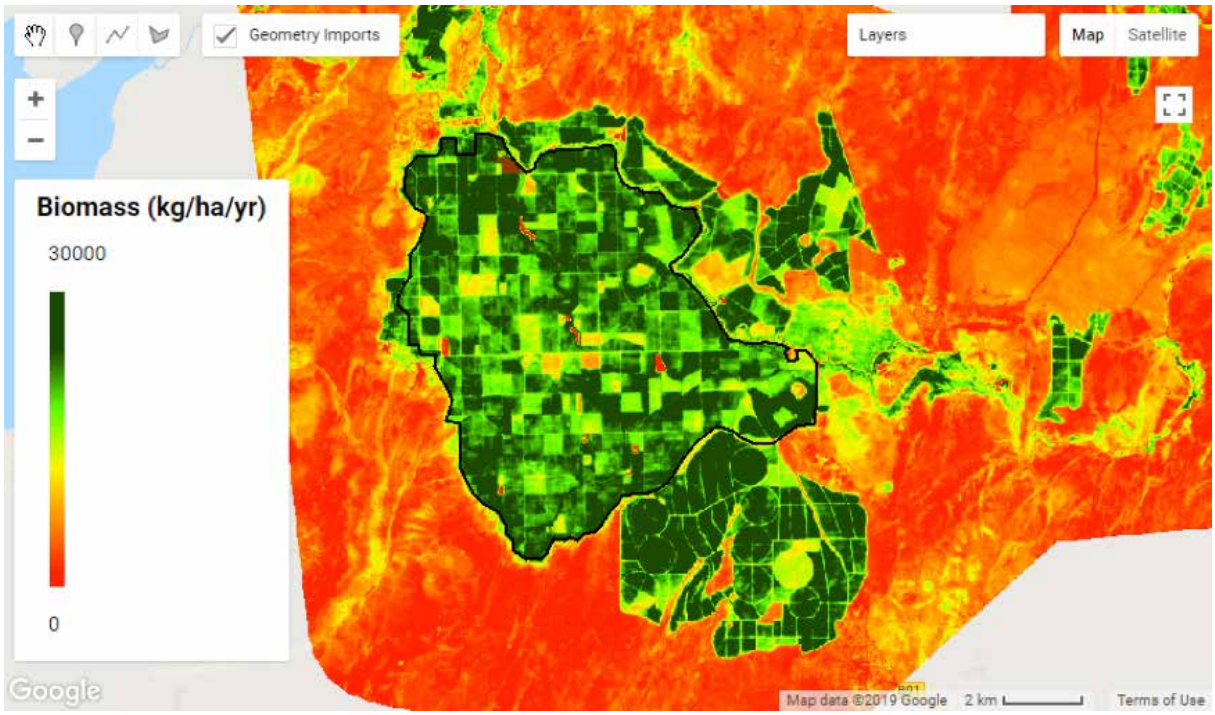

Figure 40

WaPOR derived yield for 2015 for the Wonji irrigation scheme using AGBP and specific conversion factors for sugarcane

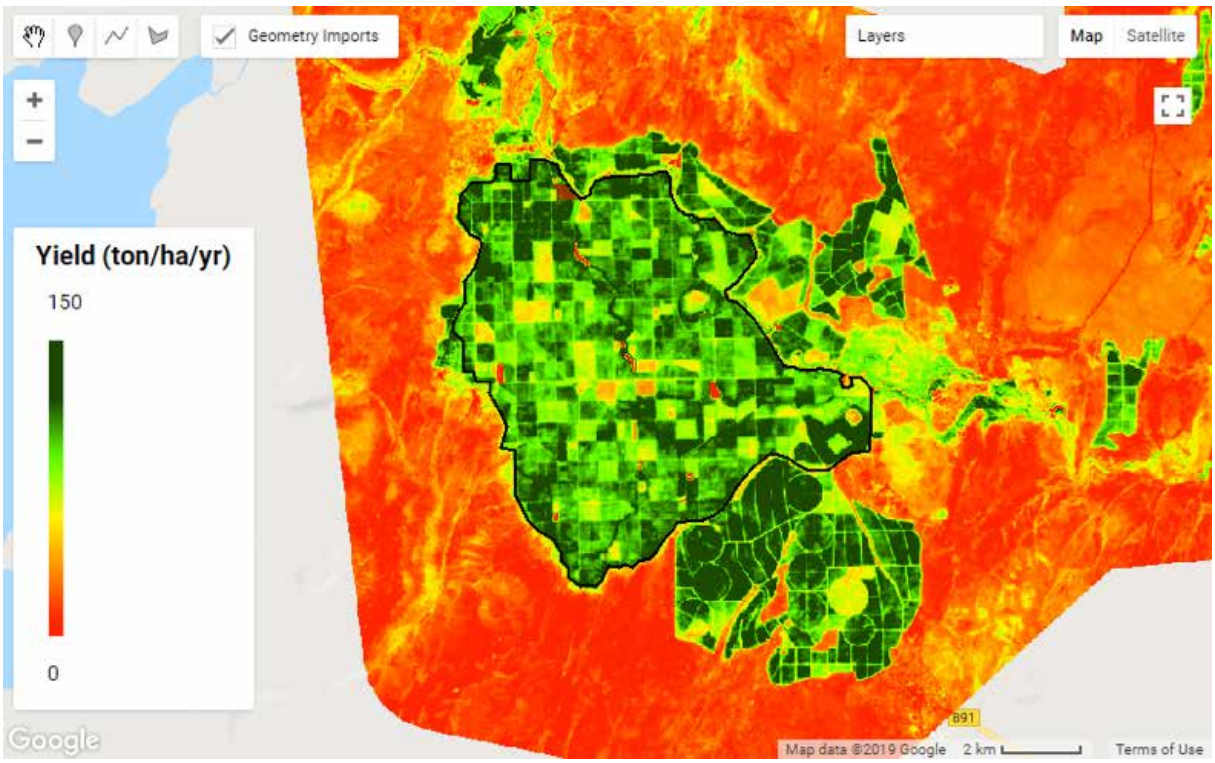

Figure 41
Sugarcane yield distribution Wonji irrigation scheme

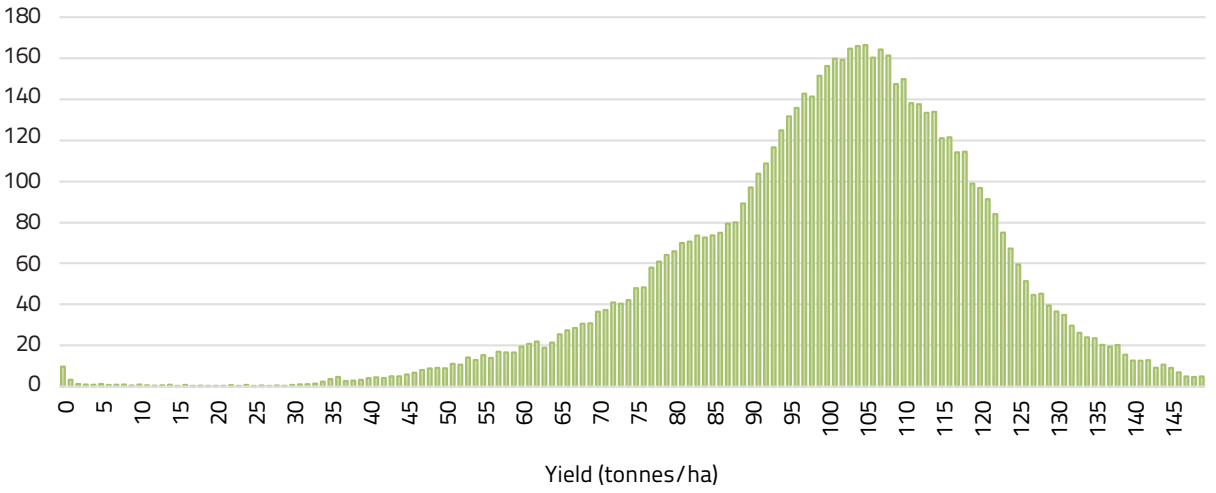

Table 27
WaPOR yield estimates for Kpong irrigation scheme for the year 2015

Crop	User defined cropping season	Harvest index	Moisture content	Average yield (tonnes/ha)	Literature values (tonnes/ha)
Sugarcane	01/01/2015-30/06/2016	1.0	0.59	100	100

Bekaa Valley irrigation

The Bekaa Valley is located in the Litani Basin in Lebanon. The farmers are growing a variety of crops, we obtained a shapefile of some grape fields (Alvarez-Carrion, 2018) and used this for the analyses. Figure 42 presents the AGBP in the area for the year 2015. The small shapes (southeast of the Bekaa Valley) are the known areas where table grapes are grown (Alvarez-Carrion, 2018).

The WaPOR yield estimation for this small area used the harvest index and moisture content as indicated in Table 28. Using these parameters the estimated yield for the grapes in these areas is 7.6 tonnes/ha, which is very close to the reported yield of 7.5 tonnes/ha (Alvarez-Carrion, 2018). The yield varied between 3.5 and 11 tonnes/ha (Figure 43). So also here, AGBP and TGBP values are accurate, but crop yield can be assessed only with proper Harvest Index and moisture content values of the fresh product.

Figure 42
WaPOR AGBP for Bekaa Valley for the year 2015

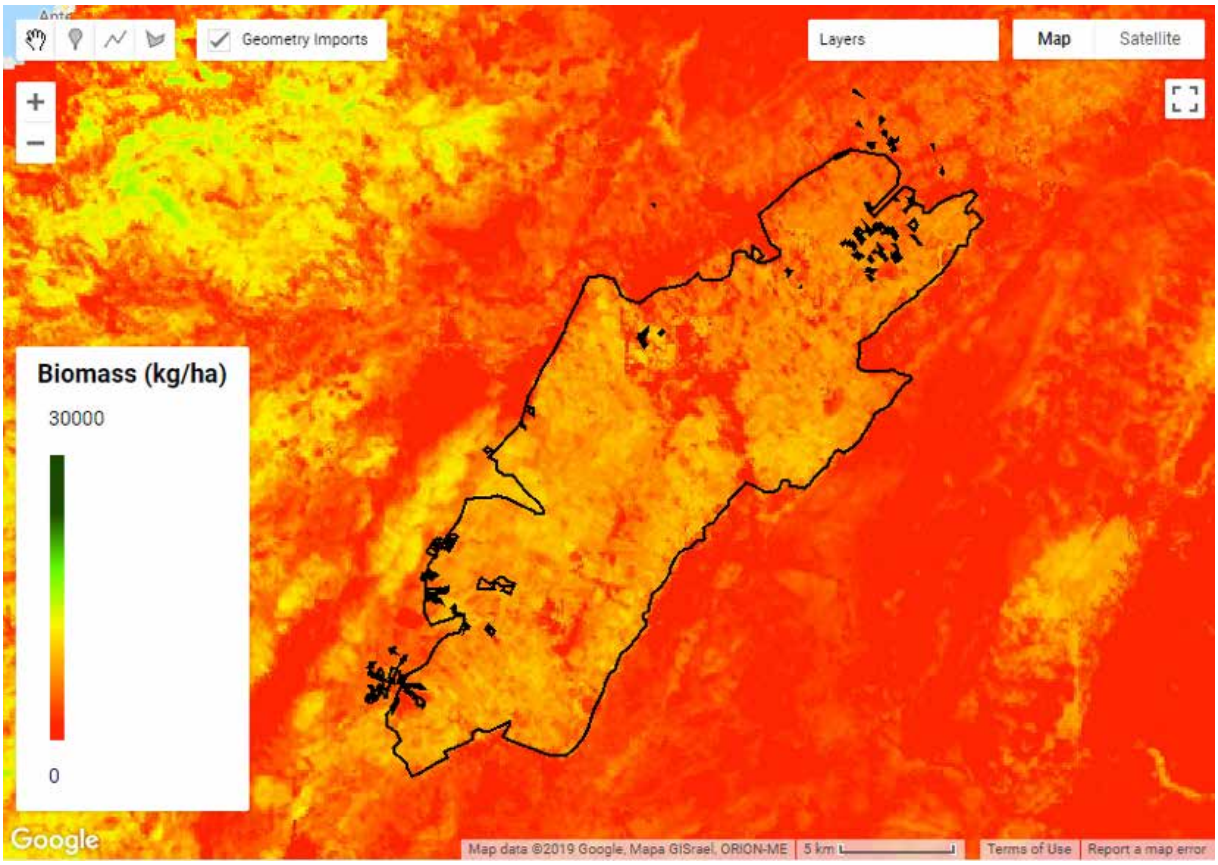

Table 28
WaPOR yield for grapes in Bekaa Valley for the year 2015

Crop	User defined cropping season	Harvest index	Moisture content	Average yield (tonnes/ha)	Literature values (tonnes/ha)
Grapes	01/01-31/12/2015	0.22	0.75	7.6	7.5

Kpong irrigation scheme

The Kpong irrigation scheme is located in Ghana. We investigated two different irrigation schemes, one with two seasons of rice (larger area in Figure 44) and one for continuous growing of bananas (smaller area in Figure 44). The accumulated AGBP for the year 2015 is presented in Figure 44. For each of the irrigation schemes the yield is calculated separately using different periods, harvest index and moisture content (Table 29). The information on cropping calendar was obtained from Gida (2010). Bananas are grown year round and the AGBP was estimated over a full year. Rice is grown twice during the year and for each season the yield is estimated.

Figure 43
Yield distribution of grapes in Bekaa Valley for the year 2015

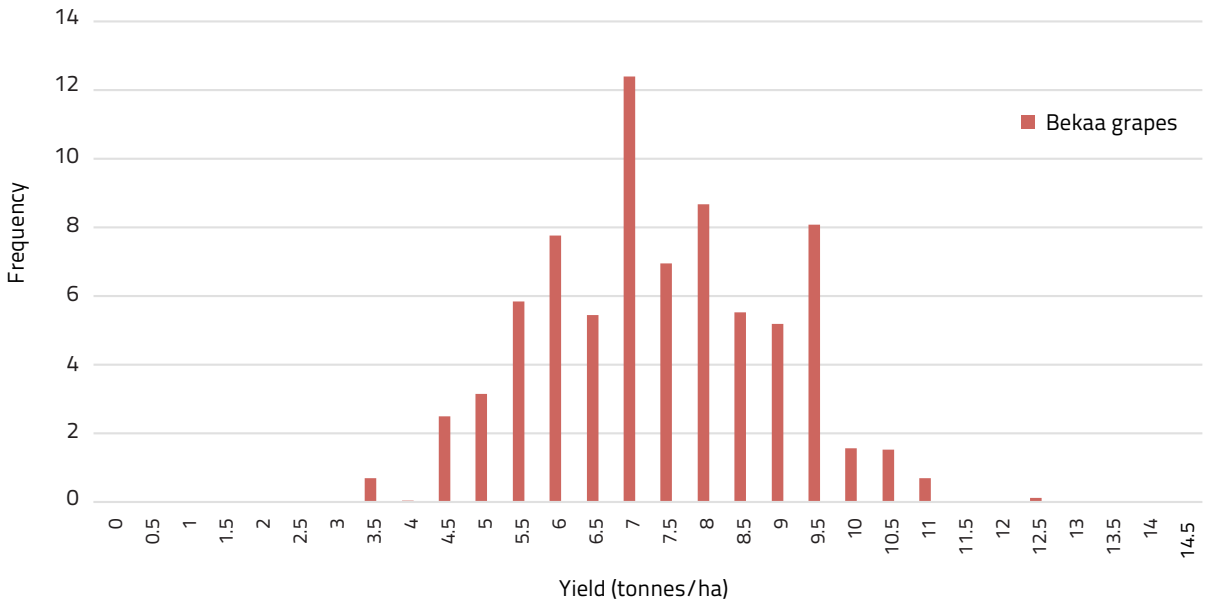

Figure 44
WaPOR AGBP at Kpong irrigation scheme for the year 2015

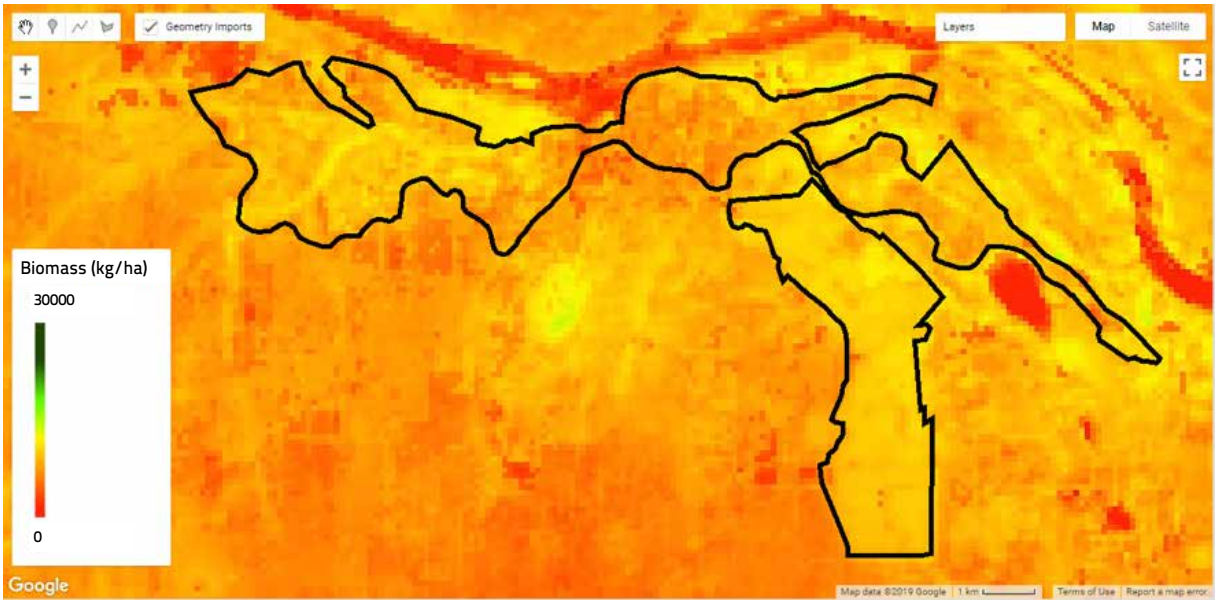

Figure 45 shows the WaPOR estimated yield for bananas. In this humid climate it is difficult to distinguish between the natural vegetation and the irrigated and or agricultural areas. Table 29 shows the estimated yield which compares very well with the reported yield by Gida (2010).

Figure 45

WaPOR yield estimation for banana plantation at Kpong irrigation scheme for the year 2015

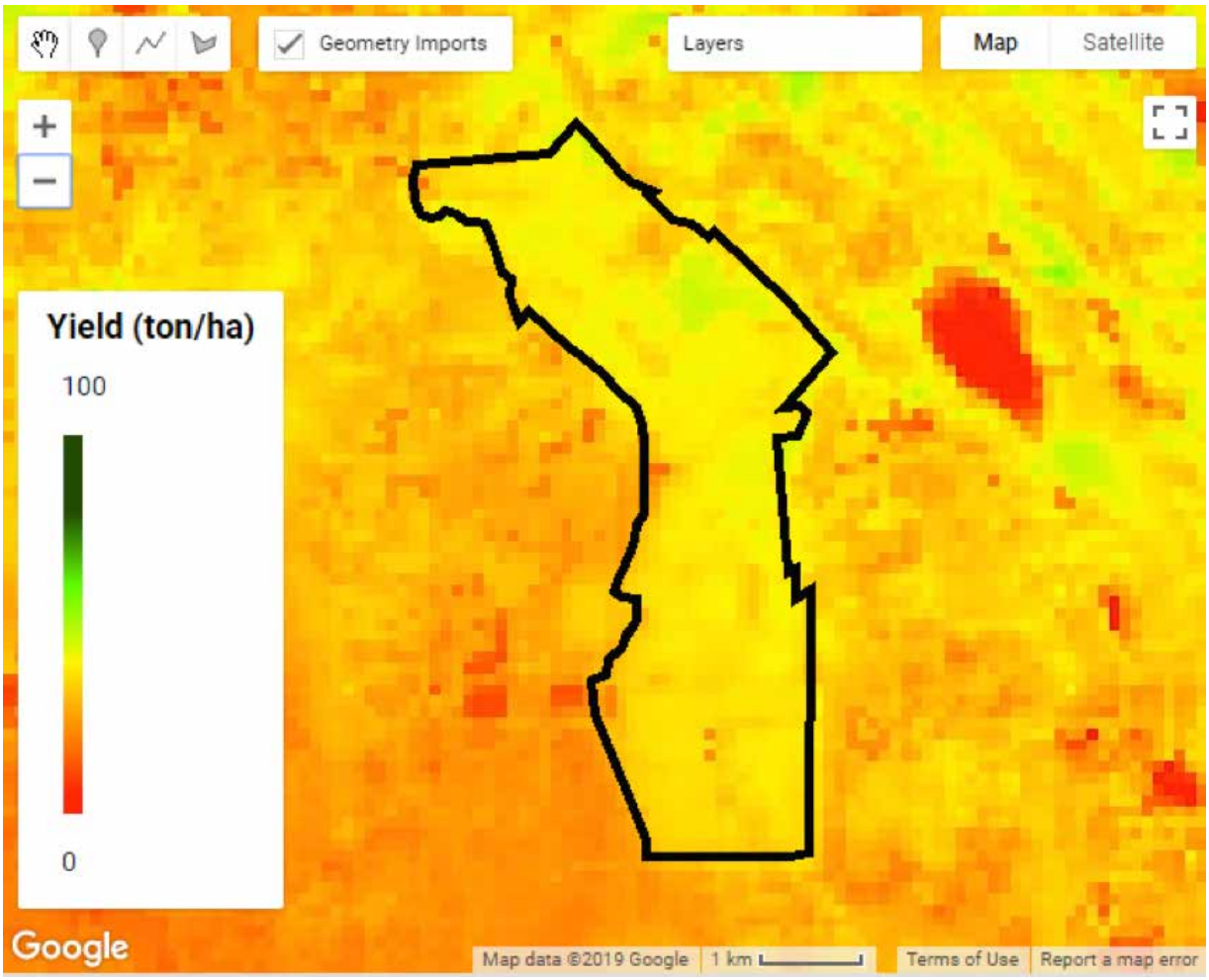

Table 29

WaPOR yield estimates for Kpong irrigation scheme for the year 2015

Crop	User defined cropping season	Harvest index	Moisture content	Average yield (tonnes/ha)	Literature values (tonnes/ha)
Bananas	01/01-31/12/2015	0.6	0.76	37.6	40
Rice main season	01/03-31/07/2015	0.55	0.2	4.2	4-5
Rice minor season	01/08-31/12/2015	0.55	0.2	4.0	4-5

Figure 46

Distribution of WaPOR estimated yield for Kpong irrigation scheme for the year 2015

Fayoum irrigation scheme

The Fayoum irrigation scheme is divided in two areas, one with permanent tree crops in orchards and an area where wheat and maize are grown on a rotational basis. The area receives very little rainfall, and most AGBP occurs on irrigated fields (Figure 47).

Yield is estimated using the cropping season as defined by Salvadore (2019). The harvest index and moisture content for each crop are presented in Table 30, and the estimated yield presented in Figure 48. The estimated yield for wheat and oranges are in the right ballpark, the estimated yield for maize is a bit on the low side (Table 30). The yield distribution (Figure 49) shows a large variation, and could be attributed to non-uniform water distribution, soil salinity and variable depth to shallow water table (see the red areas on Figure 48), which lower the yields. While wheat is the dominant winter crop, maize is cultivated side by side with berseem (and rice) during the summer. This quick analysis show the importance of having crop maps available. The user community of WaPOR should get examples on how to prepare their own crop masks, and then superimpose on WaPOR AGBP.

A.3 Conclusions

The WaPOR NPP layer is computed using a light use efficiency methodology. The maximum light use efficiency differs for different biomes and crop types, meaning that an accurate land use map is required to assign the correct values for each land use type. Correction factors for ambient conditions and soil moisture are included

Figure 47
WaPOR AGBP at Fayoum for the year 2015

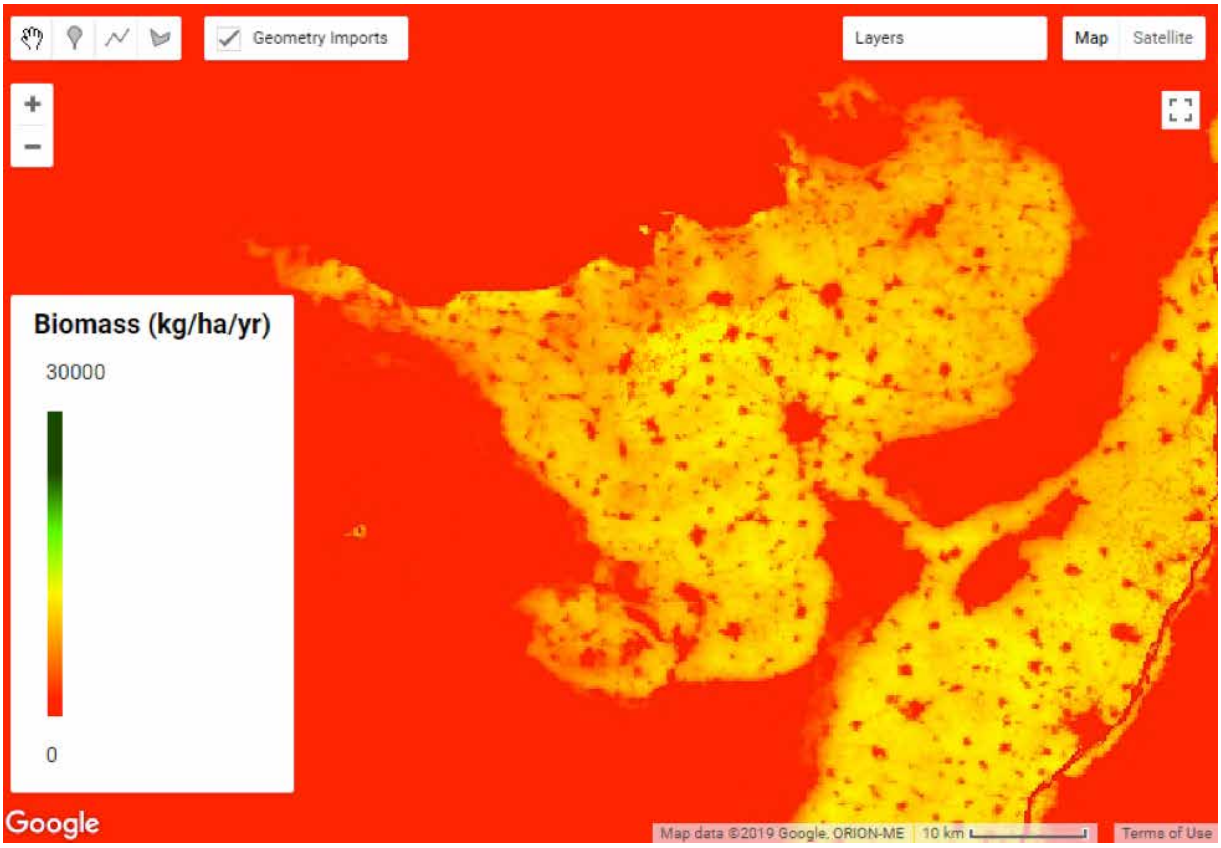

Figure 48

WaPOR derived yield for wheat (November 2015- May 2016) and maize (June-October 2016)

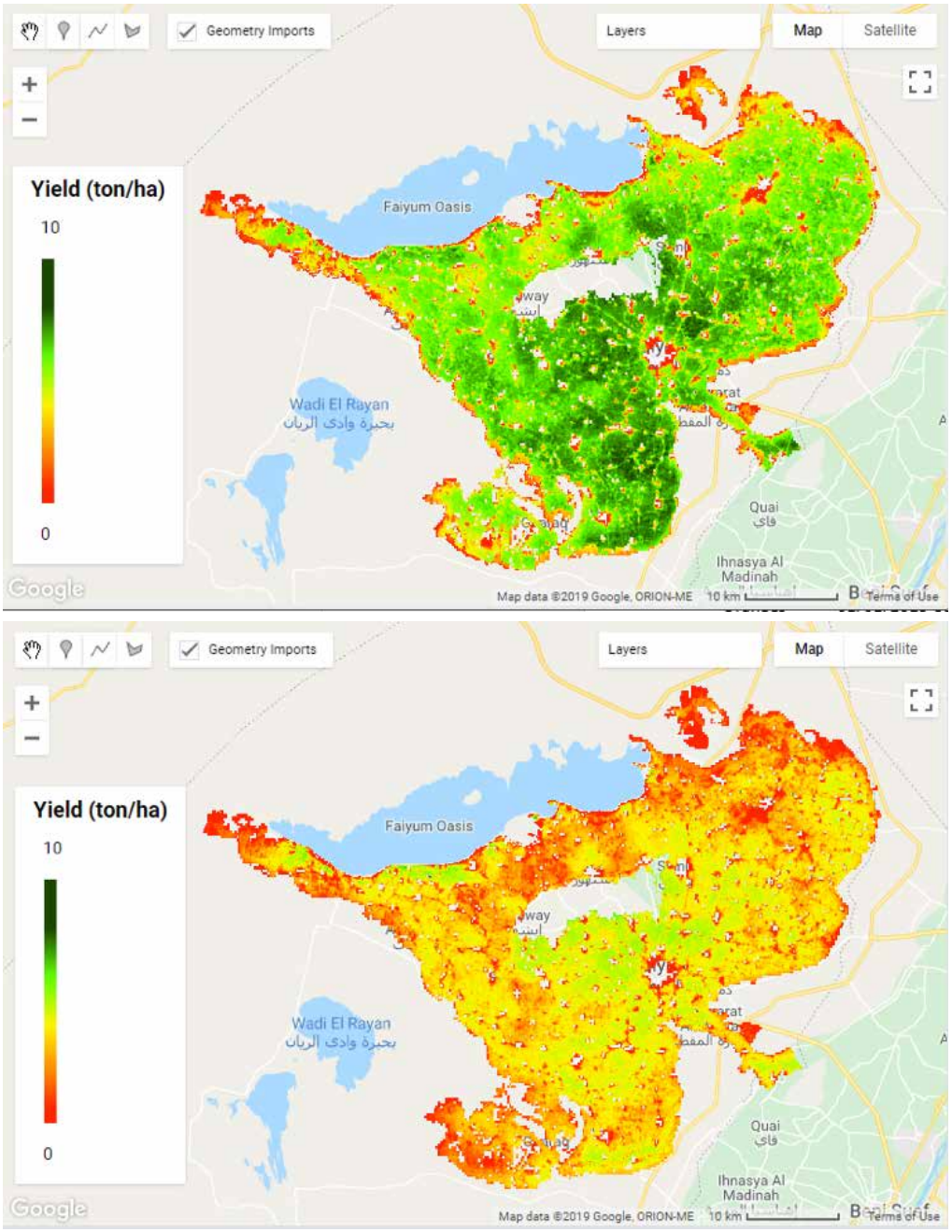

Table 30

Crop productivity Fayoum system

Crop	Cropping period	Harvest index	Moisture content	Average yield (tonnes/ha)	Literature values (tonnes/ha)*
Wheat (C3)	01/11/2015-31/05/2016	0.45	0.15	5.3	5
Maize (C4)	01/06/2016-31/10/2016	0.45	0.26	3.1	4.4
Oranges	01/01/2015-31/12/2015	0.22	0.85	17.7	20

* Salvadore, 2019

Figure 49

WaPOR yield distribution for wheat, maize and oranges in Fayoum irrigation scheme for the year 2015

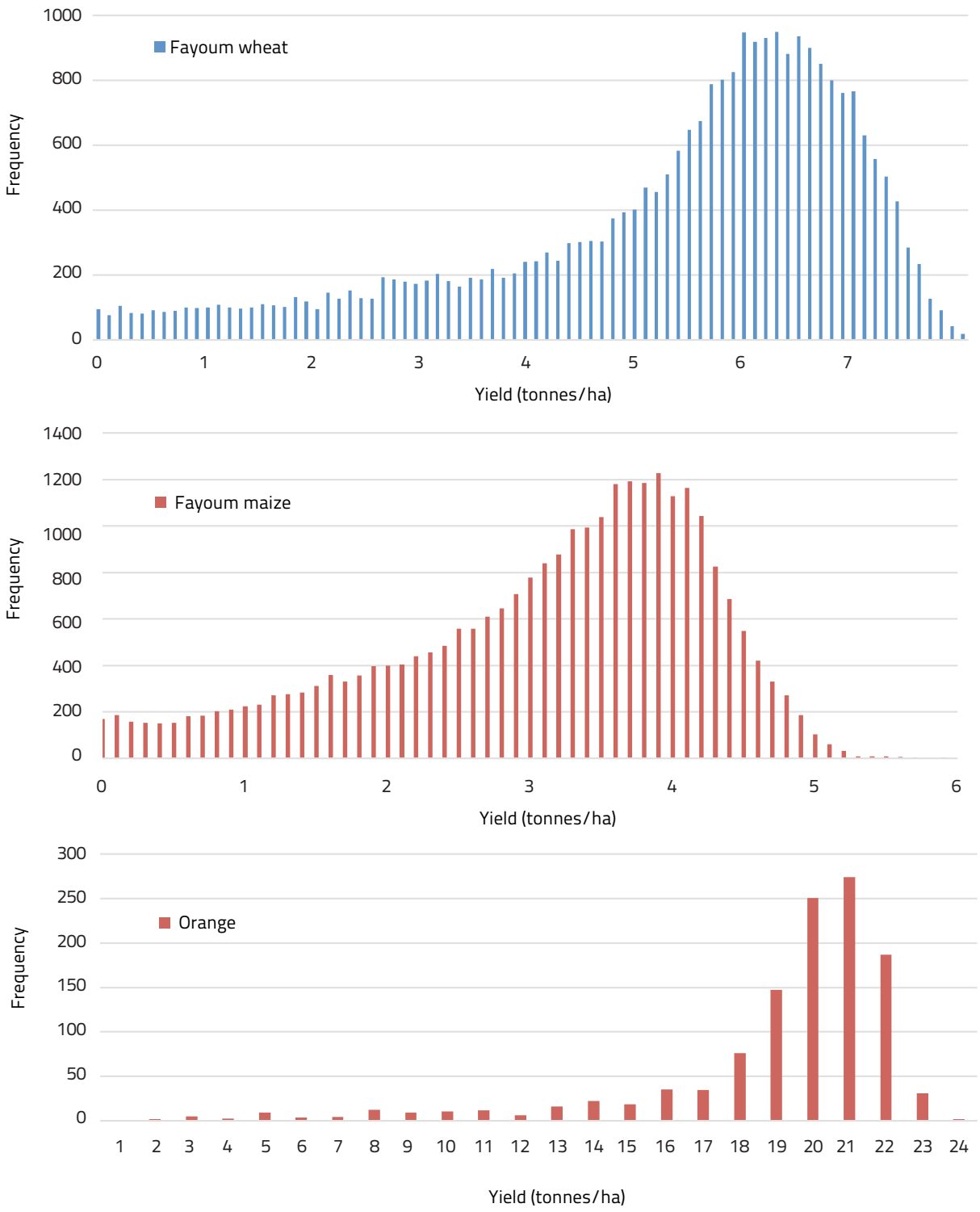

in WaPOR (FAO, 2018). NPP appears to lay in the same range for the NPP product based on MODIS images (MOD17), however there are also substantial differences between the two products. From this comparison, we cannot conclude that one of the products produces more realistic values that the other. However from the AETI comparison, WaPOR was much more accurate, and we therefore conclude that the differences observed do not necessarily mean WaPOR NPP and derived WaPOR AGBP layer is inaccurate.

The analyses show that the WaPOR AGBP layers are excellent proxies for crop yield, if the WaPOR database users have the proper skills to interpret the data. As there is a large range for total to above ground biomass production between different crop types, the first step is to revert to Total Biomass Production (TBP). The second consideration is that time integrated values of AGBP are required following the cropping season. The third one is that every crop has specific ranges of harvest index and moisture of the fresh harvestable product that need to be applied. These values require actually some local tuning. The last point is that C4 crops require an incremental TBP due to the fact that they are more efficient with solar light.

Yet, we demonstrate here examples from the Wonji sugarcane irrigation scheme in the Awash Basin that AGBP is a proxy for fresh yield. The conversion from AGBP to yield included conversion from AGBP back to TBP, crop specific ratio of ABGP over TBP, crop specific harvest index, C3 to C4 crop conversion, and moisture content of the crop. With these conversion factors, the estimation of yield for sugarcane in Wonji is within the expected range and in line with observed yield. Similar analyses for grapes in the Bekaa Valley, rice and bananas in Kpong irrigation scheme and wheat, maize and oranges in Fayoum give good results. It must be said that each conversion factor adds additional uncertainty to the yield estimations, but that the availability of WaPOR AGBP data with ten days intervals provides a solid fundament for any crop yield estimation process. You cannot estimate crop yield without spatiotemporal information on AGBP or TBP. It is the first time that such data is now available for the African continent for a period of ten years.

For the irrigation schemes located in the arid to semi-arid zones, agricultural lands can be clearly distinguished from the surrounding natural vegetation. The case studies in Ghana and Lebanon give good yield estimations, however the surrounding natural landscape reflects in similar fashion. However, total biomass production can be significantly under or over-estimated when the agricultural lands are not clearly defined.

B. Land cover classification

B.1 Introduction

The WaPOR Land Cover Classification (LCC) layer has different levels of detail for the different scales. At 250 m resolution, the WaPOR LCC has six land cover classes (natural vegetation, rainfed agriculture, irrigated agriculture, urban, bare soils and water). On the 100 m resolution, there are ten land cover classes, namely natural vegetation is split into tree cover, shrubland, grassland and wetland, whereas water is split into permanent and seasonal. At 30 m resolution, more detail of crop types are added for both rainfed and irrigated agriculture. The WaPOR LCC layer is based on NDVI and phenology and is generated using machine learning (FAO, 2018).

B.2 Data analyses

Database comparisons

The main application of the WaPOR database is agricultural productivity. Therefore, the identification of rainfed and irrigated agricultural areas are most important. Two datasets were used for comparison, the FAO based Global Map of Irrigated Area (GMIA) is part of the FAO AQUASTAT database (FAO, 2016) and the Global Irrigated Area Map (GIAM) (Dheeravath *et al.*, 2010). The GMIA includes sub-national irrigation statistics for most countries. The target year for the statistics is the year 2005. The spatial resolution of the map is 5 minutes. The information listed per country is a compilation of literature review and secondary data. The GIAM is an alternative spatial database developed by the International Water Management Institute (IWMI) using remote sensing data (http://waterdata.iwmi.org/applications/irri_area/), whereas GMIA database is a database compiled of national level data. GMIA is based on official statistics that are recognized by countries in spite of the lack of update through the statistical means[10]. The comparisons of WaPOR LCC (Level 2) for 18 countries against GMIA, and GIAM are summarized in Table 31. The three datasets do not have exactly same definitions in irrigated areas, but the direct comparison gives an indication of variations among the three sources.

Table 31

Rainfed and irrigated areas from WaPOR (2014), FAO AQUASTAT (2013-7) and GIAM (2010)

	Rainfed areas (ha)			Irrigated areas (ha)		
	WaPOR	GMIA	GIAM	WaPOR	GMIA*	GIAM
Benin	2 546 895	3 176 960	2 181 150	259 350	23 040	49 929
Ethiopia	18 398 918	15 400 700	21 381 713	872 852	858 300	2 247 969
Egypt	893 590	135 000	687 281	3 370 265	3 610 000	3 206 476
Ghana	2 100 164	7 400 000	4 371 500	203 445	30 900**	607 783
Mozambique	4 519 522	5 831 900	2 648 650	715 930	118 100	374 938
Jordan	691 069	218 600	360 256	47 872	103 400	92 006
Kenya	4 786 339	6 179 400	4 202 725	1 235 227	150 600	1 970 415
Lebanon	495 938	258 000	244 538	45 598	104 000**	250 831
Morocco	10 731 604	8 072 000	4 323 838	655 903	1 520 000	2 124 749
Mali	6 263 474	6 189 900	8 364 825	2 208 640	371 100	273 489
Occupied Palestinian territory	**402 615**	**148 000**		**13 474**	**24 000****	
Republic of South Sudan	1 102 896	2 721 900	3 757 100	141 527	38 100	31 637
Syria	6 284 334	4 392 000	2 458 456	429 646	1 341 000	1 125 514
Tunisia	5 128 812	4 745 400	488 638	159 046	486 600	1 701 626
Uganda	5 176 311	9 088 860	8 304 775	472 430	11 140	1 352 538
Yemen	164 884	1 546 000	2 546 863	627 716	454 300**	851 063
Total	**69 687 365**	**75 504 620**	**66 322 308**	**11 458 921**	**8 631 380**	**16 260 963**

* definition in AQUASTAT: Area equipped for irrigation - total

** FAO AQUASTAT statistics available before 2013

[10] http://www.fao.org/nr/water/aquastat/irrigationmap/index20.stm

Overall, it is difficult to draw conclusive observations from the comparisons, except that WaPOR lies in between GMIA and GIAM. GMIA data originates mostly from country reporting system and suffer from varying qualities in the process. GIAM on the other hand was produce

Correlation analysis in Figure 50 shows that overall WaPOR overestimated rainfed areas compared to both GMIA and GIAM. WaPOR estimated much larger rainfed areas for Morocco, occupied territories of Palestine, Syria and Tunisia. However in Ghana and Yemen, WaPOR underestimates rainfed areas compared to the other two sources. The irrigated areas of the three sources show larger variations among each other. Overall WaPOR values tend to be smaller or significantly smaller than the GIAM database. One key outlier is Mali, where WaPOR reported 2.2 million ha of irrigation while the other two sources reported 0.27 to 0.38 million ha only. For Mali, large parts of the Inner Niger Delta are classified as irrigated areas, in GMIA, these areas are likely reported under agricultural water management areas, which include wetlands and flood recession agriculture. The total area for this class in Mali in GMIA is 621 000ha, which is still well below the WaPOR estimates. Excluding Mali, for the remaining 11 countries where all three sources have data, the total irrigated areas reported by WaPOR is 101 percent of GMIA data on "Total area equipped for irrigation" but 59 percent of GIAM. GMIA is based on official national statistics and not updated regularly, it therefore does not always capture recent development in irrigation in Africa hence have a tendency to under report. Since the WaPOR LCC is reporting similar areas, it is therefore also under estimating the irrigated areas. WaPOR LCC for Ethiopia and Kenya suggest an area of 2.2 million ha, and this is a rather large discrepancy that can be associated to definitions and other factors. Nevertheless, it confirms that the WaPOR LCC seriously underestimates irrigated areas.

Comparison land use maps WA+ basins

As part of the FAO WaPOR project, IHE Delft is implementing Water Accounting studies for five river basins, Litani, Jordan, Awash, Nile and Niger. For the Water Accounting studies, a detailed land use map is required. A consultant was hired to develop detailed land use maps using a novel machine learning approach (Saah *et al.*, in preparation). It uses similar algorithms to WaPOR, such as the random forest regression method. For the land use classifications, reference data were collected from high resolution satellite imagery. Points were collected in

Figure 50

Comparisons of rainfed and irrigated areas in 18 countries from WaPOR, GMIA, and GIAM

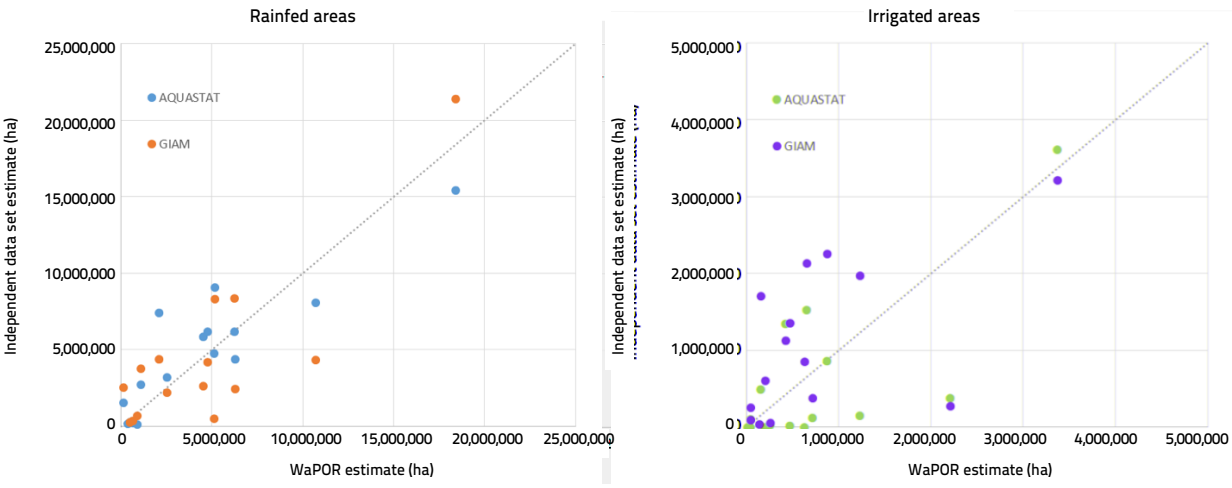

the categories water, barren, urban, field crops, tree crops, grass, forest, shrub and snow. High resolution earth observation data allowed to select locations with extended coverage of one particular class without spectral mixing from other classes. All points were sampled in one dataset (Poortinga *et al.* in prep. a&b). The resulting land use classification follows the Water Accounting Plus classification, differentiating between natural and managed land use classes. The WA+ land use classification for Litani, Jordan and Awash was available for the period 2009-2015, in addition to the land use classification for the Litani Basin developed and validated locally and made available by National Council for Scientific Research (CNRS) of Lebanon. These land use maps were compared to the WaPOR LCC 250 m and 100 m resolution (Figure 51).

In particular the comparison for the Litani River Basin is interesting, showing that the WA+ LCC is better in estimating LCC, in particular WaPOR LCC overestimates rainfed croplands and underestimates natural vegetation and bare soil. A similar trend is seen in WaPOR LCC of the Jordan River Basin, although no locally validated products were available for comparison, it is realistic to assume a similar bias (overestimating rainfed cropland) appears in the Jordan LCC. For the Awash Basin the WA+ LCC overestimated natural vegetation compared to bare soil, however in absence of a locally validated land use map, it is difficult to establish which LCC dataset is more accurate. In the Awash Basin the major difference is not related to agricultural land uses, making the bias less important for the WaPOR application. The bias in the Litani and Jordan Basin however need to be further investigated.

Figure 51

Comparison of WaPOR LCC with WA+ LCC in Jordan and Awash and local database (Litani)

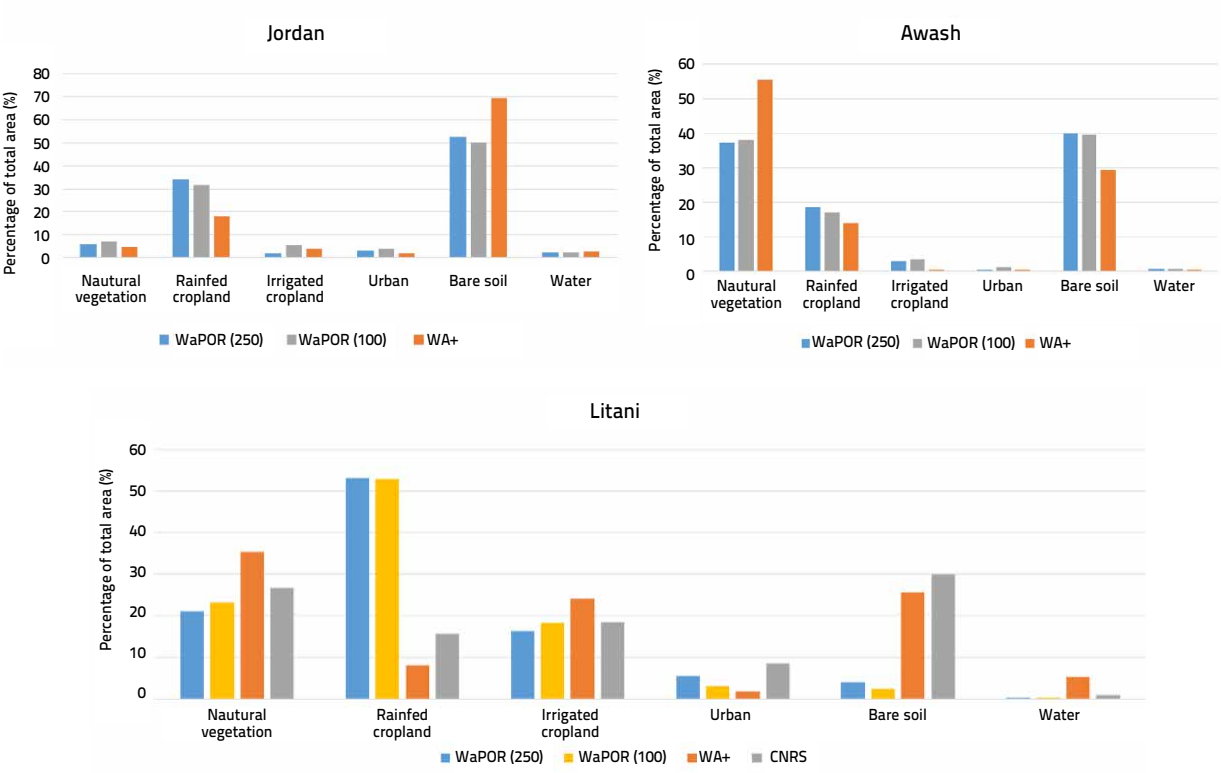

Comparison national statistics

Rwanda

In Rwanda two separate landcover maps were used to compare with WaPOR data. These two maps were from the Regional Centre for Mapping of Resources for Development (RCMRD) for year 2015 and Rwanda Water and Forestry Authority (RWFA) for year 2018. Table 32 shows that the three maps compare overall well with each other. The results of WaPOR and RCMRD in particular have a close match in natural vegetation, overall cropland area, and waterbodies.

Ground truth data comparison

We compared the 100 m resolution data of WaPOR LCC with ground truth data. We obtained some ground truth (GT) data for Ethiopia (142 fields) and Benin (115 fields) from the GIAM project. For these points specific data was therefore used to assess the classification accuracy. There were in total 142 GT points in Ethiopia collected in 2015. The 2015 GT data was used to assess the accuracy of the WaPOR 2014 LCC map. This was considered acceptable because in one year's time the conversion among four classes (natural vegetation, irrigated, rainfed agriculture, and urban areas) should be negligible. In Benin a total of 105 GT points, mostly in the southern part of the country, are available. Standard confusion matrix (Congalton and Green, 2008) were produced using these ground truth points adjusted according to the layers of the WaPOR LCC maps. In addition, where available government datasets were used to validate the WaPOR LCC maps.

Ethiopia

The accuracy for Ethiopia land cover map of 2014 is shows in Table 33. The overall accuracy is 64 percent for all four classes (91 fields out of 142 fields were identified correctly). The mapping accuracy is however higher for rainfed cropland at 79 percent (68 fields out 86 fields), and much lower for irrigated cropland at 26 percent (8 out of 34 fields). This confirms that many irrigation fields are missed by WaPOR.

Table 32

The comparisons of WaPOR LCC map with that from RCMRD and RWFA for Rwanda

	WaPOR		RCMRD		RWFA	
Class	Area [ha]	[%]	Area [ha]	[%]	Area [ha]	[%]
Natural vegetation	941 537	37.0	999 739	39.5	1 119 866	44.0
Rainfed cropland	1 329 599	52.3	1 340 508	53.0	1 220 830	48.0
Irrigated cropland	76 378	3.0	*	0.0		0.0
Urban	44 660	1.8	36 219	1.4	14 326	0.6
Bare soil	238	0.0	587	0.0	22 300	0.9
Water	151 340	5.9	152 119	6.0	166 313	6.5

* The RCMRD and RWFA maps do not separate rainfed and irrigated areas. They are presented together in the rainfed category

Table 33

Confusion matrix of WaPOR land cover map of Ethiopia for year 2014

		Groundtruth					
		Natural vegetation	Rainfed	Irrigated	Urban	Total	Error of Omission
WaPOR classification	Natural vegetation	13	18	8		39	0.67
	Rainfed	5	68	18		91	0.25
	Irrigated			8		8	0.00
	Urban	2			2	4	0.50
	Total	20	86	34	2	142	
Error of Commission		**0.35**	**0.21**	**0.76**			

Benin

The accuracy for Benin at 44 percent is much lower than for Ethiopia (Table 34). Most of the GT points are for natural vegetation and rainfed areas. The accuracy for rainfed areas are 46 percent and irrigated area at 0 percent. However, there were only two GT points for irrigated areas so this value does not represent a good indication of accuracy levels.

B.3 Conclusions

The WaPOR LCC layers provide different level of detail at different scales. At continent scale, land use is classified over six classes. Comparing the WaPOR LCC with other independent sources, shows that the accuracy was higher for rainfed cropland and other classes, compared to irrigated areas. It seems that WaPOR LCC significantly underestimates irrigated areas across the continent, and this negatively affects the utilization potential of the WaPOR database for assessing land and water productivity of irrigated areas. For two basins in the Middle East, WaPOR LCC significantly overestimates rainfed croplands over natural vegetation and bare

Table 34

Confusion matrix for WaPOR 2009 land cover map in Benin

		Groundtruth					
		Natural vegetation	Rainfed	Irrigated	Urban	Total	Error of Omission
WaPOR classification	Natural vegetation	18	42	1		61	0.70
	Rainfed	15	33	1		49	0.33
	Irrigated	2	1			3	1.00
	Urban	2				2	1.00
	Total	37	76	2	0	115	
Error of Commission		**0.51**	**0.57**	**1.00**			

soil. Comparing WaPOR LCC with GT points in Ethiopia and Benin does not show high level of accuracy (64% for Ethiopia and 44% for Benin).

Comparing a continental product such as WaPOR LCC with sub-national land cover may be misleading, as the machine learning has to be able to deal with a large range of agro-ecological zones covered by WaPOR. Developing classifiers for specific agro-ecological zones is much easier than making them work for a whole continent. However, a reliable LCC is important for the conversion of biomass production into fresh crop yield. There is an urgent need to refine WaPOR LCC, and in particular to improve the methodology of identifying new digital surveying procedures based on high resolution satellite images (e.g. Chen *et al.*, 2018)

C. Phenology

C.1 Introduction

The WaPOR phenology layer determines the start, maximum and end dekad of a cropping season, based on changes in NDVI (van Hoolst *et al.*, 2016). It is available for WaPOR Level 2 (100 m) and Level 3 (30 m).

C.2 Data analyses

Two examples of the WaPOR phenology layers are presented in Figure 52. The cropping seasons in Africa are directly linked to the Inter Tropical Conversion Zone (ITCZ), which moves across the continent. The seasons in Southern Africa starts in October the previous year, East-Africa (northern Tanzania, Kenya and Ethiopia) experiences a bimodal season, with the first starting in March and the second season starting in October. West Africa experiences rainfall starting from the coast around April and further north towards the Sahel, the season starts around June, July. These seasonal variations are generally well captured across the continent (Figure 52).

Figure 52

WaPOR phenology for selected 100 m countries expressed in terms of the start of season 1 and 2 in 2015

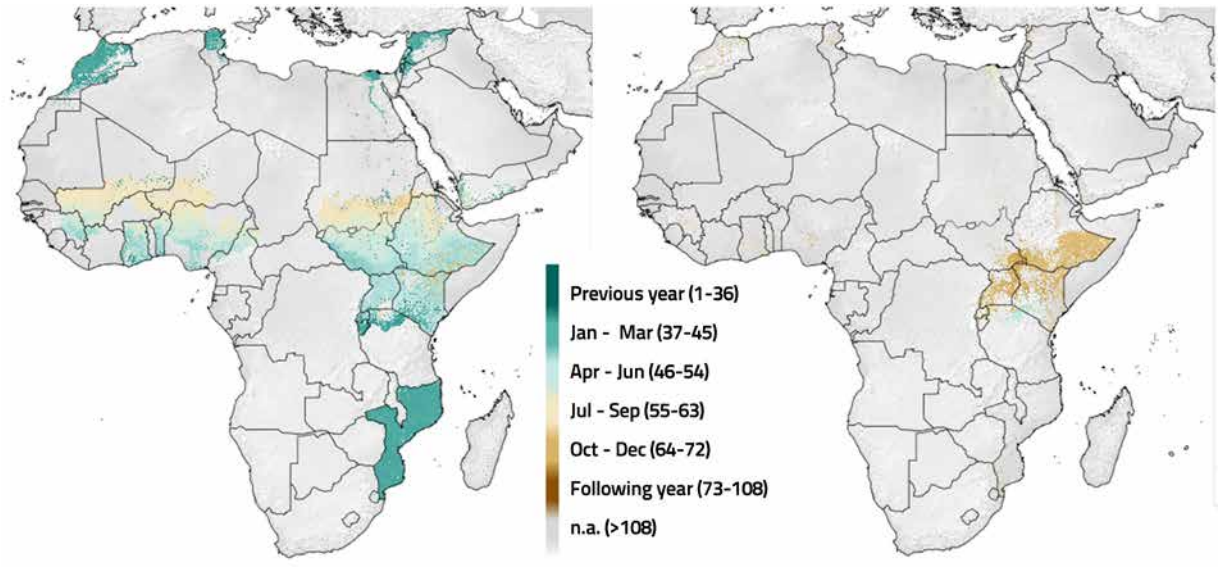

WaPOR AGBP (kg/ha

Country level analyses

A more detailed analyses is done for the start of the cropping season in Ghana (Figure 53). The WaPOR phenology layer for the cropping season shows a slight gradient of the start of the cropping season from south to north. A comparison between 2009 and 2015, shows that the cropping season in the north of Ghana was delayed significantly (by almost two months). The staple crop grown in northern Ghana is maize and the starting season of the crop is in line with the actual start of the cropping season as shown by the WaPOR phenology layer. At country level, the WaPOR phenology layer generally presents the start of the cropping season well.

Comparison for irrigation schemes

Kpong right bank irrigation is located in southern Ghana along the Lower Volta River, and supplied by the Kpong reservoir. The irrigation schemes is a combination of smallholder farmers growing rice and vegetables and commercial farmers growing bananas. The bananas grow in a rotational system, throughout the year, so there is not a predefined start of the cropping season. Rice is grown twice a year, with the first season starting in March/ April and there is an overlap between the harvesting of the first season and the sowing of the second season in August/ September (Table 35).

The WaPOR phenology for the start of the first season is presented in Figure 54. In 2015, the start of the first season for the smallholder area is anywhere from starting in the previous year (areas in red) to starting in May (bright green) the surrounding area and patches within the smallholder system start in March-April. For the banana area, the start of the season is not expected to be uniform (as the farmer tries to harvest bananas across the year). The area shows specific patches starting in particular periods. In this case, the WaPOR phenology layer is not able to accurately capture the cropping season of the irrigated rice areas (Table 36), which has a distinct season (Table 35), which affects the computation of the accumulated biomass production (AGBP and TBP) across the growing season.

Figure 53

Start of cropping season in Ghana (2009, 2015 and FAO stats)

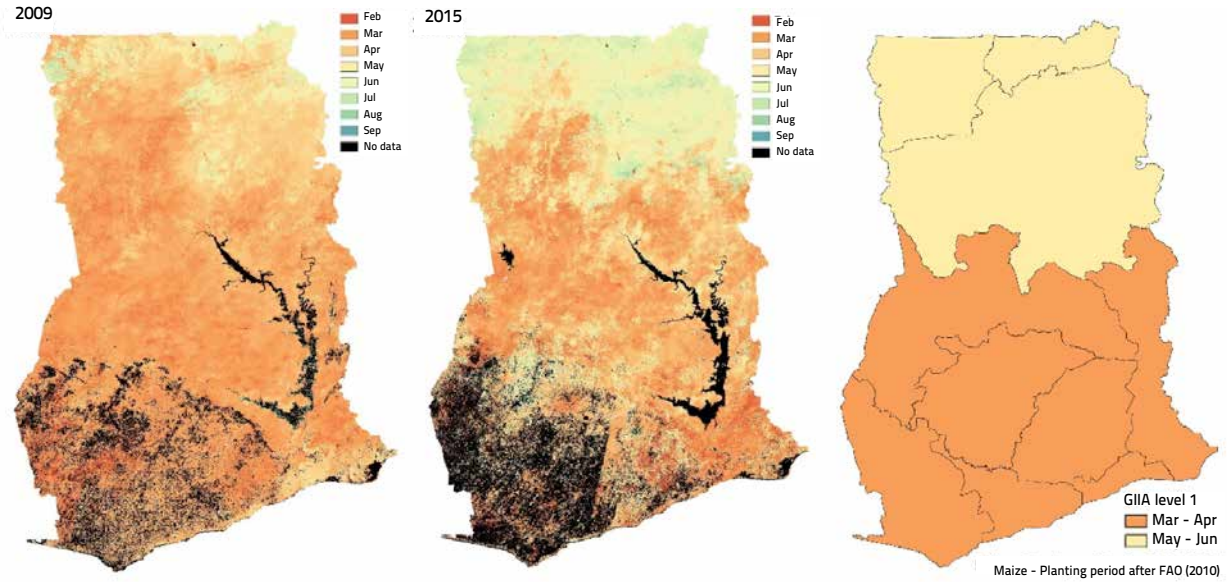

Table 35

Cropping season in Kpong irrigation scheme

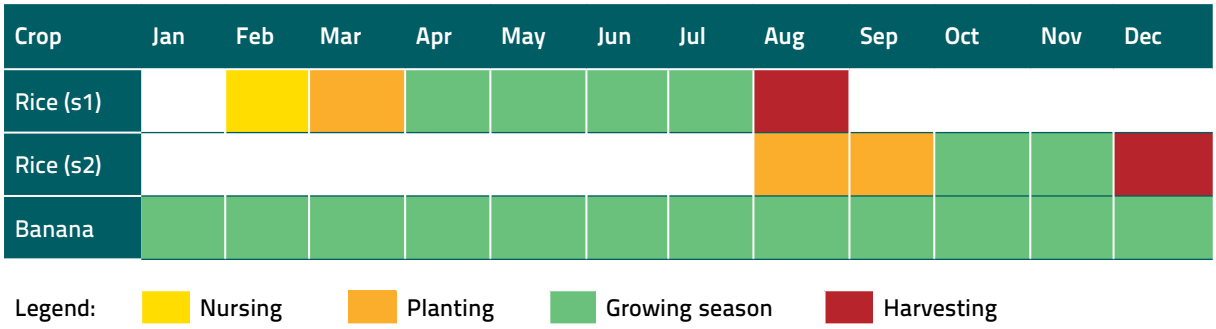

Source: Gida, 2010

The WaPOR phenology layer manages to predict the start of the first cropping season for rice (on average), however the standard deviation is very large (plus or minus 190 days). WaPOR completely misses to identify the second season of rice; the average duration of the season is similar to what is happening in the field, but again the standard deviation is very large. For bananas, the start of the season is more defined, however the start of the season for bananas is not uniform to allow for harvest throughout the year. WaPOR accurately predicts a longer growing season for bananas (Figure 54 and Table 36). When comparing the irrigation scheme with the surrounding landscape there is little to differentiate the two.

Fayoum irrigation scheme

The largest area of the Fayoum irrigation scheme is a rotational cropping system of wheat and maize (Table 37). A section of the irrigation scheme is covered with orchards. The WaPOR phenology layer seems to be able to identify the start of the wheat season (Figure 55), however the standard deviation is seven months (Table 38), potentially identifying the two starts of the cropping season and classifying them under one season. The duration of the cropping season as identified by WaPOR is also on the short side (2-3 months).

Table 36

WaPOR phenology indicators for Kpong irrigation scheme in 2015 (mean and standard deviation)

	Start of season 1	Duration of season 1	Start of season 2	Duration of season 2
Rice	20 March ± 6 month	188 ± 69	20 March ± 9 months	130 ± 37
Banana	10 April ± 3 months	251 ± 52	10 April ± 10 months	161 ± 23

Figure 54

Start of season 1 and length of season at Kpong irrigation for 2015

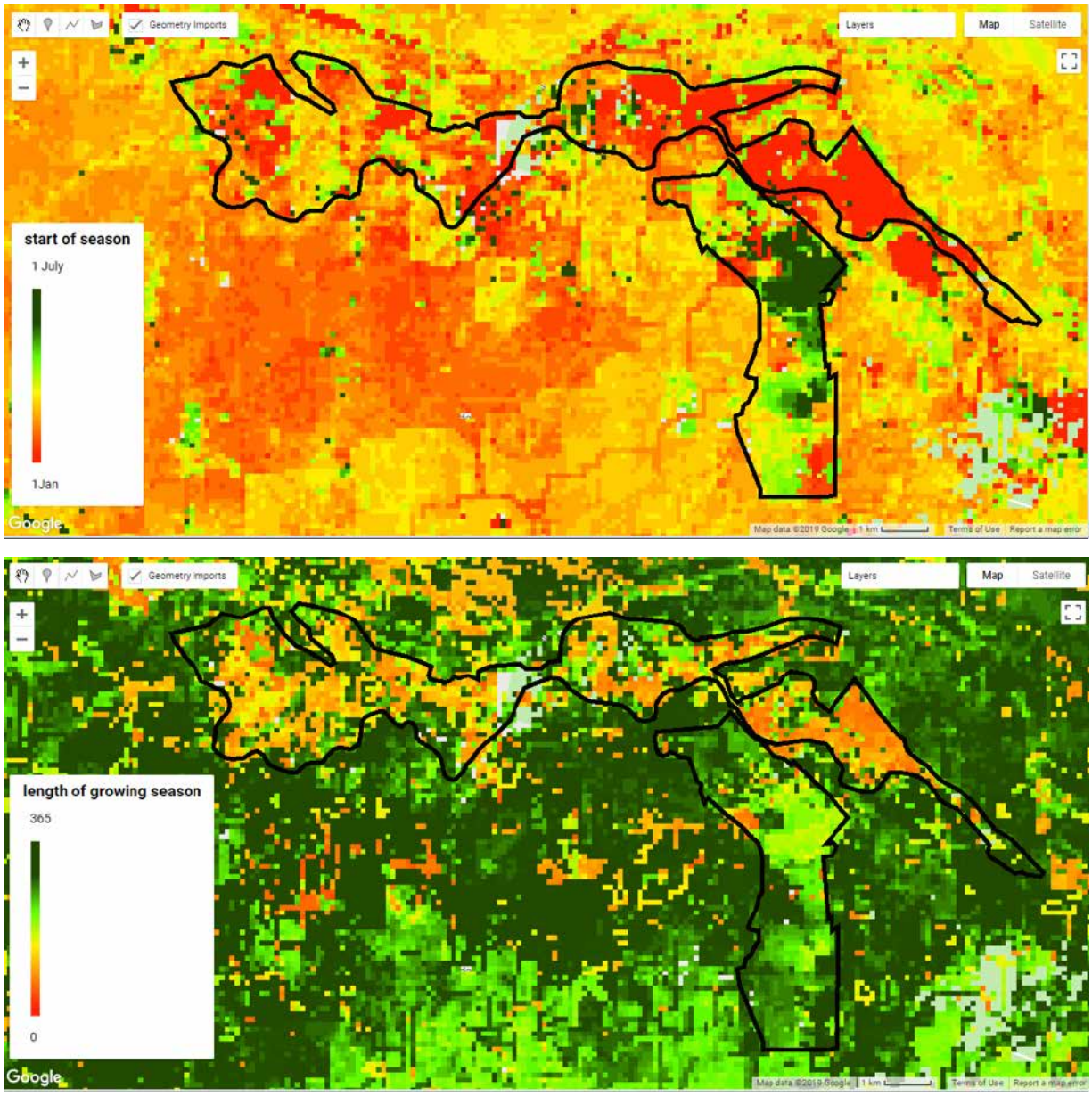

Wonji irrigation scheme

The area under investigation is planting sugarcane throughout the year to ensure continuous harvesting, there is therefore no specific time of the year when the cropping season starts. The start of the cropping season as identified by WaPOR varies across the year, consistent with what we know from the system. However, for various areas, WaPOR is not able to identify a cropping season at all, which for sugarcane is acceptable (Figure 56). The biomass map (Figure 39) also shows various areas that are left fallow, so this could be correct. The cropping season for sugar cane is somewhere between 12 and 18 months (Yilma, 2017), whereas WaPOR estimates the duration of the cropping season between six to ten months (Table 39).

Table 37

Cropping season in Fayoum irrigation scheme

Crop	Jan	Feb	Mar	Apr	May	Jun	Jul	Aug	Sep	Oct	Nov	Dec
Rice (s1)												
Rice (s2)												
Banana												

Legend: Planting Growing season Harvesting

Source: Salvadore, 2019

Figure 55

Start of season 1 and length of season at Fayoum irrigation scheme for 2015

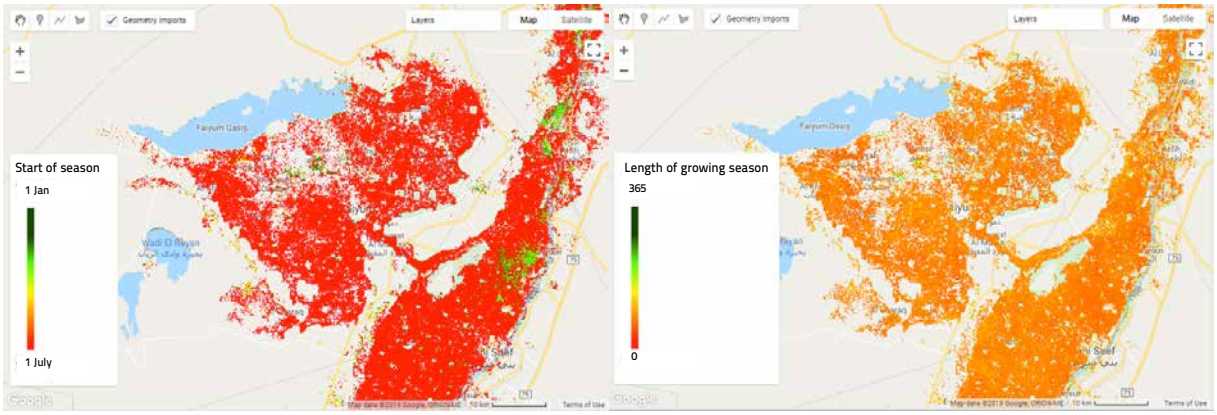

Table 38

WaPOR phenology indicators for Kpong irrigation scheme in 2015 (mean and standard deviation)

	Start of s1	Duration of s1	Start of s2	Duration of s2
Fayoum	10 October ± 7 months	73 ± 14	10 October ± 7 months	73 ± 14

Bekaa Valley irrigation

The irrigation in the Bekaa Valley, located in Lebanon follows the seasonality. An example of the cropping season of a typical crop in the Bekaa Valley, potatoes, is provided in Table 40 (Alvarez-Carrion, 2018). Another wide spread crop is wheat, which has for the winter varieties a cropping season of 100-170 days and for the summer varieties 180-300 days. Because of the heterogeneity of the crop production in the Bekaa Valley it is difficult to identify if the cropping season is well determined (Figure 57; Table 41).

Figure 56

Start of season 1 and length of season at Kpong irrigation for 2015

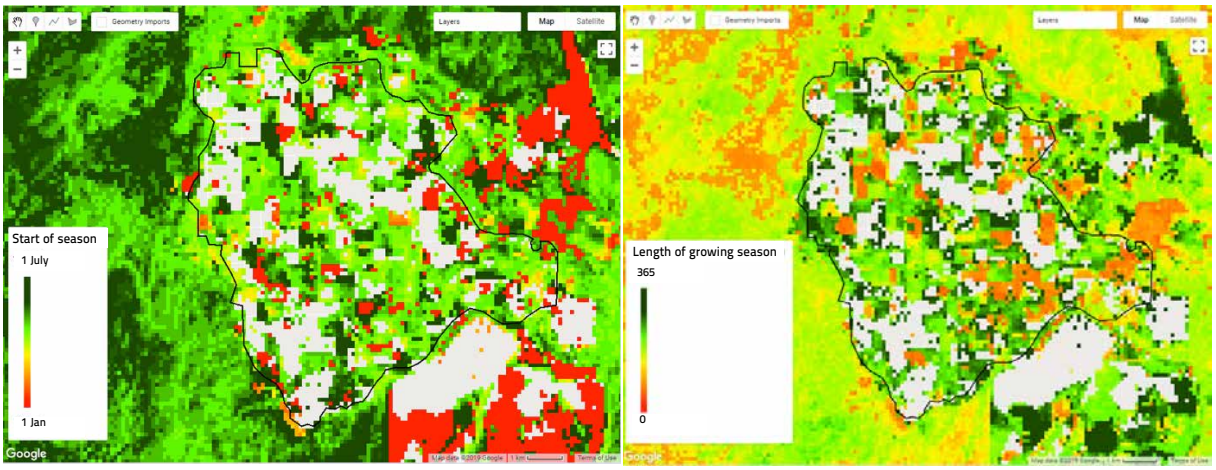

Table 39

WaPOR phenology indicators for Kpong irrigation scheme in 2015 (mean and standard deviation)

	Start of s1	Duration of s1	Start of s2	Duration of s2
Wonji	10 November ± 1 year	186 ± 61	20 April ± 10 months	104 ± 44

Consistency season 1 and season 2

The WaPOR phenology produces separate layers for the start of season 1 and season 2. An analysis was done on the start and end of all seasons identified by WaPOR for an area in Rwanda (Braliwa farms) (Figure 58). The area is located in East Africa and experiences a bi-modal rainy season, with one season starting around October until January and a second season from March to June. The season 1 (each red line in Figure 58 represents one pixel), in 2009 line up nicely. For 2010, some pixels span both the season November-January and March-June, other pixels have the season October-January identified as season 2 for 2009 (green lines) and others have identified the same season as season 1 for the year 2010. For the season October 2011-January 2012, the pixels are evenly identified as 2011 season 2 and 2012 season 1. For some pixels the same season is both identified as season 2 of a previous year and season 1 of the following year (Annex E).

Table 40

Cropping season of potatoes in Bekaa Valley irrigation

Crop	Jan	Feb	Mar	Apr	May	Jun	Jul	Aug	Sep	Oct	Nov	Dec
Rice (s1)	G	H	H	H							P	P
Rice (s2)				P	P	G	G	H	H			
Banana						P	P	G	H	H		

Legend: P Planting G Growing season H Harvesting

Source: Alvarez-Carrion, 2018

Figure 57

Start of growing season 1 and length of growing season Bekaa Valley

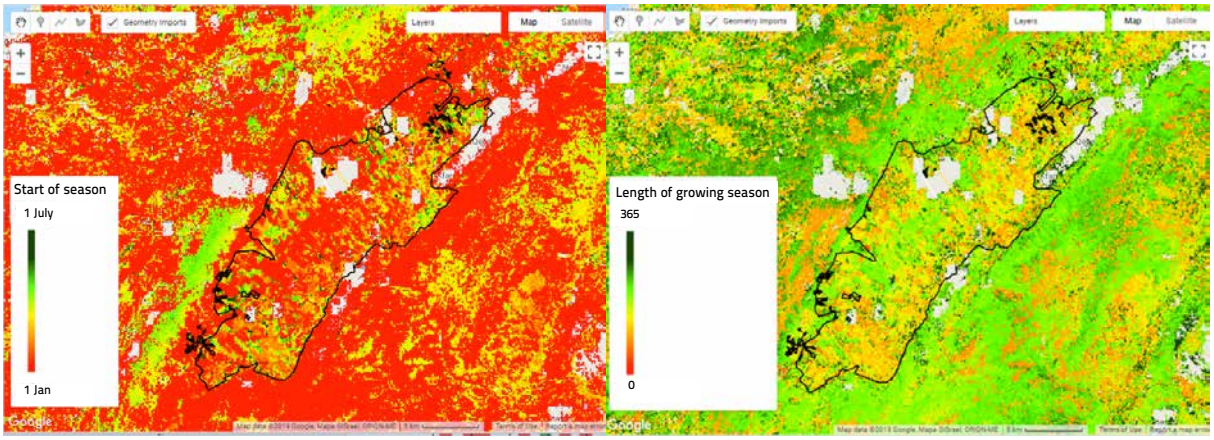

Table 41

WaPOR phenology indicators for Bekaa Valley irrigation in 2015 (mean and standard deviation)

	Start of season 1	Duration of season 1	Start of season 2	Duration of season 2
Bekaa Valley	20 Feb ± 6 months	162 ± 41	20 Feb ± 8 months	85 ± 24
Bekaa_grapes	1 Feb ± 2 months	166 ± 47	20 March ± 8 months	101 ± 31

Figure 58

Season 1 and season 2 pixel identification

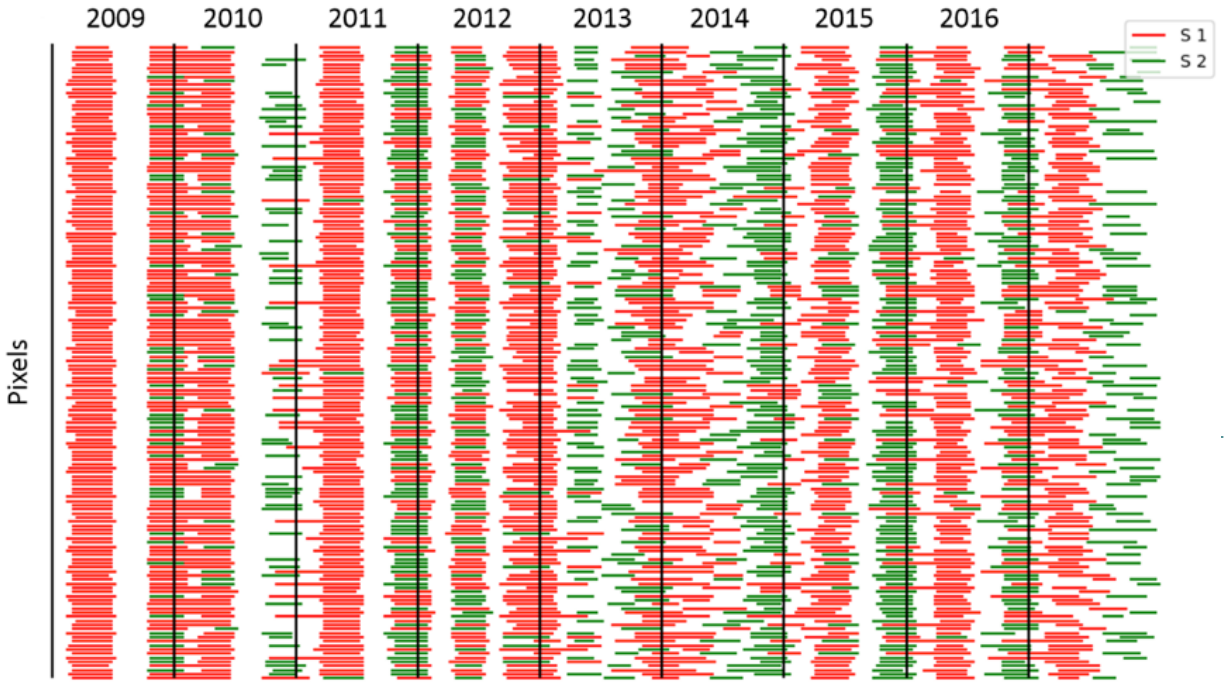

C.3 Conclusions

The WaPOR phenology layer generally presents the cropping season as expected at basin and national level, following the general seasonality. However, when zooming into specific areas, the phenology layers has some serious issues in adequately representing the cropping seasons. This is crucial for the WaPOR portal, as water productivity is calculated on seasonal basis at Level 2, together with its inputs: seasonal AGBP and seasonally cumulated AETI. If the season is not well defined, all other parameters are affected by this error. Also, the shift between the two seasons, creates maps that are composed of pixels showing two different seasons. This makes it difficult to analyse the data, also it hampers identifying trends between one year to the next (as it is not clear if season 1 for year 1 is the same period as season 1 for year 2).

The main observation is that both crop types and cropping seasons cannot be obtained from WaPOR. Users have to prepare their own crop masks and select the local cropping calendar. Only with this extra GIS processing, land productivity, water productivity and crop water consumption can be properly estimated. It is recommended that FAO and/or FRAME consortium will make this limitation and opportunity clear to website visitors.

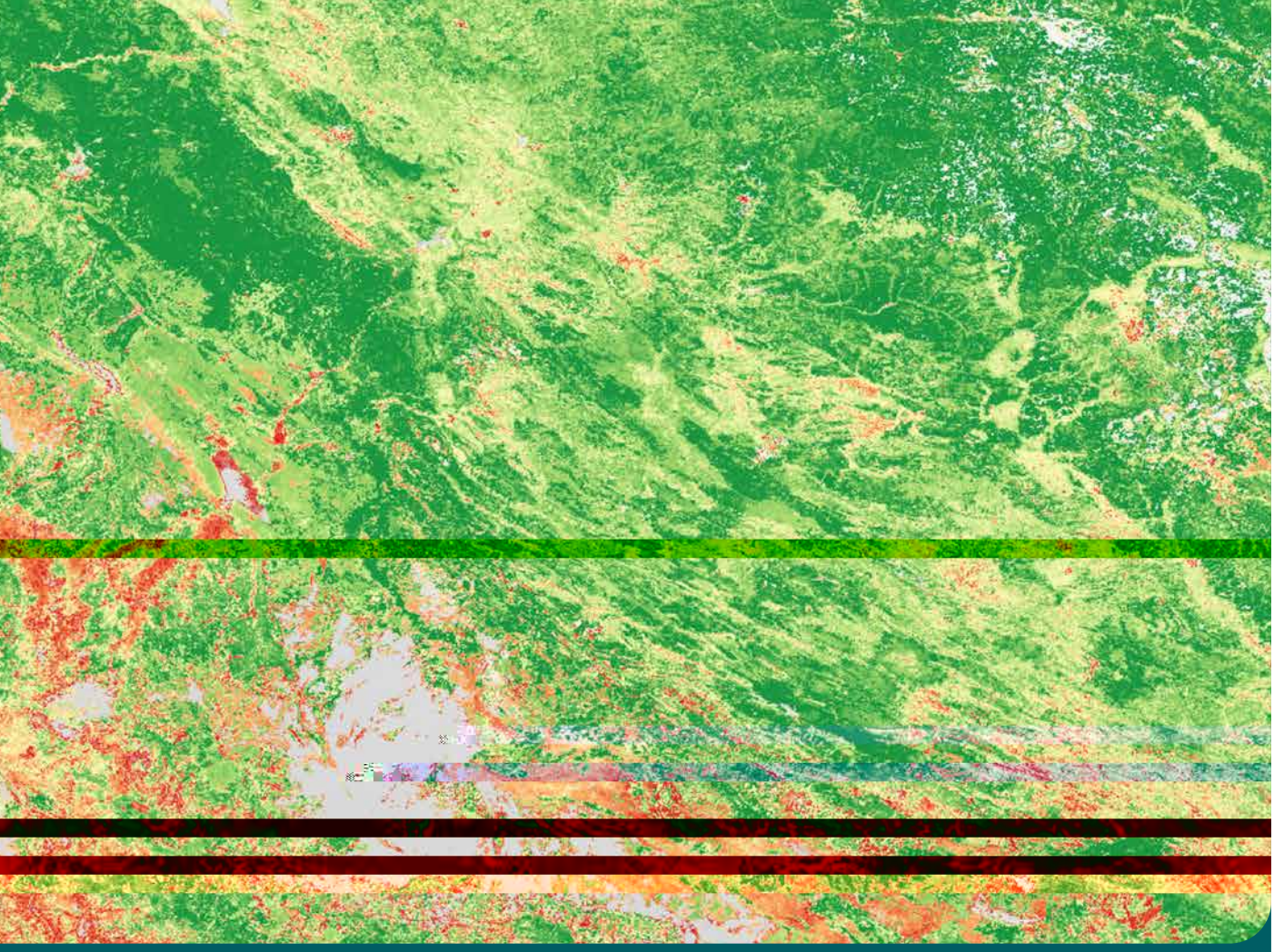

Detail of WaPOR Map "Net Biomass Water Productivity 2014 - Iraq and Iran"

5. Water productivity

A. Gross Water Productivity

A.1 Introduction

The WaPOR Water Productivity (WP) layers are based on a simple calculation of AGBP over AETI (gross biomass WP or GBWP) and AGBP over T (net biomass WP or NBWP). The uncertainty of water productivity is therefore directly related to the datasets of AGBP, AETI and T. The WaPOR data portal provides WP for integrated time intervals. The 250 m resolution integrates WP on annual basis, whereas the 100 m and 30 m resolution data integrates based on the WaPOR defined seasons.

A2. Data Analyses

The WaPOR values for gross and net WP are presented in Figure 59. The average continental value of GBWP is 0.66 and for NBWP is 1.20. At first sight it is obvious that the arid zones exhibit lower WP values. This can be explained by the fact that relative humidity and T are inversely related (low humidity will induce high T flux) while the C flux is unaffected. The H_2O and CO_2 fluxes have to pass through the same stomatal aperture, and this climatological control of WP by air humidity (thus also indirectly induced by air temperature) was recognized since the 1960s

(Bierhuizen and Slayter, 1965). Indeed, the humid areas of Central Africa and the Atlas mountains in Morocco and Algeria show the highest WP values, and these agro-ecosystems behave according to the theoretical expectations.

Some more attention should be provided to NBWP because biomass production per unit of transpiration is often suggested to be conservative. It is also commonly referred to as the Transpiration Efficiency. Transpiration Efficiency (TE) is a main feature in AquaCrop (Raes *et al.*, 2011). The average value of 1.2 kg/m^3 for NBWP for the continent is on the low side, as the conservative relationship between biomass and transpiration for C3 crops should be between 1.5 and 2.0 kg/m^3 (Raes *et al.*, 2011; Steduto *et al.*, 2007).

Spatial data comparison

We compared WaPOR gross WP with a similar product of Servir Mekong produced by Poortinga and co-workers (Simons *et al.*, 2017). The global WP map created by Servir uses the MODIS Terra NPP values and the SSEBop AETI calculations and is therefore expressed in 0.1*kg C/m^3 (Figure 60). We used the WaPOR NPP data and WaPOR AETI to calculate WP in the same manner (converting to DM using the same conversion factors would result in the same biases). The comparison shows large deviations between the two products, this can be both a result of the differences in AETI or NPP. NPP differences between WaPOR and MOD17 (averaged for Terra and Aqua though) were discussed in the earlier section on NPP, so we think the major difference originates from AETI values estimated by SSEBop. Because WaPOR AETI was properly checked with water balances, it is believed that WaPOR WP values are more accurate than the WP version created by Servir.

Figure 59

Average WaPOR gross biomass WP (GBWP) and net biomass WP (NBWP) for 2009-2017. Note that GBWP and NBWP are based on AGBP, thus ignore 35% of the total dry matter production

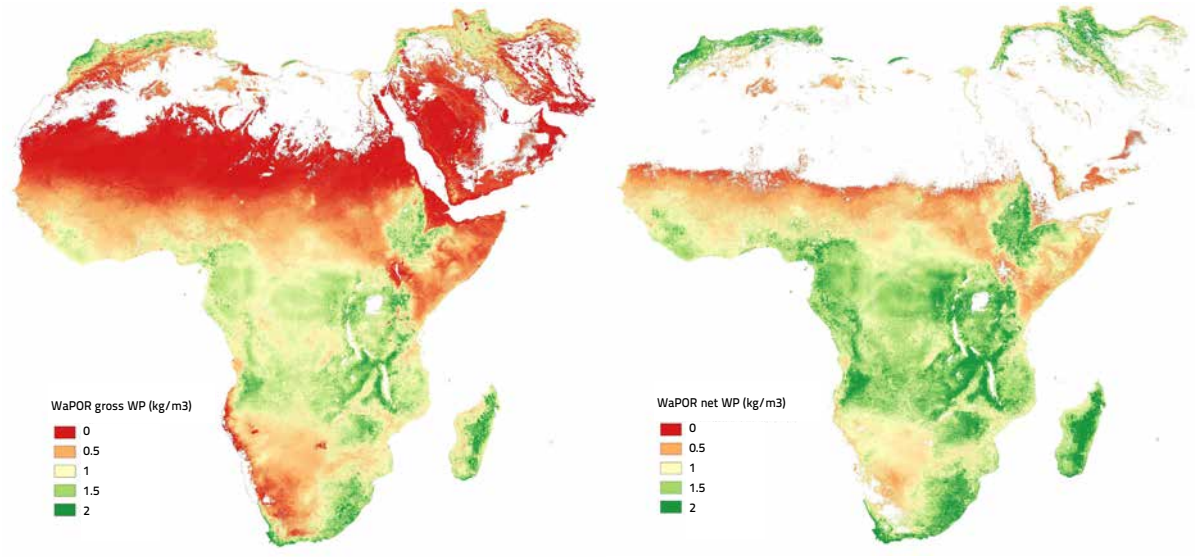

Figure 60

Servir WP in 0.1*kg C/m^3 and difference between Servir and WaPOR WP in 0.1*kg C/m^3 (2009-2013)

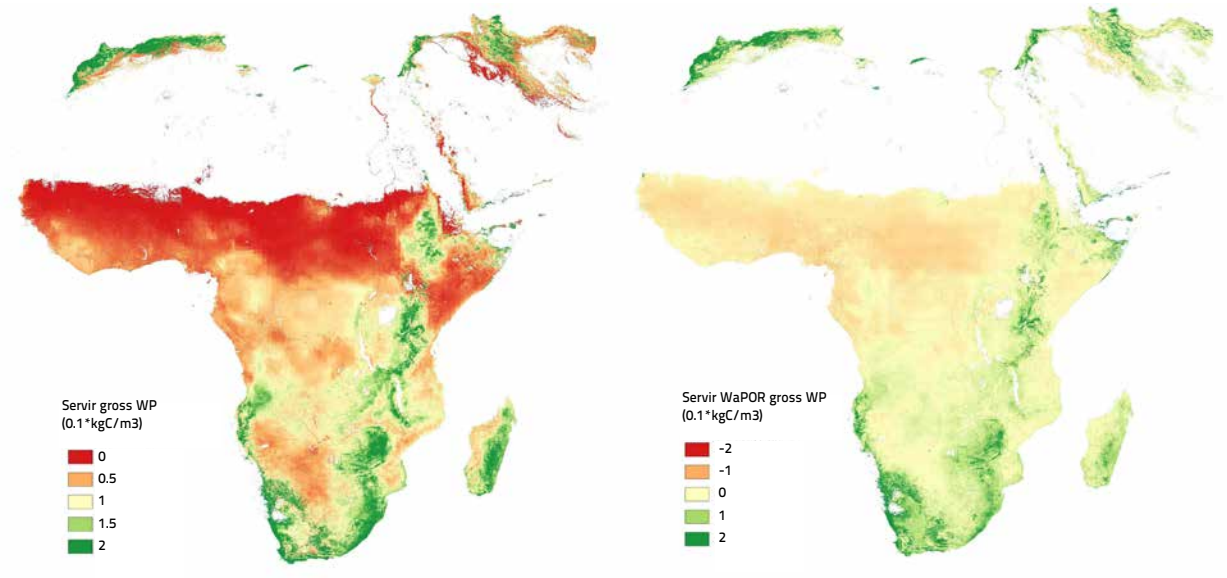

Water productivity for selected irrigation scheme

Gross and net Water Productivity (WP) was calculated for three of the four irrigation schemes. The Bekaa Valley with the diverse cropping system was not included for the analyses. WP is defined as the yield per unit of water (kg/m^3), the gross WP uses the total water consumption (AETI), whereas the net WP uses T for unit of water beneficially consumed.

Wonji irrigation scheme

The gross WP for sugar cane in the Wonji irrigation scheme, was calculated using the 30 m resolution data (Figure 61). Gross WP is 5.22 kg/m^3 (Table 42), which is on the low side compared to the range of 5.9-6.6 kg/m^3 found by Yilma (2017). The values found by Yilma were individual plot values, whereas the WaPOR data is an integrated value of the entire area, including fallow plots and buildings and areas with open water, thereby lowering the average value for gross WP. The WaPOR estimated value for gross WP is therefore in the correct range.

Figure 61
Gross WP for Wonji (30 m resolution)

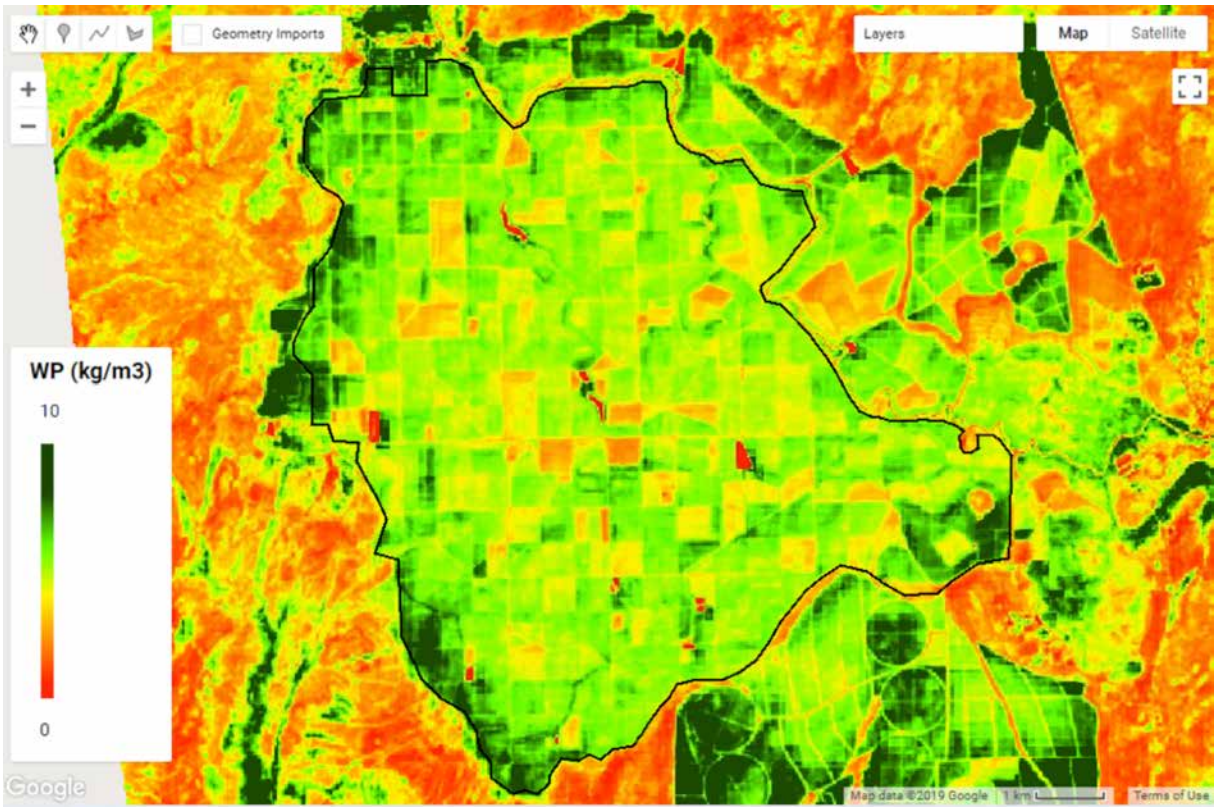

Table 42
Key indicators for Water Productivity in Wonji irrigation scheme

	Yield (tonnes/ha)	AETI (mm/season)	T (mm/season)	Gross WP (kg/m^3)	Net WP (kg/m^3)
Sugarcane	99.85	1,926	1,638	5.22	6.13

Fayoum irrigation scheme

The gross and net WP for the Fayoum irrigation scheme are presented in Figure 62 and Table 43. Salvadore (2019) found for wheat gross WP of 0.94, for maize 0.75 and for oranges 1.55 kg/m^3. The values found using WaPOR data are slightly higher. The areas presumed to be fallow (low biomass production, see also Figure 48) around the edges of the irrigation scheme show the highest gross WP. This indicates that WP on its own is not a good indicator for agricultural productivity. Considering these differences, the WaPOR gross WP values provide a good reference for WP calculations.

Figure 62

Gross Water Productivity wheat and maize

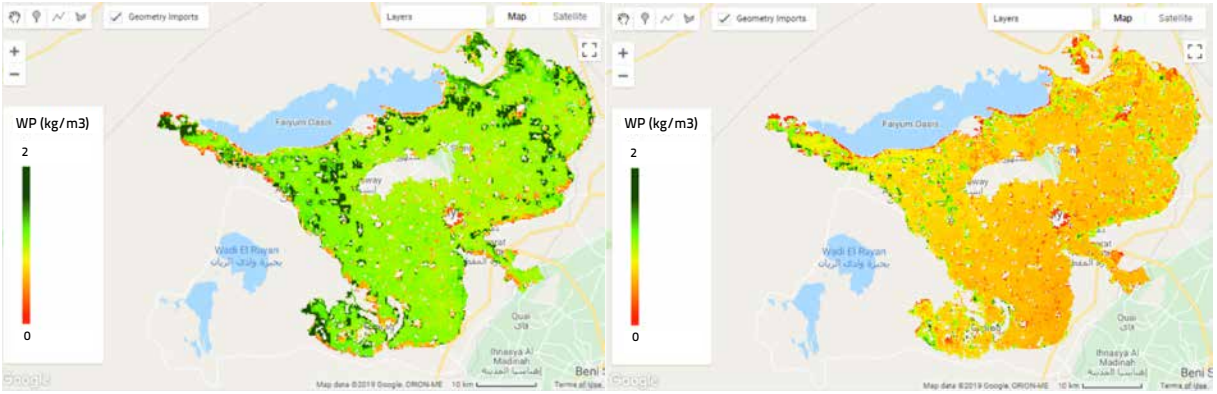

Table 43

Key indicators for Water Productivity in Wonji irrigation scheme

	Yield (tonnes/ha)	AETI (mm/season)	T (mm/season)	Gross WP (kg/m^3)	Net WP (kg/m^3)
Wheat	5.28	248	178	1.11	1.25
Maize	3.14	244	159	0.69	0.87
Oranges	24.69	485	333	1.83	2.02

Kpong irrigation scheme

The gross WP for Kpong irrigation scheme is presented in Figure 63 and 64 and Table 44. The gross WP for rice 1.18 and for banana it is 4.85 kg/m^3. We did not have locally verified values to compare the gross WP with. However, what is clear is that in humid climate, the differentiation between agricultural land and natural vegetation is not clear. For rice during both seasons, the surrounding landscape seems to have higher WP compared to the irrigated system. Without a detailed land use map it is not possible to correctly estimate agricultural water productivity, as natural vegetation would be erroneously included in the biomass production estimations.

Figure 63

Kpong gross WP rice season 1 (top) and season 2 (bottom)

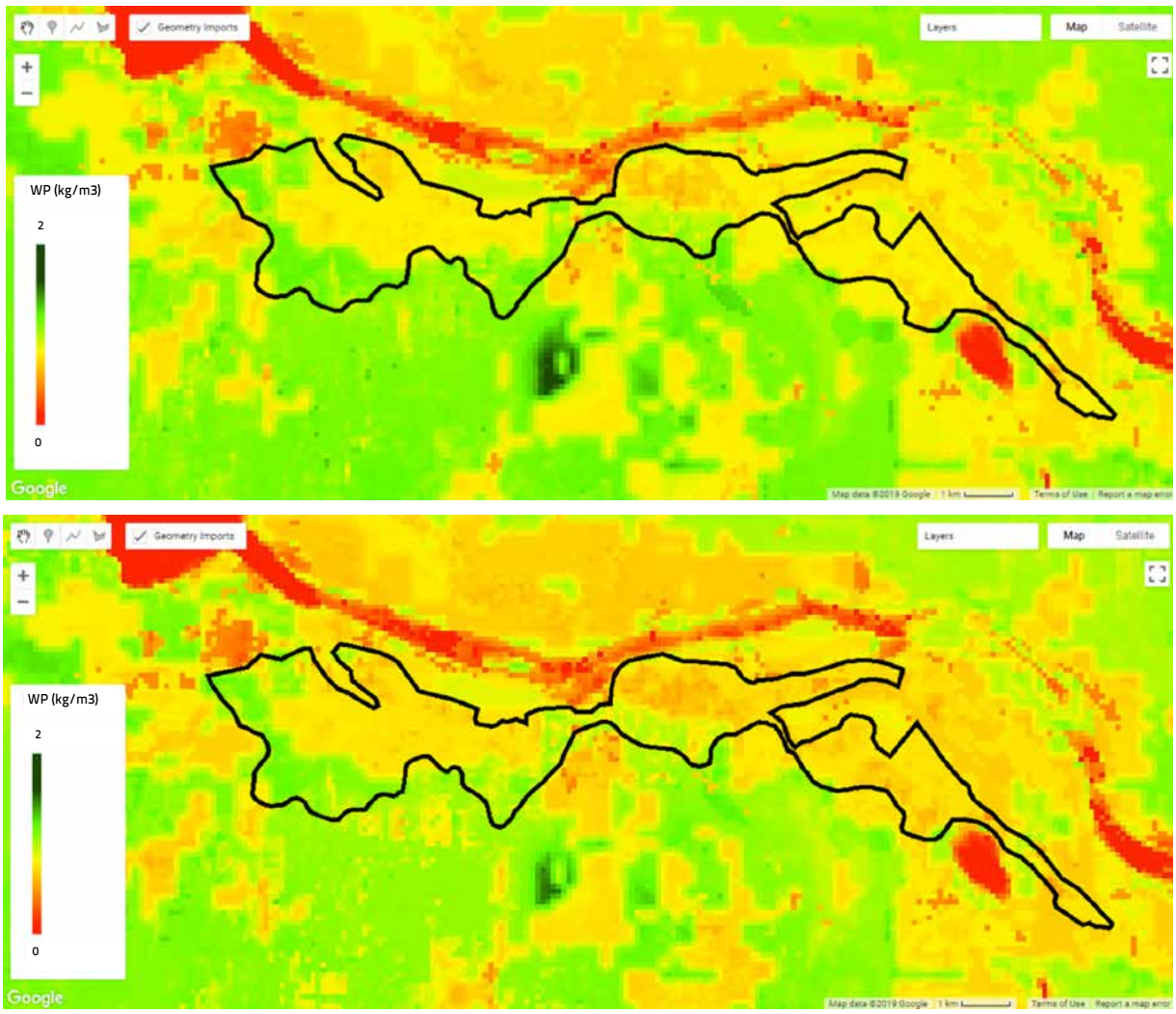

Table 44

Kpong gross WP rice season 1 (top) and season 2 (bottom)

	Yield (tonnes/ha)	AETI (mm/season)	T (mm/season)	Gross WP (kg/m^3)	Net WP (kg/m^3)
Banana	37.59	1,022	793	3.72	4.85
Rice s1	4.15	495	356	0.86	1.25
Rice s2	3.99	503	382	0.82	1.11

Figure 64
Kpong gross WP bananas

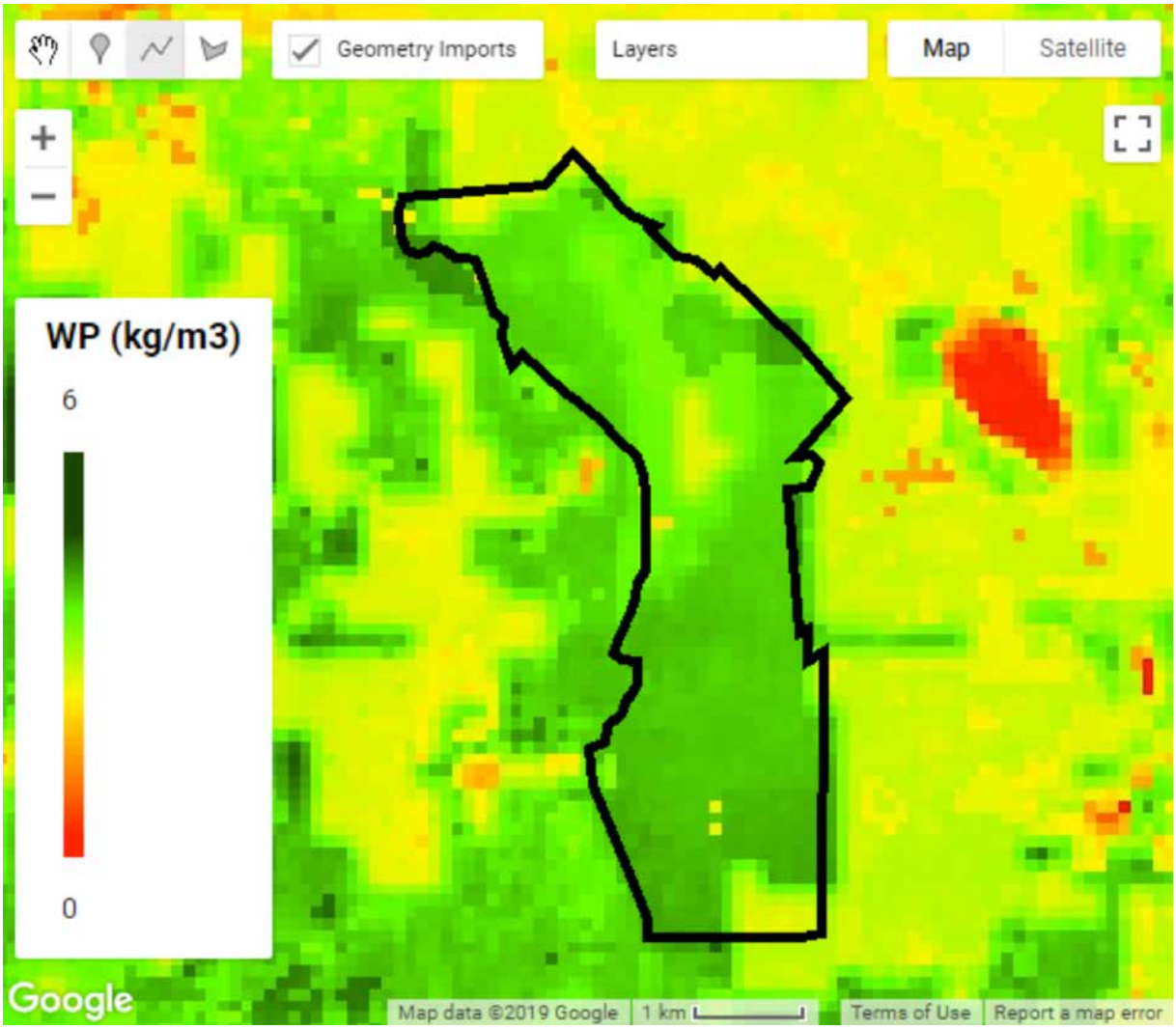

C3. Conclusions

The WaPOR gross WP using user defined cropping season, harvest index and moisture content values, provides very good estimation of WP. The gross WP estimates for sugarcane (Ethiopia) and wheat (Egypt) highlight the challenges of deriving such indicators from remote sensing. In the Ethiopia case, the areal gross WP is lower than the field observation as the area incorporates non-agricultural or fallow land in the analyses. For Egypt, fallow land increases the areal gross WP, as fallow areas (with low AGBP and even lower AETI) reflect with a high WP. The inaccuracy of WP in those cases seems to originate from wrong identification of cultivated areas and not from erroneous WP assessment.

For the humid area in Ghana, the main challenges is the differentiation of natural vegetation versus agricultural lands. The surrounding landscape has equal or higher WP compared to the irrigated areas. It is expected that rainfed agricultural areas will face similar challenges in distinguishing between natural and agricultural lands, as both follow similar phenological patterns.

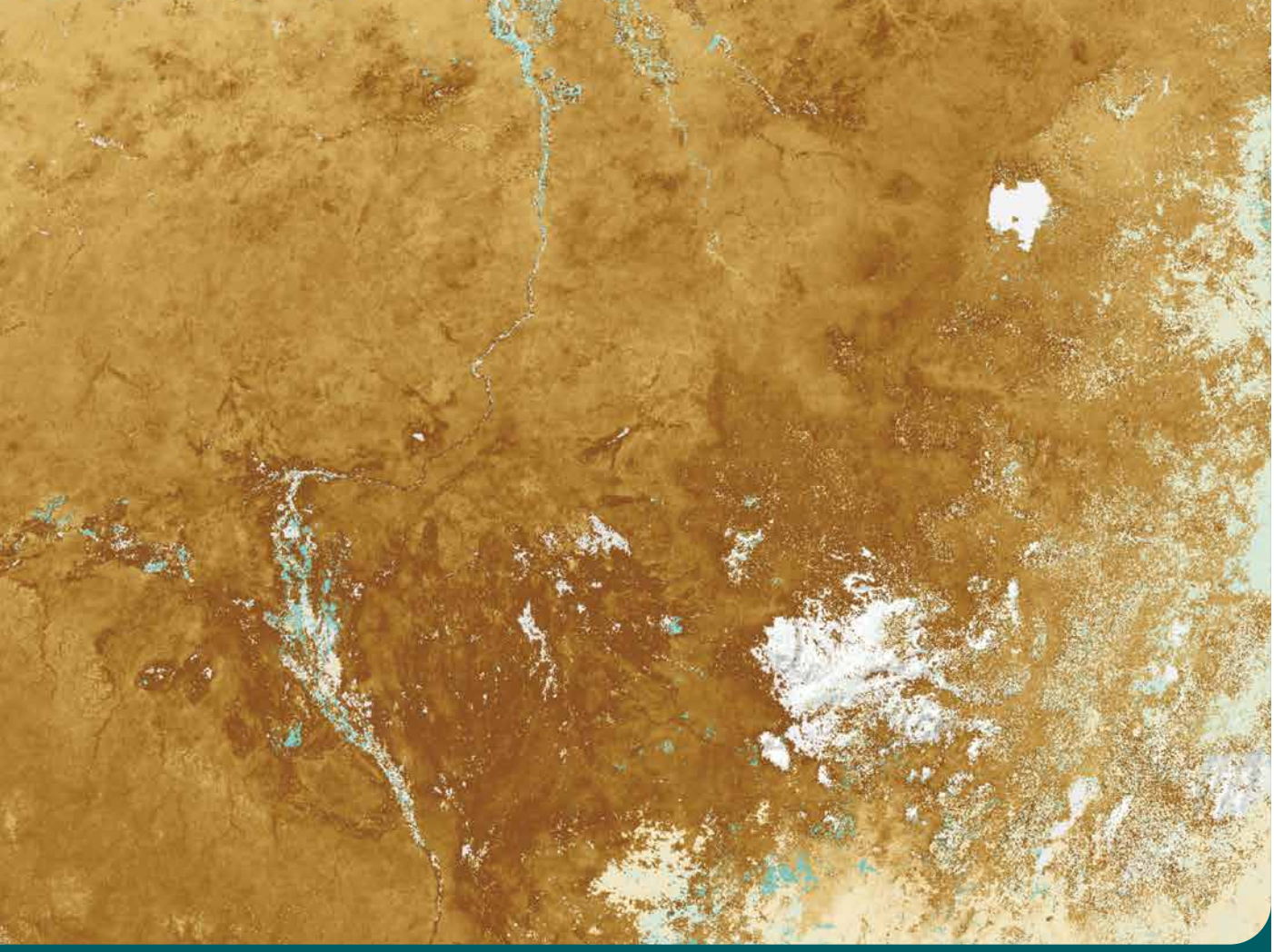

Detail of WaPOR Map "Phenology Season end 2010 - Central African Republic, Sudan, South Sudan and Ethiopia"

6. Synthesis

Rainfall in WaPOR is based on the spatial CHIRPS rainfall product. This is an existing product that is widely tested in the international literature. Research in Africa and Asia supports the selection of this product. Not only the quality is good, the spatial resolution of 5 km x 5 km is superior as well and the data goes back as far as 1983, which makes it suitable for climate change studies and impact on crop production. For a proper independent validation of CHIRPS, it is required to have access to a network with a high density of rainfall gauges. There is currently a spatial mismatch between the coverage of CHIRPS and that of rain gauges. Therefore areas with a higher density of rain gauges need to be searched for further validation of the CHIRPS product. Due to the fact that CHIRPS is an existing product, we have deliberately chosen to focus for now on the validation of the AETI and biomass production products.

Obviously, WaPOR follows the FAO standard guidelines on reference evapotranspiration as laid out in FAO Irrigation and Drainage paper 56. Because the methodology is a global standard, the quality control should focus on the inputs for the FAO 56 equation. While WaPOR makes use of MERRA, it seems there are also advantages of using GLDAS. More routine weather stations should be involved in the next phase of the validation analysis to verify whether MERRA or GLDAS is more accurate. For now, it is convenient to conclude that no suspicious results of RET were found.

While AETI cannot be measured in a straightforward manner, most of the in situ techniques available for an independent ground truth have been explored. These techniques range from eddy covariance flux towers, soil water balances at field scale to river basin water balances. Field measurements from many different countries in North Africa, Near East and Eastern Africa could be included in the analysis. While this would take more time, it helps in drawing consistent conclusions.

The overall finding is that the accumulated AETI for a year is rather good, and that spatially aggregated AETI values for river basins or sub-basins (e.g. 11 sub-basins of the Nile system) match even better. Some error in the accumulated and spatially aggregated AETI of WaPOR seems to be introduced at higher aridity. For instance, the Nile Delta, Fayoum Depression and Jordan River show higher deviation. Various mismatches with local fields and for shorter periods were detected. During the period of full crop development, AETI hardly exceeds 5 mm/d. The latter is essential for FAO, as a significant part of the applications will be related to crop water productivity analysis for a shorter period and for particular fields.

The breakdown of AETI into T, E and I has emphasized that T/AETI is higher than comparative remote sensing models and international literature. While we believe that T/AETI is at the higher side indeed, for instance the Transpiration Efficiencies (or NBWP in WaPOR terms) seem too low, T should increase during peak growing season and decrease in the emergence, senescence and fallow period. The interactions between LAI, PCP, soil moisture and light extinction coefficient α need to be investigated with more attention.

The biomass production and the related NPP fluxes are rather good for pristine growing conditions. The crop yield for various crops can now be computed in a physical manner, provided that the proper conversion factors are used. This is a leap forward as compared to solutions based on empirical relationships with NDVI. With WaPOR a decent bio-physical methodology is available with consistent data across a period of ten years.

The WP is based on biomass production, and not on crop yield. GBWP is a surrogate for WP by absence of crop information. The default constants of root-shoot ratio and maximum light use efficiency are questionable, and require more time for validation. It is easier to compare WP for yield for which more international literature is available, however this requires local knowledge to convert AGBP or TBP to yield.

Problematic are the layers on rainfed and irrigated crops, along with their cropping calendar. These two parameter are related because cropland has specific days of emergence and harvest and confusion between cropland and other land use will immediately impact the detection of the duration of the cropping and irrigation seasons. With user knowledge on the location of the field, crop type and cropping season, the WaPOR database is able to derive acceptable results.

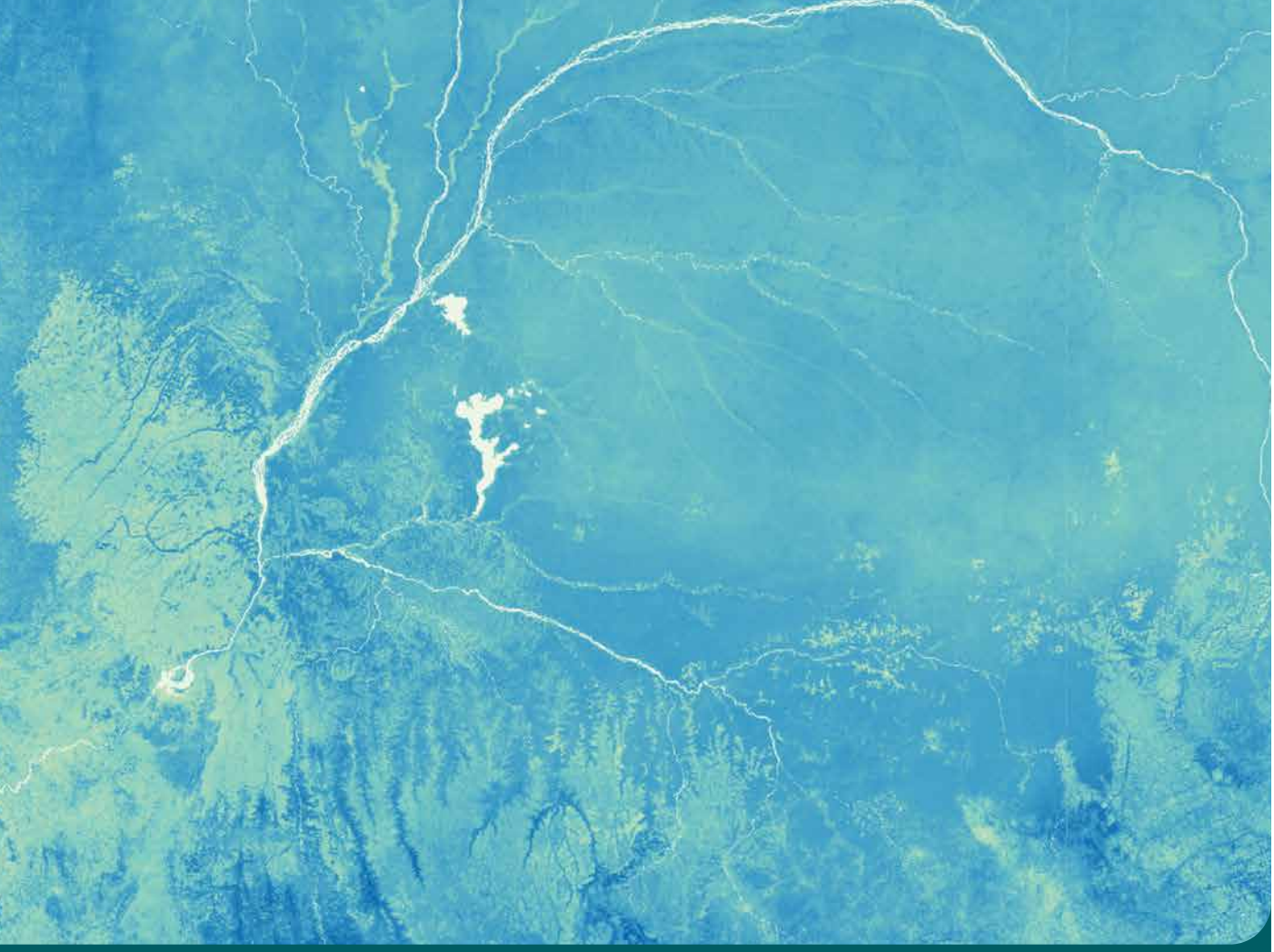

Detail of WaPOR Map "Annual Transpiration 2009 - Democratic Republic of the Congo, Republic of the Congo and Gabon"

7. Next steps

A disturbing role of aridity on the accuracy of AETI values for different products has been found, with WaPOR performing better than other products, but still with some bias. The causing factors for this sensitivity need to be found out as a collaborative effort with the WaPOR team. Not unlikely, the combined soil moisture, temperature and vapor pressure deficit stress plays a regulating role on the stomatal behavior that requires correction.

The estimates of T in WaPOR is inspected and evaluated. While local sapflow measurements showed the opposite, we believe that T is genuinely high. The breakdown of T in smaller periods needs to be investigated. Additional analysis with basal crop coefficients using NDVI are required for assessing the potential transpiration rates. Furthermore, T data layers should be compared with AGBP and TBP values for specific land use and crop types. The WP parameter introduced in AquaCrop is normalized for atmospheric evaporative demand, defined by ET_o, and for the CO_2 concentration of the atmosphere. The normalized biomass water productivity (WP*) proved to be nearly constant for a given crop when mineral nutrients are not limiting, regardless of water stress except for extremely severe cases. Normalization NBWP for evaporative demands and atmospheric CO_2 concentration has to be executed and the conservation behavior of the normalized AGBP should be verified.

More sources of land cover and land use need to be consulted to improve the WaPOR LCC. High resolution data bases became available recently such as the CCI land cover at 20 m spatial resolution from the Joint Research Centre JRC (http://2016africalandcover20m.esrin.esa.int/), GeoWiki from IIASA (https://www.geo-wiki.org/), the Global Food Security-Support Analysis Data at 30 m from USGS (https://www.usgs.gov/centers/wgsc/science/global-food-security-support-analysis-data-30-m?qt-science_center_objects=0#qt-science_center_objects) and the global land cover map of Tsinghua University (http://data.ess.tsinghua.edu.cn/). Together with new solutions to detect irrigation processes, this could be considered to improve the current WaPOR maps on rainfed and irrigated cropland.

References

Abatzoglou, J. T., Dobrowski, S. Z., Parks, S. A., & Hegewisch, K. C. 2018. TerraClimate, a high-resolution global dataset of monthly climate and climatic water balance from 1958–2015. Scientific data, 5, 170191.

Alemohammad, S. H., Fang, B., Konings, A. G., Aires, F., Green, J. K., Kolassa, J., Miralles, D., Prigent, C., & Gentine, P. 2017. Water, Energy, and Carbon with Artificial Neural Networks (WECANN): a statistically based estimate of global surface turbulent fluxes and gross primary productivity using solar-induced fluorescence. Biogeosciences, 14(18), 4101-4124.

Allen, R. G., Pereira, L. S., Raes, D., & Smith, M. 1998. Crop evapotranspiration-Guidelines for computing crop water requirements-FAO Irrigation and drainage paper 56. Fao, Rome, 300(9), D05109.

Allen, R. G., Pereira, L. S., Smith, M., Raes, D., & Wright, J. L. 2005. FAO-56 dual crop coefficient method for estimating evaporation from soil and application extensions. Journal of irrigation and drainage engineering, 131(1), 2-13.

Alvarez-Carrion, S.M. 2018. Water Productivity score computation using spatial remote sensing data sources in the Bekaa valley, Lebanon. UNESCO-IHE MSc thesis. 70 pages

Anderson, M. C., Norman, J. M., Mecikalski, J. R., Otkin, J. A., & Kustas, W. P. 2007. A climatological study of evapotranspiration and moisture stress across the continental United States based on thermal remote sensing: 1. Model formulation. Journal of Geophysical Research: Atmospheres, 112(D10).

Archibald, S. A., Kirton, A., Merwe, M. R. van der, Scholes, R. J., Williams, C. A. and Hanan, N. 2009. Drivers of inter-annual variability in Net Ecosystem Exchange in a semi-arid savanna ecosystem, South Africa, Biogeosciences, 6(2), 251–266.

Arnold, J.G., Bieger, K., White, M.J., Srinivasan, R., Dunbar, J.A., Allen, P.M. 2018. Use of decision tables to simulate management in SWAT+. Water (Switzerland) 10, 1–10. https://doi.org/10.3390/w10060713

Arnold, J.G., Srinivasan, R., Muttiah, R.S., Williams, J.R. 1998. LARGE AREA HYDROLOGIC MODELING AND ASSESSMENT PART I: MODEL DEVELOPMENT. J. Am. Resour. Assoc. 34, 73–89. https://doi.org/10.1016/S0899-9007(00)00483-4

Awange, J. L., Ferreira, V. G., Forootan, E., Andam-Akorful, S. A., Agutu, N. O., & He, X. F. 2016. Uncertainties in remotely sensed precipitation data over Africa. International Journal of Climatology, 36(1), 303-323.

Baldocchi, D. D., Hincks, B. B., and Meyers, T. P.: Measuring Biosphere-Atmosphere Exchanges of Biologically Related Gases with Micrometeorological Methods, Ecology, 69, 1331– 1340, 1988.

Bastiaanssen, W. G. M., Cheema, M. J. M., Immerzeel, W. W., Miltenburg, I. J., & Pelgrum, H. 2012. Surface energy balance and actual evapotranspiration of the transboundary Indus Basin estimated from satellite measurements and the ETLook model. Water Resources Research, 48(11).

Bastiaanssen, W.G.M., Karimi, P., Rebelo, L.M., Duan, Z., Senay, G., Muthuwatte, L., Smakhtin, V. 2014. Earth observation based assessment of the water production and water consumption of Nile basin agro-ecosystems. Remote Sens. 6, 10306–10334. https://doi.org/10.3390/rs61110306

Bastidas-Obando, E., Bastiaanssen, W.G.M., Jarmain, C. 2017. Estimation of transpiration fluxes from rainfed and irrigated sugarcane in South Africa using a canopy resistance and crop coefficient model. Agric. Water Manag. 181, 94–107. https://doi.org/10.1016/j.agwat.2016.11.024

Belete, M., Deng, J., Zhou, M., Wang, K., You, S., Hong, Y., Weston, M. 2018. A new approach to modelingwater balance in Nile River Basin, Africa. Sustain. 10, 1–14. https://doi.org/10.3390/su10030810

Bieger, K., Arnold, J.G., Rathjens, H., White, M.J., Bosch, D.D., Allen, P.M., Volk, M., Srinivasan, R. 2017. Introduction to SWAT+, a Completely Restructured Version of the Soil and Water Assessment Tool. J. Am. Water Resour. Assoc. 53, 115–130. https://doi.org/10.1111/1752-1688.12482

Bierhuizen, J.F., and R.O. Slayter. 1965. Effect of atmospheric concentration of water vapor and CO2 in determining transpiration-photosynthesis relationships of cotton leaves. Agric. Meteorol. 2:259–270.

Bouchet, R. J., 1963. Evapotranspiration réelle evapotranspiration potentielle, signification climatique, pp. 134–142, in International Association of Scientific Hydrology, General Assembly of Berkeley, Transactions, vol. 2, Evaporation, Berkeley, California.

Calera, A., Martínez, C., Meliá, J. 2001. A procedure for Obtaining Green Plant Cover: Relation to NDVI in a Case of Study for Barley. International Journal of Remote Sensing, vol 22, no 17, 3357-3362.

Cheema, M.J.M. and W.G.M. Bastiaanssen 2012. Local calibration of remotely sensed rainfall from the TRMM satellite for different periods and spatial scales in the Indus Basin, Int. J. Of Rem. Sens., 33(8): 2603-2627

Chen, Y., Lu, D., Luo, L., Pokhrel, Y., Deb, K., Huang, J., & Ran, Y. 2018. Detecting irrigation extent, frequency, and timing in a heterogeneous arid agricultural region using MODIS time series, Landsat imagery, and ancillary data. Remote Sensing of Environment, 204, 197-211.

Chiti, T., Certini, G., Grieco, E. and Valentini, R. 2010. The role of soil in storing carbon in tropical rainforests: the case of Ankasa Park, Ghana, Plant Soil, 331, 453-461.

Choudhury, B. J., & DiGirolamo, N. E. 1998. A biophysical process-based estimate of global land surface evaporation using satellite and ancillary data I. Model description and comparison with observations. Journal of Hydrology, 205(3-4), 164-185.

Conway, G. 2009. The science of climate change in Africa: impacts and adaptation. Grantham Institute for Climate Change Discussion Paper, 1, 24.

De Bruin, H. A. R., Trigo, I. F., Bosveld, F. C., & Meirink, J. F. 2016. A thermodynamically based model for actual evapotranspiration of an extensive grass field close to FAO Reference, suitable for remote sensing application. Journal of Hydrometeorology, 17(5), 1373-1382.

Dee, D. P., Uppala, S. M., Simmons, A. J., Berrisford, P., Poli, P., Kobayashi, S., Andrae, U., Balmaseda, M.A., Balsamo, G., Bauer, P., Bechtold, P., Beljaars, A.C.M., van de Berg, L., Bidlot, J., Bormann, N., Delsol, C., Dragani, R., Fuentes, M., Geer, A.J., Haimberger, L., Healy, S.B., Hersbach, H., Hólm, E.V., Isaksen, L., Kållberg, P., Köhler, M., Matricardi, M., McNally, A.P., Monge-Sanz, B.M., Morcrette, J.-J., Park, B.-K., Peubey, C., de Rosnay, P., Tavolato, C., Thépaut, J.-N., & Vitart, F. 2011. The ERA-Interim reanalysis: Configuration and performance of the data assimilation system. Quarterly Journal of the royal meteorological society, 137(656), 553-597.

Dembélé, M., & Zwart, S. J. 2016. Evaluation and comparison of satellite-based rainfall products in Burkina Faso, West Africa. International journal of remote sensing, 37(17), 3995-4014.

Dheeravath, V., Thenkabail, P.S., Chandrakantha, G., Noojipady, P., Reddy, G.P.O., Biradar, C.M., Gumma, M.K., Velpuri, M. 2010. Irrigated areas of India derived using MODIS 500 m time series for the years 2001 - 2003. ISPRS Journal of Photogrammetry and Remote Sensing, 65 (1), 42-59.

Dinku, T., Funk, C., Peterson, P., Maidment, R., Tadesse, T., Gadain, H., & Ceccato, P. 2018. Validation of the CHIRPS satellite rainfall estimates over eastern of Africa. Quarterly Journal of the Royal Meteorological Society.

Dobrowski, S. Z., Abatzoglou, J., Swanson, A. K., Greenberg, J. A., Mynsberge, A. R., Holden, Z. A., & Schwartz, M. K. 2013. The climate velocity of the contiguous United States during the 20th century. Global change biology, 19(1), 241-251.

El-Quosy, Dia and Samia El-Guindy. 1989. Water and salt balance of the Nile Delta, a new approach, in (eds.) M.H Amer and N.A. de Ridder, Land Drainage in Egypt, Chapter 10: 243-253

FAO. 2016. AQUASTAT website. Food and Agriculture Organization of the United Nations (FAO). Website accessed on 2018/12/27.

FAO. 2018. WaPOR Database Methodology: Level 1. Remote Sensing for Water Productivity Technical Report: Methodology Series. Rome, FAO. 72 pages. http://www.fao.org/3/I7315EN/i7315en.pdf

FAO. 2019. El Nino and rainfall. http://www.fao.org/emergencies/resources/maps/detail/en/c/339920/ Accessed on 19-01-2019

Fisher, J.B., Melton, F., Middleton, E., Hain, C., Anderson, M., Allen, R., Mccabe, M.F., Hook, S., Baldocchi, D., Townsend, P.A., Kilic, A., Tu, K., Miralles, D.D., Perret, J., Lagouarde, J.-P., Waliser, D., Purdy, A.J., French, A., Schimel, D., Famiglietti, J.S., Stephens, G., Wood, E.F. 2017. The future of evapotranspiration: Global requirements for ecosystem functioning, carbon and climate feedbacks, agricultural management, and water resources. Water Resour. Res. 53, 2618–2626. https://doi.org/10.1002/2016WR020175

Foley, J.A., C.J. Kucharik, and D. Polzin. 2005. Integrated Biosphere Simulator Model (IBIS), Version 2.5. ORNL DAAC, Oak Ridge, Tennessee, USA. https://doi.org/10.3334/ORNLDAAC/808

Funk, C., Peterson, P., Landsfeld, M., Pedreros, D., Verdin, J., Shukla, S., Husak, G., Rowland, J., Harrison, L., Hoell, A., Michaelsen, J. 2015. The climate hazards infrared precipitation with stations—a new environmental record for monitoring extremes. Scientific data, 2, 150066.

Ghana Irrigation Development Authority (GIDA). 2010. Feasibility of the Accra Plains Irrigation Project – Detailed study for the 5000 ha. Final report, 300 pages

Gilmont, M., Al Naber, M., Tal, N., and Alhaddadin, R. 2019. Water Productivity Decoupling – Verification of agricultural potential for Jordan and Israel using farm-level surveys and remote sensing in Jordan Valley. Draft Project Report

Gilmont, M., Nassar, L., Rayner, S., Tal, N., Harper, E., Salem, H.S. 2018. The Potential for Enhanced Water Decoupling in the Jordan Basin through Regional Agricultural Best Practice, Land, 7, 63; doi:10.3390/land7020063

Guerschman, J.P., Van Dijk, A.I., Mattersdorf, G., Beringer, J., Hutley, L.B., Leuning, R., Pipunic, R.C., & Sherman, B.S. 2009. Scaling of potential evapotranspiration with MODIS data reproduces flux observations and catchment water balance observations across Australia. Journal of Hydrology, 369(1-2), 107-119.

Ha, L.T., W.G.M. Bastiaanssen, A. van Griensven, A.I.J.M. van Dijk, and G.l B. Senay. 2017. SWAT-CUP for Calibration of Spatially Distributed Hydrological Processes and Ecosystem Services in a Vietnamese River Basin Using Remote Sensing, https://doi.org/10.5194/hess-2017-251

Hargreaves, G.H., and Z.A. Samani. 1985. Reference crop evapotranspiration from temperature. Applied Engineering. in Agric. 1:96-99

Harris, I.C.; Jones, P.D. 2017. CRU TS4.00: Climatic Research Unit (CRU) Time-Series (TS) version 4.00 of high-resolution gridded data of month-by-month variation in climate (Jan. 1901- Dec. 2015). Centre for Environmental Data Analysis, 25 August 2017. doi:10.5285/edf8febfdaad48abb2cbaf7d7e846a86

HarvestChoice. 2011. "Longterm Average Annual Rainfall (mm)." International Food Policy Research Institute, Washington, DC., and University of Minnesota, St. Paul, MN. Available online at http://harvestchoice.org/node/4963.

Heinsch, F. A., Reeves, M., Votava, P., Kang, S., Milesi, C., Zhao, M., Glassy, J., Jolly, W.M., Loehman, R., Bowker, C.F., Kimball, J.S., Nemani, R.R., & Running, S.W. 2003. GPP and NPP (MOD17A2/A3) Products NASA MODIS Land Algorithm. MOD17 User's Guide, 1-57.

Herman, A., V. B. Kumar, P. A. Arkin, and J. V. Kousky. 1997. "Objectively Determined 10-Day African Rainfall Estimates Created for Famine Early Warning Systems." International Journal of Remote Sensing 18 (10): 2147–2159. doi:10.1080/014311697217800

Hessels, T. M. 2015. Comparison and Validation of Several Open Access Remotely Sensed Rainfall Products for the Nile Basin. MSc thesis TU Delft

Hilhorst, B.; Burke, J.; Hoogeveen, J.; Fremken, K.; Faures, J.-M.; Gross, D. 2011. Information Products for Nile Basin Water Resources Management; FAO: Rome, Italy; p. 130

Hsu, K.-L., X. Gao, S., Sorooshian, and Gupta, H.V. 1997. "Precipitation Estimation from Remotely Sensed Information Using Artificial Neural Networks." Journal of Applied Meteorology 36 (9): 1176–1190. doi:10.1175/1520-0450(1997)0362.0.CO;2.

Hu, G., & Jia, L. 2015. Monitoring of evapotranspiration in a semi-arid inland river basin by combining microwave and optical remote sensing observations. Remote Sensing, 7(3), 3056-3087.

Jiménez, C., Prigent, C., Mueller, B., Seneviratne, S.I., McCabe, M.F., Wood, E.F., Rossow, W.B., Balsamo, G., Betts, A.K., Dirmeyer, P.A., Fisher, J.B., Jung, M., Kanamitsu, M., Reichle, R.H., Reichstein, M., Rodell, M., Sheffield, J., Tu, K., Wang, K. 2011. Global intercomparison of 12 land surface heat flux estimates. J. Geophys. Res. Atmos. 116, 1–27. https://doi.org/10.1029/2010JD014545

Joyce, R.J., Janowiak, J.E., Arkin, P.A., Xie, P. 2004. CMORPH: a method that produces global precipitation estimates from passive microwave and infrared data at high spatial and temporal resolution. J. Hydrometeorol. 5 : 487–503

Jung, M., Reichstein, M., Ciais, P., Seneviratne, S. I., Sheffield, J., Bonan, G., Chen, J., Cescatti, A., de Jeu, R.A.M., Dolman, A. J., Eugster, W., Gerten, D., Gianelle, D., Gobron, N., Goulden, M. L., Heinke, J., Kimball, J., Law, B.E., Montagnani, J., Mu, Q., Mueller, B., Oleson, K., Papale, D., Richardson, A., Roupsard, O., Running, S., Tomelleri, E., Viovy, N., Weber, U., Williams, C., Wood, E., Zaehle, S., & Zhang, K. 2010. Recent decline in the global land evapotranspiration trend due to limited moisture supply. Nature 467:951– 954

Jung, H.C., Getirana, A., Policelli, F., McNally, A., Arsenault, K.R., Kumar, S., Tadesse, T., Peters-Lidard, C.D. 2017. Upper Blue Nile basin water budget from a multi-model perspective. J. Hydrol. 555, 535–546. https://doi.org/10.1016/j.jhydrol.2017.10.040

Jung, M., Reichstein, M. & Bondeau, A. 2009. Towards global empirical upscaling of FLUXNET eddy covariance observations: validation of a model tree ensemble approach using a biosphere model. Biogeosciences 6, 2001–2013.

Karimi, P., Molden, D., Notenbaert, A., Peden, D. 2012. Nile basin farming systems and productivity. In The Nile River Basin, Water, Agriculture, Governance and Livelihoods; Chalmers, K., Godfrey, J., Eds.; Edgar Elger: Cheltenham, UK, 2012; pp. 133–153

Kiptala, J.K., Mohamed, Y., Mul, M.L., Zaag, P. 2013. Mapping evapotranspiration trends using MODIS and SEBAL model in a data scarce and heterogeneous landscape in Eastern Africa. Water Resour. Res. 49, 8495–8510.

Kongo, M.V., Jewitt, G.W.P., & Lorentz, S.A. 2011. Evaporative water use of different land uses in the upper-Thukela river basin assessed from satellite imagery. Agricultural water management, 98(11), 1727-1739.

Kucharik, C.J., Foley, J.A., Delire, C., Fisher, V.A., Coe, M.T., Lenters, J.D., Young-Molling, C., Ramankutty, N., Norman, J.M., & Gower, S.T. 2000. Testing the performance of a dynamic global ecosystem model: water balance, carbon balance, and vegetation structure. Global Biogeochemical Cycles, 14(3), 795-825.

Łabędzki, L. 2011. Evapotranspiration Edited. InTech, Rijeka, Croatia.

Li, A., Bian, J., Lei, G., & Huang, C. 2012. Estimating the maximal light use efficiency for different vegetation through the CASA Model combined with time-series remote sensing data and ground measurements. Remote sensing, 4(12), 3857-3876.

Madani, N., Kimball, J.S., & Running, S.W. 2017. Improving global gross primary productivity estimates by computing optimum light use efficiencies using flux tower data. Journal of Geophysical Research: Biogeosciences, 122(11), 2939-2951.

Maidment, R.I., D. Grimes, R.P. Allan, E. Tarnavsky, M. Stringer, T. Hewison, R. Roebeling, and E. Black. 2014. "The 30 Year TAMSAT African Rainfall Climatology and Time Series (TARCAT) Data Set." Journal of Geophysical Research: Atmospheres 119 (18): 10,619–610,644. doi:10.1002/ 2014JD021927

Marchesini, B., L., Bombelli, A., Chiti, T., Consalvo, C., Forgione, A., Grieco, E., Mazzenga, F., Papale, D., Stefani, P., Vittorini, E., Zompanti, R., & Valentini, R. 2011. Ankasa flux tower: a new research facility for the study of the carbon cycle in a primary tropical forest in Africa. Africa and the Carbon Cycle, 11.

Marshall, M., Tu, K., Funk, C., Michaelsen, J., Williams, P., Williams, C., Ardö, J., Boucher, M., Cappelaere, B., De Grandcourt, A., Nickless A., Nouvellon, Y., Scholes, R., & Kutsch, W. 2013. Improving operational land surface model canopy evapotranspiration in Africa using a direct remote sensing approach. Hydrology and Earth System Sciences 17, 1079–1091

Martens, B., Miralles, D.G., Lievens, H., Van Der Schalie, R., De Jeu, R.A.M., Fernández36 Prieto, D., Beck, H.E., Dorigo, W.A., Verhoest, N.E.C. 2017. GLEAM v3 : satellite-based land evaporation and root-zone soil moisture. Geosci. Model Dev. 10, 1903–1925, doi:10.5194/gmd-10-1903-2017.

Mianabadi, A., Coenders–Gerrits, M., Shirazi, P., Ghahraman, B., & Alizadeh, A. 2019. A global Budyko model to partition evaporation into interception and transpiration. Hydrology and Earth System Sciences Discussions https://doi.org/10.5194/hess-2018-638, in review.

Michel, D., Jiménez, C., Miralles, D.G., Jung, M., Hirschi, M., Ershadi, A., Martens, B., McCabe, M.F., Fischer, J.B., Mu, Q., Seneviratne, S.I., Wood, E.F., & Fernàndez-Prieto, D. 2016. TheWACMOS-ET project–Part 1: Tower-scale evaluation of four remote-sensing-based evapotranspiration algorithms. Hydrology and Earth System Sciences, 20(2), 803-822.

Miralles, D.G., De Jeu, R.A.M., Gash, J.H., Holmes, T.R.H., and Dolman, A.J. 2011a. Magnitude and variability of land evaporation and its components at the global scale, Hydrol. Earth Syst. Sci., 15, 967–981, doi:10.5194/hess-15-967-2011.

Miralles, D.G., Holmes, T.R.H., De Jeu, R.A.M., Gash, J.H., Meesters, A.G.C.A., and Dolman, A.J. 2011b. Global land-surface evaporation estimated from satellite-based observations, Hydrol. Earth Syst. Sci., 15, 453–469, doi:10.5194/hess-15-453-2011

Miralles, D.G., Jiménez, C., Jung, M., Michel, D., Ershadi, A., Mccabe, M.F., Hirschi, M., Martens, B., Dolman, A.J., Fisher, J.B., Mu, Q., Seneviratne, S.I., Wood, E.F., Fernández-Prieto, D. 2016. The WACMOS-ET project-Part 2: Evaluation of global terrestrial evaporation data sets. Hydrol. Earth Syst. Sci 20, 823–842. https://doi.org/10.5194/hess-20-823-2016

Monteith, J.L. 1965. Evaporation and environment. 19th Symposia of the Society for Experimental Biology 19: 205-234.

Mu, Q., F. A. Heinsch, M. Zhao, and S. W. Running. 2007. Development of a global evapotranspiration algorithm based on MODIS and global meteorology data, Remote Sens. Environ., 111, 519–536.

Mu, Q., Heinsch, F.A., Zhao, M., Running, S.W. 2011. Development of a global evapotranspiration algorithm based on MODIS and global meteorology data. Remote Sensing of Environment 111, 519–536. https://doi.org/10.1016/j.rse.2007.04.015

Mu, Q., M. Zhao, and S. W. Running. 2011. Improvements to a MODIS global terrestrial evapotranspiration algorithm, Remote Sens. Environ., 115, 1781–1800.

Mueller, B., Hirschi, M., Jimenez, C., Ciais, P., Dirmeyer, P. A., Dolman, A. J., Fisher, J. B., Jung, M., Ludwig, F., Maignan, F., Miralles, D. G., McCabe, M. F., Reichstein, M., Sheffield, J., Wang, K., Wood, E. F., Zhang, Y., and Seneviratne, S. I. 2013. Benchmark products for land evapotranspiration: LandFluxEVAL multi-data set synthesis, Hydrol. Earth Syst. Sci., 17, 3707–3720, doi:10.5194/hess-17-3707-2013, 2013.

New, M., Lister, D., Hulme, M., Makin, I. 2000. A high-resolution data set of surface climate over global land areas. Climate Research, Vol 21: 1-25, http://dx.doi.org/10.3354/cr021001

Nile Basin Initiative. 2014. Mapping Actual Evapotranspiration over the Nile Basin.

Novella, N., and W. Thiaw. 2010. Validation of Satellite-Derived Rainfall Products over the Sahel, 1–9. Camp Springs, MD: Wyle Information Systems/CPC/NOAA.

Novella, N. S., and W. M. Thiaw. 2013. "African Rainfall Climatology Version 2 for Famine Early Warning Systems." Journal of Applied Meteorology and Climatology 52 (3): 588–606. doi:10.1175/ JAMC-D-11-0238.1

Paca, V. H. da Motta, G. E. Espinoza-Dávalos, T.M. Hessels, D. Medeiros Moreira, G.F. Comair and W.G.M. Bastiaanssen. 2019. The spatial variability of actual evapotranspiration across the Amazon River Basin based on remote sensing products validated with flux towers, Ecological Processes, Springer, https://doi.org/10.1186/s13717-019-0158-8

Penman, H.L. 1963. Vegetation and hydrology. Technical Communication No. 53. Harpenden, England: Commonwealth Bureau of Soils. 125p.

Pôças, I., Paço, T. A., Paredes, P., Cunha, M., & Pereira, L. S. 2015. Estimation of actual crop coefficients using remotely sensed vegetation indices and soil water balance modelled data. Remote Sensing, 7(3), 2373-2400.

Poméon, T., Jackisch, D., & Diekkrüger, B. 2017. Evaluating the performance of remotely sensed and reanalysed precipitation data over West Africa using HBV light. Journal of hydrology, 547, 222-235.

Poortinga *et al.* (in prep. a). Water accounting for the Awash river basin

Poortinga *et al.* (in prep. b). Water accounting for the Jordan and Litani river basins

Raes, D., Steduto, P., Hsiao, T.C. & Fereres, E. 2011. Aquacrop – Reference Manual. Available at: http://www.fao.org/nr/water/aquacrop.html

Ramadan, F.M, D.S. Alnaggar and H.M van Leeuwen. 1989. The Fayoum water and salt balance model, in (eds) M.H Amer and N.A. de Ridder, Land Drainage in Egypt, chapter 11: 255-294

Richard, Y., S. Trzaska, P. Roucou, and M. Rouault. 2000. Modification of the southern African rainfall variability/ENSO relationship since the late 1960s. Climate Dyn., 16, 883–895, doi:10.1007/s003820000086.

Rockström, J. 2003. Water for food and nature in drought–prone tropics: vapour shift in rain–fed agriculture. Philosophical Transactions of the Royal Society of London B: Biological Sciences, 358(1440), 1997-2009.

Rodell, M., P.R. Houser, U. Jambor, J. Gottschalck, K. Mitchell, C.-J. Meng, K. Arsenault, B. Cosgrove, J. Radakovich, M. Bosilovich, J.K. Entin, J.P. Walker, D. Lohmann, and D. Toll. 2004. The Global Land Data Assimilation System, Bull. Amer. Meteor. Soc., 85(3), 381-394.

Ruimy, A., Kergoat, L., & Bondeau, A. 1999. Comparing global models of terrestrial net primary productivity (NPP): Analysis of differences in light absorption and light-use efficiency. Global Change Biology, 5(S1), 56-64.

Running, S. W., & Zhao, M. 2015. Daily GPP and annual NPP (MOD17A2/A3) products NASA Earth Observing System MODIS land algorithm. MOD17 User's Guide.

Running, S., Mu, Q., Zhao, M. 2015. MOD17A3H MODIS/Terra Net Primary Production Yearly L4 Global 500m SIN Grid V006 [Data set]. NASA EOSDIS Land Processes DAAC. doi: 10.5067/MODIS/MOD17A3H.006

Saah, D., Tenneson, K., Poortinga, A., Nguyen, Q., Aung, K.S., Markert, K.N., Clinton, N., Anderson, E.R., Cutter, P., Goldstein, J., Housman, I.W., Bhandari, B., Potapov, B.V., Chishtie, F., Matin, M., Uddin, K., Pham Ngoc, H., Khanal, N., Maharjan, S., Ellenberg, W.L., Bajracharya, B., Bhargava, R., Maus, P., Patterson, M., Silverman, J., Sovann, C., Phuong, D.M., Giang, N., V., Bounthabandit, S., Aryal, R.R., Mon, M.S., Sato, K., Lindquist, E., Kono, M., Towashiraporn, P., Ganz, D., (in prep). A novel modular free and open-source system for landcover mapping using cloud-based remote sensing and machine learning

Salvadore, E. 2019. Capacity Development in support to the establishment of the Water Accounting Unit within the Egyptian Ministry of Water Resources & Irrigation, IHE-Delft

Samain, B., Simons, G. W., Voogt, M. P., Defloor, W., Bink, N. J., & Pauwels, V. 2012. Consistency between hydrological model, large aperture scintillometer and remote sensing based evapotranspiration estimates for a heterogeneous catchment. Hydrology and Earth System Sciences, 16(7), 2095-2107.

Schuol, J., Abbaspour, K.C., Yang, H., Srinivasan, R., Zehnder, A.J.B. 2008. Modeling blue and green water availability in Africa. Water Resour. Res. 44, 1–18. https://doi.org/10.1029/2007WR006609

Sellers, P.J., Dickinson, R.E., Randall, A., Betts, A.K., Hall, F.G., Berry, J.A., Collatz, G.J., Denning, A.S., Mooney, H.A., Nobre, C.A., Sato, N., Field, C.B., Henderson- Sellers, A. 1997. Modelling the Exchanges of Energy, Water, and Carbon between Continents and the Atmosphere. Science, Vol 275, 52-509.

Senay, G.B., N.M. Velpuri, S. Bohms, Y. Demissie, and M. Gebremichael. 2014, Understanding the hydrologic sources and sinks in the Nile Basin using multisource climate and remote sensing data sets, Water Resour. Res., 50, doi:10.1002/2013WR015231.

Senay, G.B., Asante, K., Artan, G. 2009. Water balance dynamics in the Nile Basin. Hydrol. Process. Hydrol. Process 23, 3675–3681. https://doi.org/10.1002/hyp.7364

Simons, G., Bastiaanssen, W., Ngô, L.A., Hain, C.R., Anderson, M., & Senay, G. 2016. Integrating global satellite-derived data products as a pre-analysis for hydrological modelling studies: A case study for the Red River Basin. Remote Sensing, 8(4), 279.

Simons, G., Poortinga, A., Bastiaanssen, W., Saah, D., Troy, D., Hunink, J.E., de Klerk, M., Rutten, M., Cutter, P., Rebelo, L., Thanh Ha, L., Phuong Nam, V., Hessels, T., Fenn, M., Bean, B., Ganz, D., Droogers, P., Erickson, T & Clinton, N. 2017. On Spatially Distributed Hydrological Ecosystem Services: Bridging the Quantitative Information Gap using Remote Sensing and Hydrological Models. White Paper, 45 pages

Steduto, P., Hsiao, T. C., & Fereres, E. 2007. On the conservative behavior of biomass water productivity. Irrigation Science, 25(3), 189-207.

Steduto, P., Hsiao, T. C., Fereres, E., & Raes, D. 2012. Crop yield response to water (Vol. 1028). Rome: fao.

Su, Z. (2002), The Surface Energy Balance System (SEBS) for estimation of turbulent heat fluxes, Hydrol. Earth Syst. Sci., 6, 85–99.

Sugita, M., Matsuno, A., El-Kilani, R.M.M., Abdel-Fattah, A., Mahmoud, M.A. 2017: Crop evapotranspiration in the Nile Delta under different irrigation methods, Hydrological Sciences Journal, DOI:10.1080/02626667.2017.1341631

Tagesson, T., Fensholt, R., Guiro, I., Rasmussen, M. O., Huber, S., Mbow, C., Garcia, M., Horion, S., Sandholt, I., Holm-Rasmussen, B., Göttsche, F. M., Ridler, M.-E., Olén, N., Lundegard Olsen, J., Ehammer, A., Madsen, M., Olesen, F. S. and Ardö, J. 2015. Ecosystem properties of semiarid savanna grassland in West Africa and its relationship with environmental variability, Glob. Chang. Biol., 21(1), 250–264

Tarnavsky, E., D. Grimes, R. Maidment, E. Black, R. P. Allan, M. Stringer, R. Chadwick, and F. Kayitakire. 2014. "Extension of the TAMSAT Satellite-Based Rainfall Monitoring over Africa and from 1983 to Present." Journal of Applied Meteorology and Climatology 53 (12): 2805–2822. doi:10.1175/JAMC-D-14-0016.1.

Trambauer, P., Dutra, E., Maskey, S., Werner, M., Pappenberger, F., Van Beek, L.P.H., Uhlenbrook, S. 2014. Comparison of different evaporation estimates over the African continent. Hydrol. Earth Syst. Sci 18, 193–212. https://doi.org/10.5194/hess-18-193-2014

Tran, B., Salvadore, E., Matar, A., Espinoza-Davalos, E., Opstal, J., Mul, M., Bastiaanssen, W,. 2019. Water Accounting in the Litani River Basin: Understanding the state of the water resources with an emphasis on irrigated agriculture. Technical report submitted to FAO, Rome.

Twine, T.E., Kustas, W.P., Norman, J.M., Cook, D.R., Houser, P.R., Meyers, T.P., Prueger, J.H., Starks, P.J., Wesely, M.L. 2000. Correcting eddy-covariance flux underestimates over a grassland. Agric. For. Meteorol. 103, 279–300. https://doi.org/10.1016/S0168-1923(00)00123-4

Valentini, R., Nicolini, G., Stefani, P., de Grandcourt, A., and Stivanello, S. 2016. FLUXNET2015 GH-Ank Ankasa. Ghana: N. p., Web. doi:10.18140/FLX/1440229.

Van Hoolst, R., Eerens, H., Haesen, D., Royer, A., Bydekerke, L., Rojas, O., Li, Y & Racionzer, P. 2016. FAO's AVHRR-based Agricultural Stress Index System (ASIS) for global drought monitoring. International Journal of Remote Sensing, 37(2), 418-439.

Vanderkelen, I., van Lipzig, N. P., & Thiery, W. 2018a. Modelling the water balance of Lake Victoria (East Africa), part 1: observational analysis. Hydrol. Earth Syst. Sci, , 22, 5509–5525.

Vanderkelen, I., Van Lipzig, N. P., & Thiery, W. 2018b. Modelling the water balance of Lake Victoria (East Africa), part 2: future projections. Hydrol. Earth Syst. Sci, 22, 5527–5549.

Vinukollu, R.K., Meynadier, R., Sheffield, J., Wood, E.F. 2011. Multi-model, multi-sensor estimates of global evapotranspiration: climatology, uncertainties and trends. Hydrol. Process. 25, 3993–4010. https://doi.org/10.1002/hyp.8393

Wang-Erlandsson, L., Bastiaanssen, W. G. M., Gao, H., Jägermeyr, J., Senay, G. B., van Dijk, A. I. J. M., Guerschman, J. P., Keys, P. W., Gordon, L. J., and Savenije, H. H. G. 2016. Global root zone storage capacity from satellite-based evaporation, Hydrol. Earth Syst. Sci., 20, 1459-1481

Wang-Erlandsson, L., Van Der Ent, R.J., Gordon, L.J., Savenije, H.H.G. 2014. Contrasting roles of interception and transpiration in the hydrological cycle - Part 1: Temporal characteristics over land. Earth Syst. Dyn. 5, 441–469, doi:10.5194/esd-5-441-2014.

Wartenburger, R., Seneviratne, S.I., Hirschi, M., Chang, J., Ciais, P., Deryng, D., Elliott, J., Folberth, C., Gosling, S.N., Gudmundsson, L., Henrot, A.-J., Hickler, T., Ito, A., Khabarov, N., Kim, H., Leng, G., Liu, J., Liu, X., Masaki, Y., Morfopoulos, C., Muller, C., Schmied, H., Nishina, K., Orth, R., Pokhrel, Y., Pugh, T., Satoh, Y., Schaphoff, S., Schmid, E., Sheffield, J., Stacke, T., Steinkamp, J., Tang, Q., Thiery, W., Wada, Y., Wang, X., Weedon, G., Yang, H., Zhou, T. 2018. Evapotranspiration simulations in ISIMIP2a-Evaluation of spatio-temporal characteristics with a comprehensive ensemble of independent datasets. Environ. Res. Lett. 13. https://doi.org/10.1088/1748-9326/aac4bb

Wei, Z., Yoshimura, K., Wang, L., Miralles, D. G., Jasechko, S., & Lee, X. 2017. Revisiting the contribution of transpiration to global terrestrial evapotranspiration. Geophysical Research Letters, 44(6), 2792-2801.

Wolters, W., Ghobrial, N. S., van Leeuwem H. M., and Bos M. G. 1989 "Managing the water balance of The Fayoum Depression, Egypt". Irrigation and Drainages Systems, 3, pp. 103-123.

Xie, P., Yoo, S. H., Joyce, R., & Yarosh, Y. 2011. Bias-corrected CMORPH: A 13-year analysis of high-resolution global precipitation. In Geophysical Research Abstracts (Vol. 13, pp. EGU2011-1809).

Yilma, W.A. 2017. Computation and spatial observation of water productivity in Awash river basin. UNESCO-IHE MSc thesis. 74 pages

Zhang, Y., Peña-Arancibia, J.L., Mcvicar, T.R., Chiew, F.H.S., Vaze, J., Liu, C., Lu, X., Zheng, H., Wang, Y., Liu, Y.Y., Miralles, D.G., Pan, M. 2016. Multi-decadal trends in global terrestrial evapotranspiration and its components OPEN. Sci. Rep. 6. https://doi.org/10.1038/srep19124

Annex A: SWAT Model set-up

The Soil and Water Assessment Tool (SWAT) is a widely applied catchment model, integrating hydrological, agricultural, soil and plant growth processes. SWAT has been used widely to support water resources and/or agricultural management at river basin scale (Arnold *et al.*, 1998). The newly develop SWAT+ version was released in September 2018. SWAT+ is using the same equations, but a different structure and formats of the programming codes and the in- and output files, allowing for a higher flexibility to connect different elements of the river basin (Bieger *et al.*, 2017). In the new SWAT+ version, it is easier to implement routing over the landscape (flow moving from upland areas through lower areas) or wetland-flooding interactions. Another new feature of SWAT+ are the use of 'decision tables' as a standardized and flexible way to represent management activities, such as irrigation or dam operations (Arnold *et al.*, 2018).

The model functions such that a basin, along with a stream and channel network, is delineated from a Digital Elevation Map (DEM) and optionally a stream network. Once the basin is defined it is divided into sub-basins and Landscape Units (LSUs) according to the sections of the streams and channels. These are then further subdivided into Hydrological Response Units (HRUs) which consist of unique land use, slope and soil characteristics.

The setup of the SWAT+ Africa model was conducted using QSWAT+, a graphical user interface (GUI) using Quantum Geographic Information System (QGIS). There are three phases involved using SWAT+ for water management: preprocessing, setting up the model and post-processing. Figure A1 shows the steps involved for setting up a SWAT+ model. Steps 1-3 are performed using SWAT+ and 4-5 are performed using a different program, SWAT+ Editor (Celray *et al.*, 2018). Data inputs required for development of a SWAT+ model are a Digital Elevation Map (DEM), Land use and Soil Maps, Climate data (precipitation, minimum and maximum temperature, relative humidity, solar radiation and wind speed). Table A1 details the data sources used for the setup of the Africa SWAT+ model.

Figure A1
Steps for setting up a SWAT+ model in QSWAT+

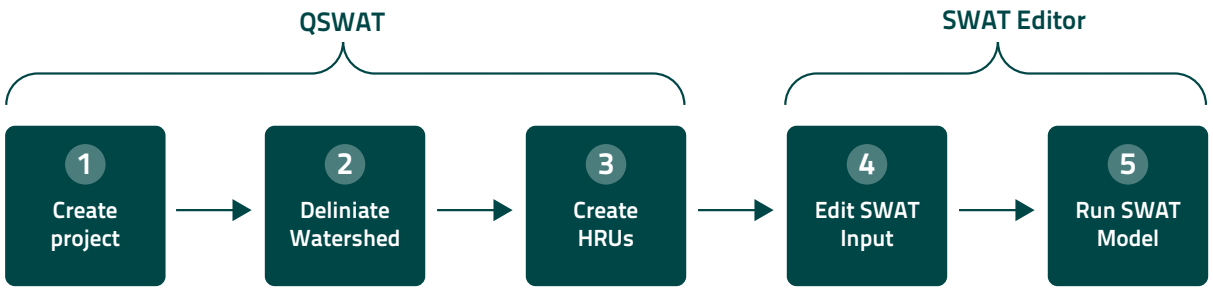

Table A1

Input data and details used for setting up the SWAT+ Africa model

Data Type	Data Source	Data Description
Digital Elevation Model (DEM)	Shutter Radar Topography Mission (SRTM)	Resampled to 300 m x 300 m resolution
Soil Map	Africa Soil Information Service (AFSIS)	Resampled to 0.25 degree x 0.25 degree resolution
Land Use/Land Cover Map	Land Harmonisation Project (LUH2)	0.25 degree x 0.25 degree resolution netCDF file format Year: 1979
Weather data Precipitation (kg m-2 s-1) Solar radiation (W m-2) Temperature (K) Wind Speed (m s-1) Relative Humidity (%)	EarthH_2Observe, WFDEI and ERA-Interim data Merged and Bias-corrected for ISI-MIP (EWEMBI)	0.5 degree x 0.5 degree resolution
Weather generator	Climate Forecast System Reanalysis (CFSR)	World dataset that ships with SWAT+ Editor

The following section details the model settings used for the development of the Africa model. During the watershed delineation step, a threshold of 3 500 km² was used for both channels and streams resulting in 5 664 landscape units (LSUs). LSUs are new to SWAT+ and are similar to sub-basins, however are based on the channel network rather than only on the stream network. SWAT+ allows the setting of sub-basins to equal the LSUs. Outlets are positioned based on inland GRDC stations (Figure A2) and on all points where rivers flow to the oceans. The next step is the creation of the HRUs using the land use and soil maps and slope classes. The slope classes used were 0 percent and 9999 percent. HRU delineation thresholds were set to 0 percent, 0 percent, and 0 percent for land use, soil and slope respectively. Due to the land use map used as input, the final HRUs were created by splitting the initial HRUs based on the pixel composition information. This information was derived from the input land use map resulting in a total of 930 870 HRUs.

Figure A2

PBIAS for the GRDC station flow data compared with SWAT+ simulation

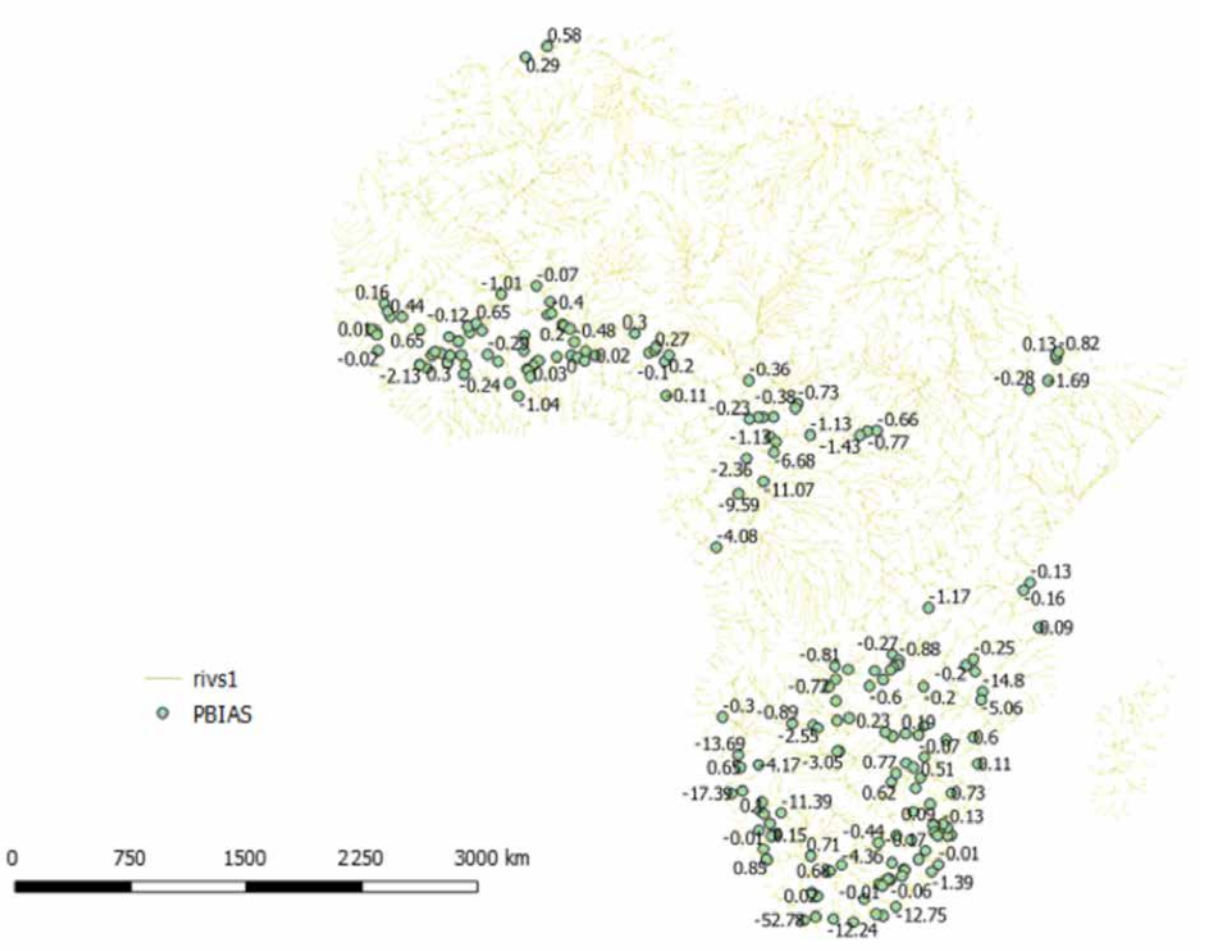

Figure A3

PBIAS for the GRDC station flow data compared with SWAT+ simulation

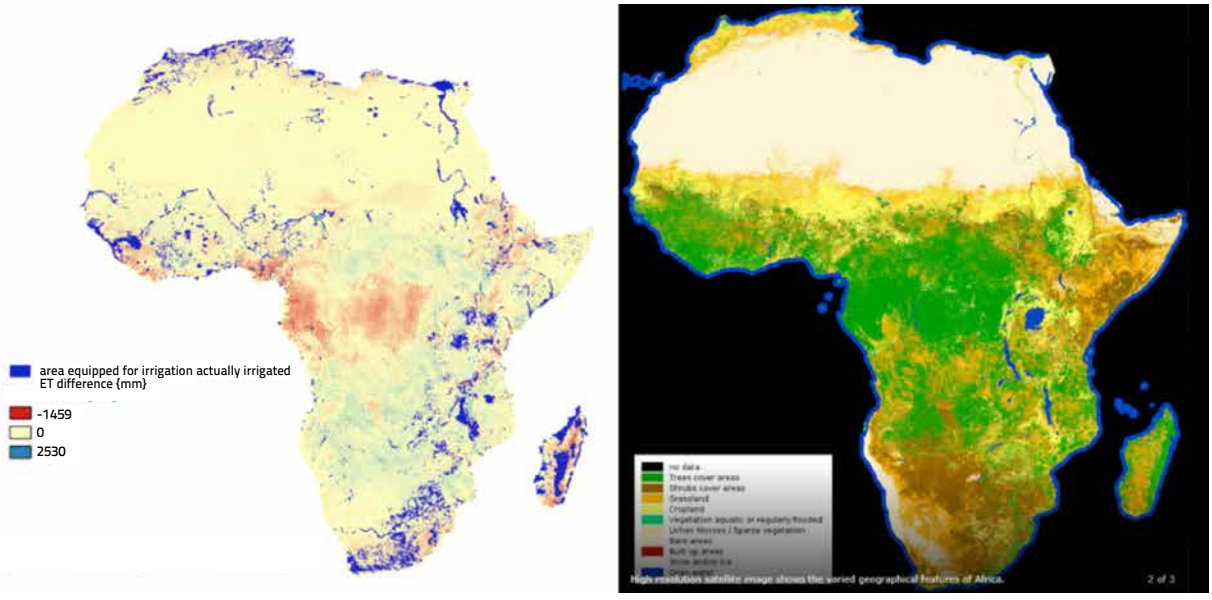

Annex B: Comparison WaPOR AETI to other remote sensing AETI products using water balance at river basin scale

Figure B1

PCP-Q comparison with different remote sensing products

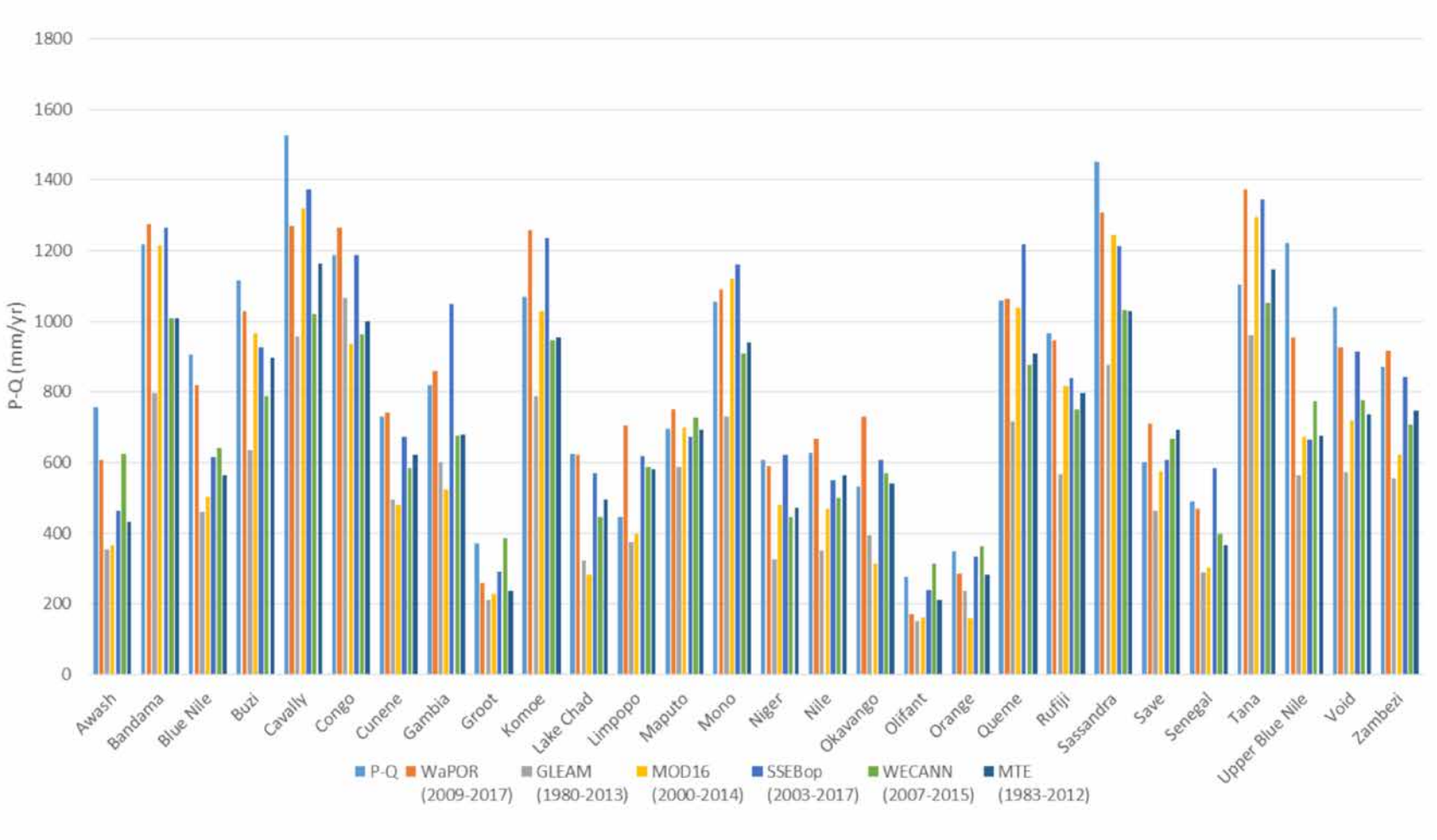

Annex C: Comparison Fluxnet vs WaPOR AETI

Figure C1

Comparison Fluxnet towers and WaPOR AETI (areas indicated were removed from the analyses)

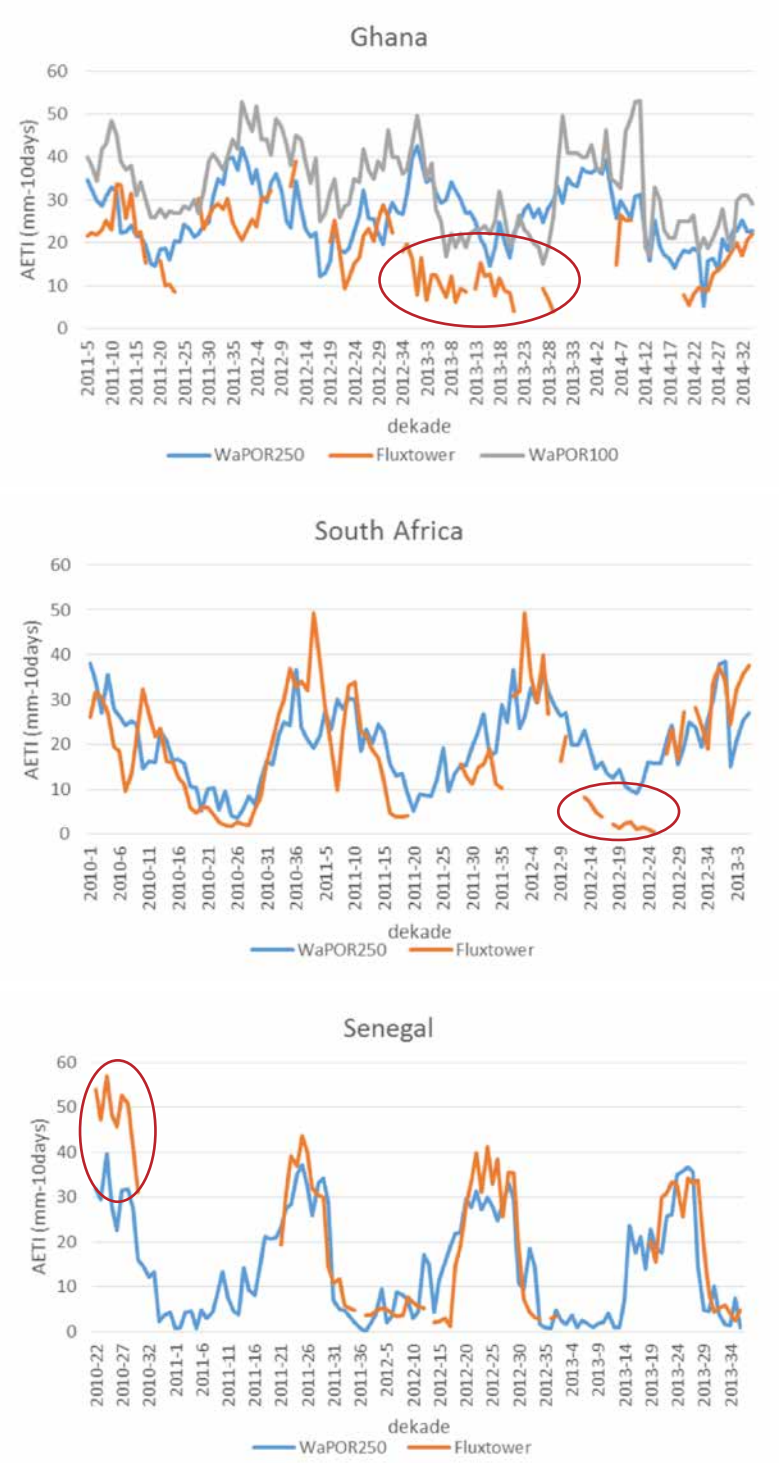

Annex D: E, I and AETI comparison ETmonitor and WaPOR

Actual

Figure D3

GLDAS AETI and comparison with WaPOR AETI for 2010

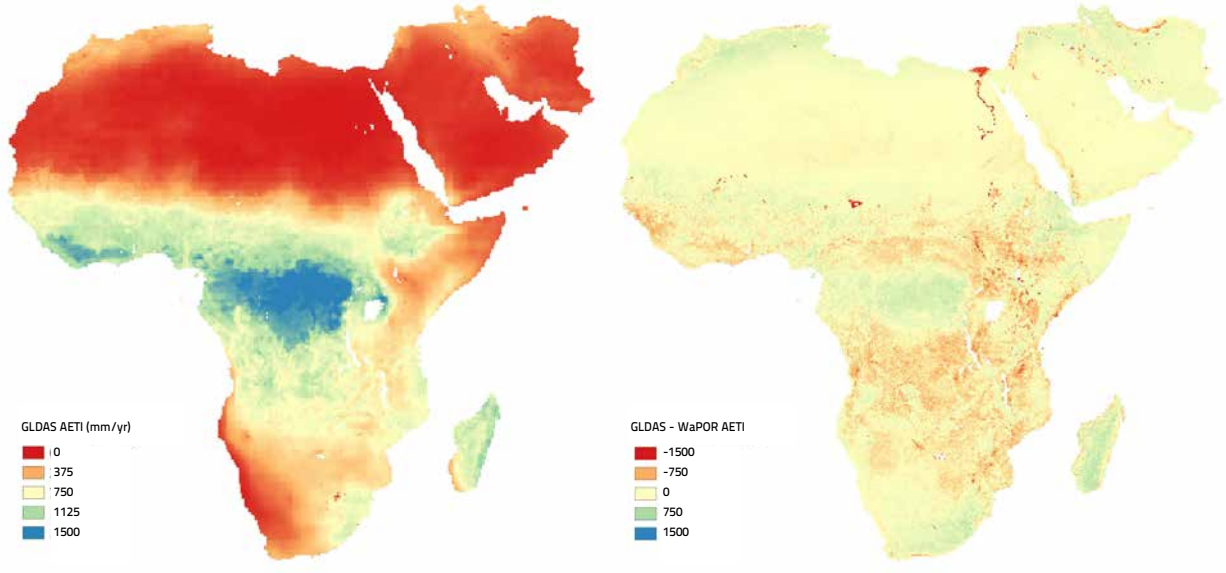

Evaporation 2010

Figure D4

WaPOR E for 2010

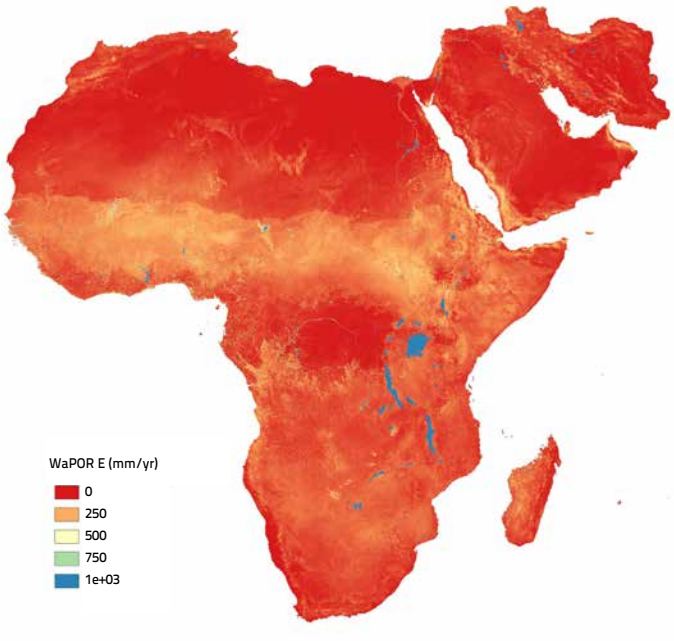

Figure D5

ETMonitor E and Comparison with WaPOR E for 2010

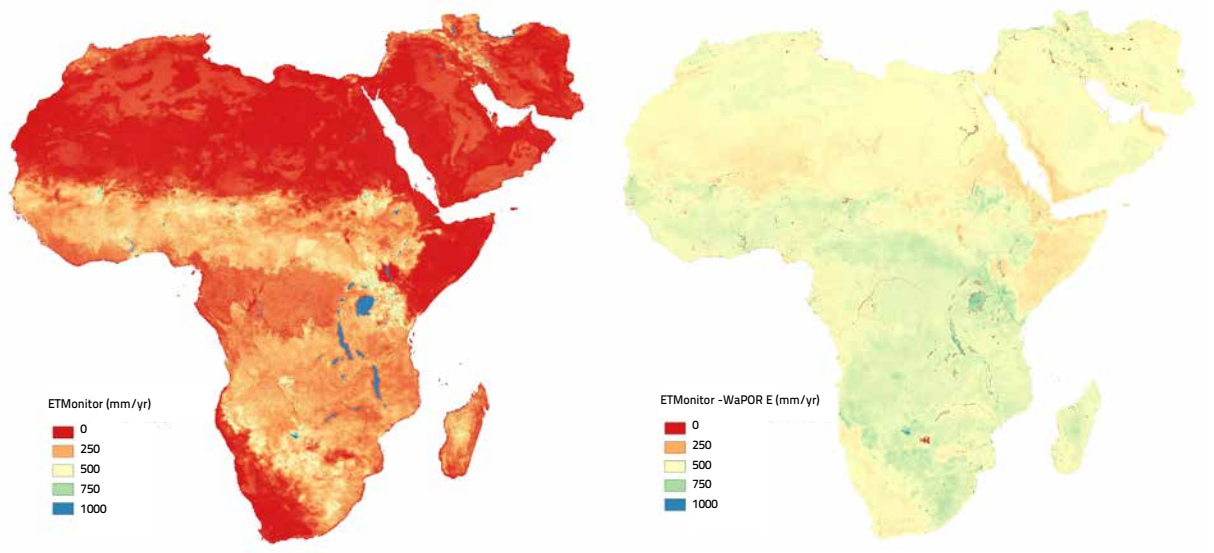

Figure D6

GLDAS E and comparison with WaPOR E for 2010

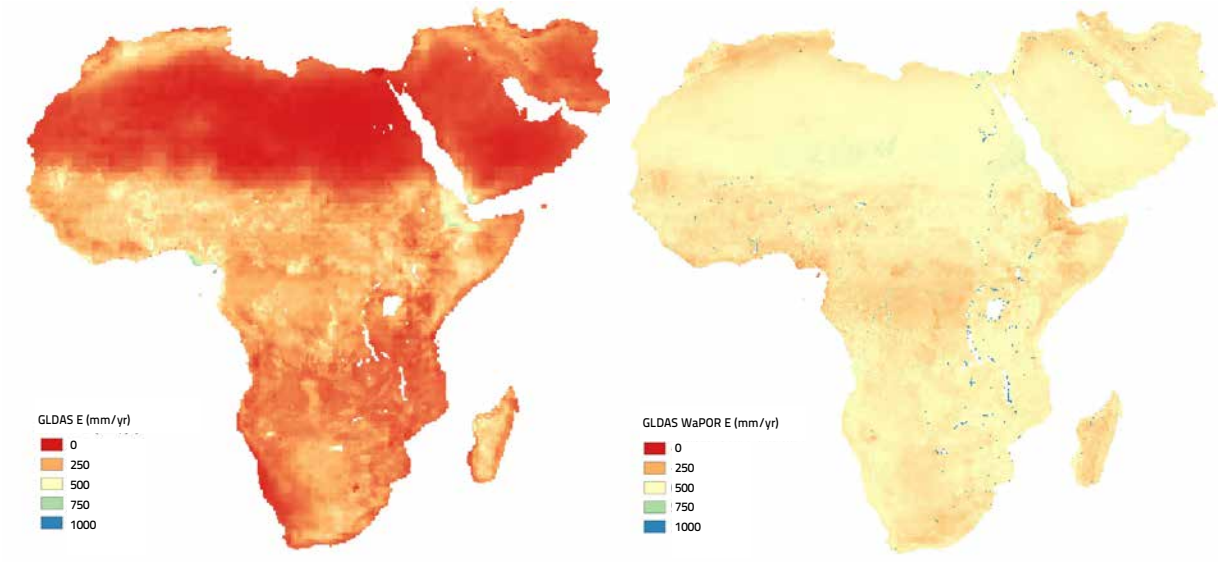

Interception 2010

Figure D7

WaPOR I for 2010

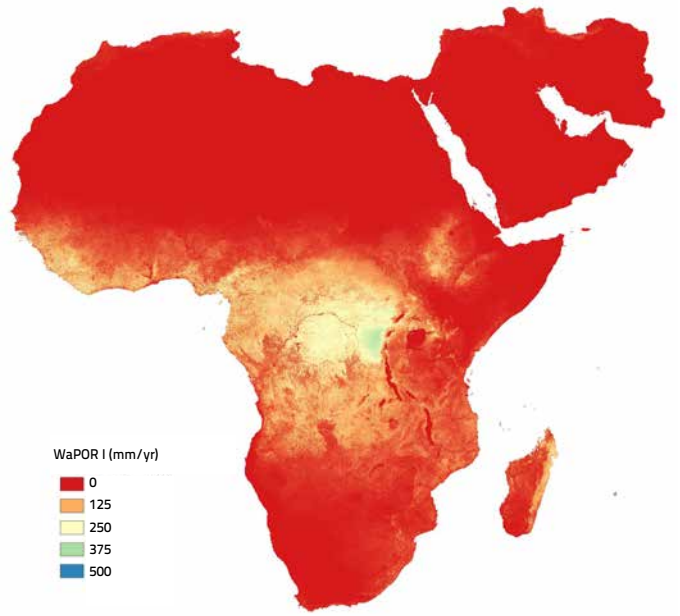

Figure D8

ETMonitor I and comparison with WaPOR I

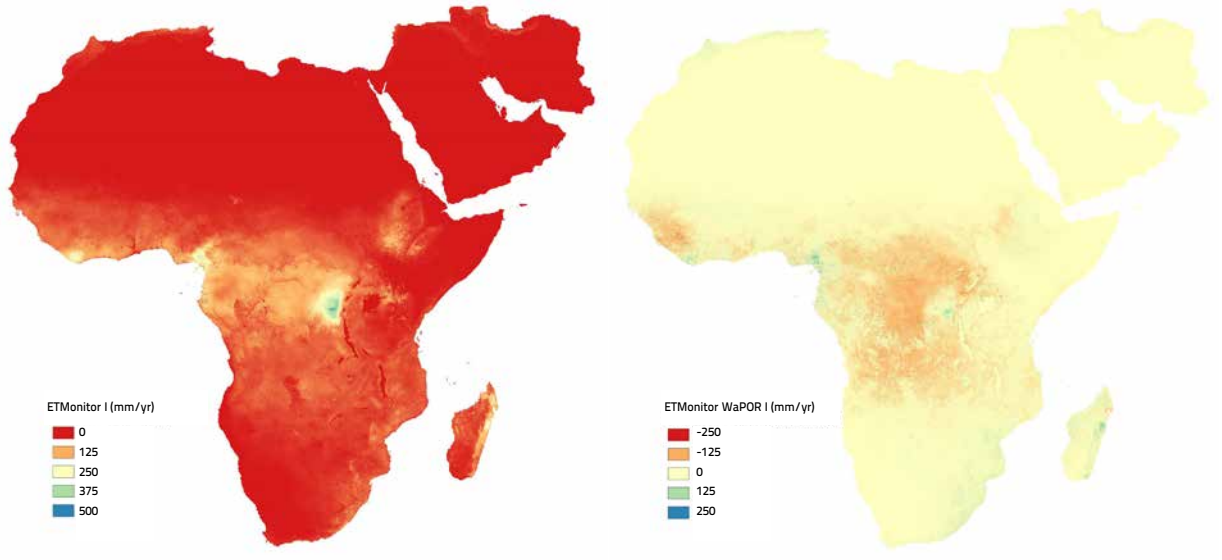

Figure D9

GLDAS I and comparison with WaPOR I

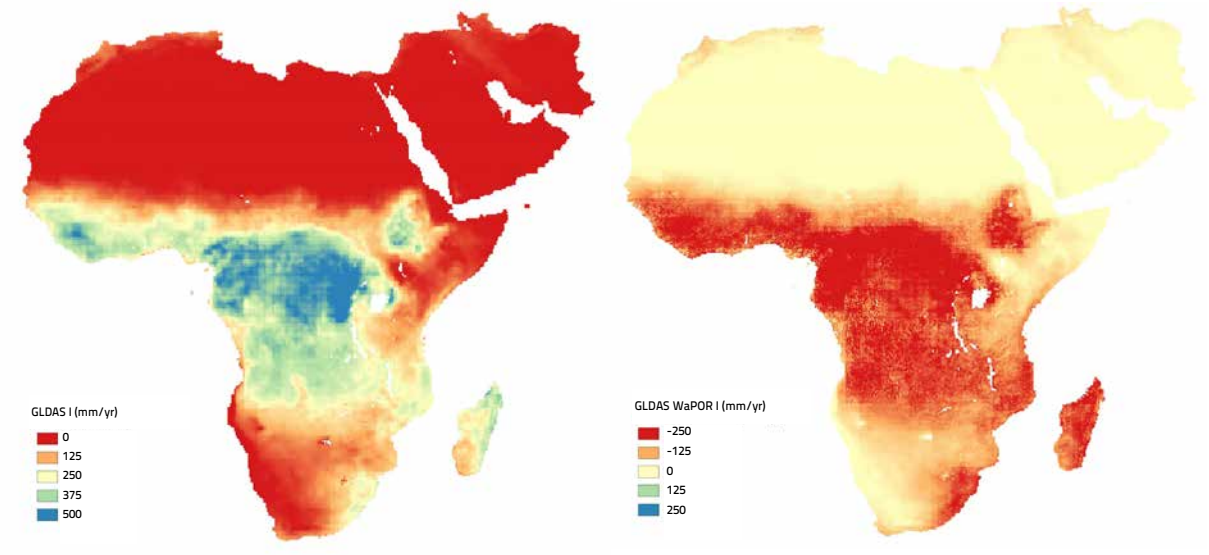

Figure D10

Budyko I and comparison with WaPOR I

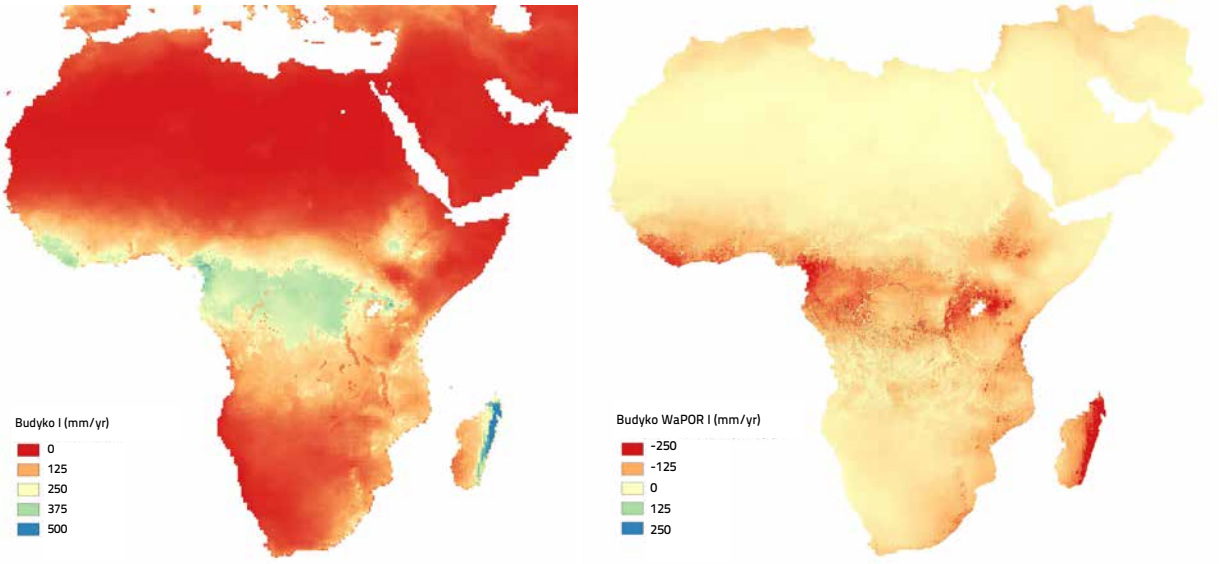

Annex E: WaPOR phenology start of cropping season

Figure E1

Overlap in identification of cropping season 1 and 2

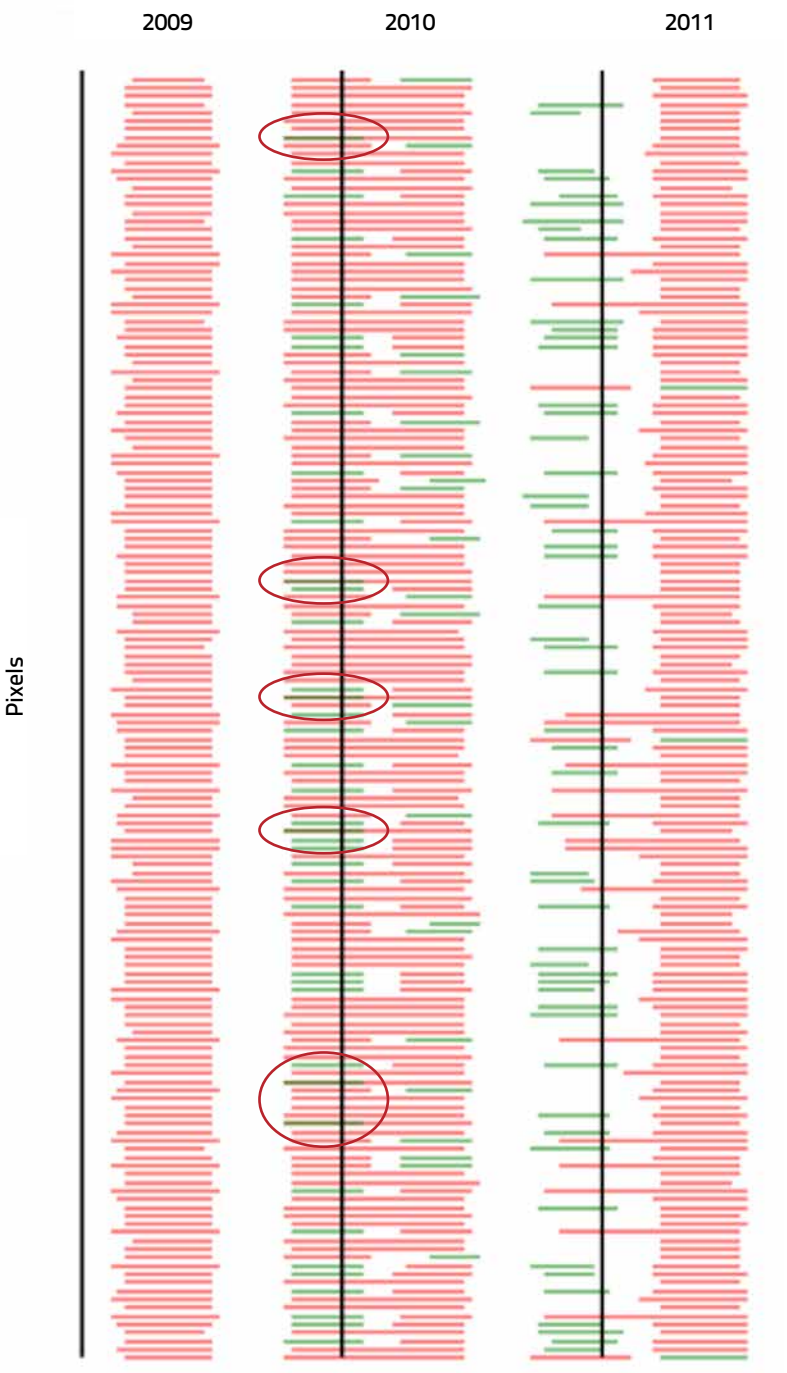

Annex F: Proposed methodological improvements arising from the QA report

This Annex was contributed by eLEAF and VITO, who are responsible within the FRAME[1] consortium for data production to the WaPOR database. It was added to the WaPOR version 1 data Quality Assessment report to summarise, where relevant, the changes that will be made to the methodologies for production of the version 2 (v2.0) WaPOR data components. Where no changes are applied to the methodology of the v 1.0 data components, information is provided to explain the possible sources of error that can influence the data components, explaining why at this moment in time no methodological changes are applied.

A. E, T, I individually

The following changes were made to the v2.0 input data sources: Soil moisture has increased in high vegetation areas, and the land cover input was changed from GlobCover to the v2.0 Land cover data.

B NPP

The v2.0 NPP data product is affected by changes in the input data, specifically the land cover and soil moisture. Based on the validation results, the Light Use Efficiency value applied for cropland (2.49) in v1.0 was replaced by a LUE value of 2.7 for cropland in v2.0. This change was made to avoid double accounting of water stress because a soil moisture stress factor is included in the NPP calculation. A value of 2.7 represents the LUE under optimal water availability conditions (e.g. for irrigated cropland).

In addition, the autotrophic respiration (AR) factor of 0.5 (ratio NPP/GPP) was also under discussion. However, the consensus between experts is that a fixed ratio is currently the best method available. Even though improvements can be achieved by making this AR factor land-cover and land-use dependent, there is insufficient calibration data available over Africa, making the 0.5 factor the best available option.

C. AGBP

In v1.0, the AGBP in level 2 was calculated based on the phenology data. The NPP was summed over the length of each detected growing season, while also taking into account the conversion to the above-ground biomass, as well as the conversion to Dry Matter Productivity. This meant that AGBP was only calculated for those pixels where a growing season was detected. This posed problems for vegetated areas where no clear growing season could be detected, such as evergreen forests (mainly in the tropical areas) and perennial crops with a growing season longer

[1] The FRAME consortium consists of eLEAF, VITO, ITC, University of Twente and Waterwatch foundation commissioned by and in partnership with the Land and Water Division of FAO. For more information regarding FRAME, contact eLEAF (http://www.eleaf.com/). Contact persons. FRAME project manager: Steven Wonink (steven.wonink@eleaf.com). Managing Director: Maurits Voogt (maurits.voogt@eleaf.com)

than one year (e.g. sugar cane). To circumvent this issue, an additional check is incorporated for v2.0: the mean annual NPP is computed for all pixels without a detected growing season. If this mean annual NPP falls above a certain threshold, the pixel is flagged as an evergreen and the AGBP is calculated as the annual sum of NPP. It is also proposed to distribute Total Biomass Production instead of AGBP.

D. Land cover

In v1.0, WaPOR-specific LC maps were used in combination with the official Copernicus 100m Africa land cover map. However, for v2.0, the LC maps will be entirely based on the Copernicus Global Land – Land Cover product, released in May 2019. As by this time only the 2015 global map will be available, this map will be used as the base map for all years. The distinction of irrigated/rainfed areas will be added on an annual basis, resulting in annual LC maps. This irrigation labelling will be based on the original Water Deficit Index (WDI) from v1.0, where an additional temporal check is added. For each year, a 5-year window will be evaluated, labelling that target year as irrigated if the WDI was lower than 0.9 for more than 2 years in that window.

E. Phenology

Phenology is derived from the NDVI-time series, where the evolution in time depicts when the area is greening up to when the senescence of the vegetation is occurring. A greening-up is represented by a sudden increase in the NDVI, while senescence is shown as a decrease in the NDVI. For an accurate delineation of the growing season from the NDVI time series, it is essential to have reliable data available. A common issue which may occur, especially for the start of the growing season (SOS), is high cloud cover, as the main growing season usually coincides with the rainy season. To this end, it is important to check the NDVI quality layer included in the WaPOR database. To make this quality-information easier to interpret, an overall quality layer will be added to the WaPOR database, showing the mean percentage of cloud-free observations per pixel. Areas with a low number of observations have a higher chance of poorly delineated growing seasons, or un-detected growing seasons in case of very sparse valid observations. It is thus important to keep the quality layers in mind when using phenology and/or any seasonal/annual product.

An additional issue to take into account when using the phenology data is the assignment of a growing season to a specific year in case the growing season extends over multiple years. The current assignment is based on the End of Season (EOS), where a growing season is assigned to the calendar year where the EOS is located. A buffer of one month is considered, where EOS values in January of year T are still assigned to the calendar year T-1. Regardless of this threshold for assigning a growing season to a calendar year, issues will arise for areas where the EOS lies around this threshold. Due to natural fluctuations in the timing and length of growing seasons, the assignment of the growing seasons may vary between years, resulting in variations in numbers of growing seasons in these areas (when only one growing season is present, some years will have two growing seasons assigned, while the next year will have no growing season), or a change in the order of the growing season between years (i.e. the rainy season may sometimes be the first season, and sometimes the second season). This issue is demonstrated in figure 58 of the WaPOR quality assessment report.

WaPOR quality assessment

Technical report on the data quality of the WaPOR FAO database version 1.0

This report describes the quality assessment of the FAO's data portal to monitor Water Productivity through Open access of Remotely sensed derived data (WaPOR 1.0). The WaPOR 1.0 data portal has been prepared as a major output of the project: ´Using Remote Sensing in support of solutions to reduce agricultural water productivity gaps', funded by the Government of The Netherlands. The WaPOR database is a comprehensive database that provides information on biomass production (for food production) and evapotranspiration (for water consumption) for Africa and the Near East in near real time covering the period 1 January 2009 to date. This report is the result of an independent quality assessment of the different datasets available in WaPOR prepared by IHE-Delft. The quality assessment checks the consistency of the different layers and compares the individual layers to various other independent data sources, including: spatial data; auxiliary data and in-situ data. The report describes the results of the quality assessment per data layer for each specific theme as available on the portal

ISBN 978-92-5-131535-4

9 789251 315354

CA4895EN/1/06.19